

COMMITTEE CERTIFICATION OF APPROVED VERSION

The committee for Johanna Carolina Sierra certifies that this is the approved version of the following dissertation:

MECHANISM OF ACTION OF AexU, A NEW TYPE III SECRETION SYSTEM EFFECTOR FROM AN EMERGING HUMAN PATHOGEN *Aeromonas hydrophila*

Committee:

Ashok K. Chopra, Ph.D., C.Sc.

Johnny W. Peterson, Ph.D.

Vladimir Motin, Ph.D.

Eric M. Smith, Ph.D.

Judith A. Johnson, Ph.D.

Dean, Graduate School

**MECHANISM OF ACTION OF AexU, A NEW TYPE III
SECRETION SYSTEM EFFECTOR FROM AN EMERGING
HUMAN PATHOGEN *Aeromonas hydrophila***

By

Johanna Carolina Sierra

Dissertation

Presented to the Faculty of the University of Texas Medical Branch Graduate School of
Biomedical Sciences at Galveston in Partial Fulfillment of the Requirements for the
Degree of

Doctor of Philosophy

Approved by the Supervisory Committee

Ashok K. Chopra, Ph.D., C.Sc

Johnny W. Peterson, Ph.D.

Vladimir Motin, Ph.D.

Eric M. Smith, Ph.D.

Judith A. Johnson, Ph.D.

Keywords: *Aeromonas hydrophila*, Type III secretion system, AexU, ADP-
ribosyltransferase activity, GAP activity, septicemic mouse model of infection

August 2010

Galveston, Texas

© 2010, Johanna Carolina Sierra

To my parents Cecilia and German and grandmother Isabel because all their sacrifice allowed me to complete this journey. To Giovanni for his love and patience.

ACKNOWLEDGMENTS

I would like to acknowledge my mentor Dr. Ashok Chopra for his guidance and continuous encouragement. Special thanks to the members of my committee, Drs J.W. Peterson, V. Motin. E.M. Smith and J.A. Johnson for their support through the completion of this work. I would also like to acknowledge all the members of Dr. Chopra's laboratory for providing help during my training. My special gratitude to Giovanni Suarez for his advice and help multiple times during this process. I am grateful to the Graduate School and the Department of Microbiology and Immunology. I would like to acknowledge Dr. V.L. Popov for providing his expertise in the use of the Electron Microscope. I sincerely thank the McLaughlin Endowment committee and the Vale-Asche Foundation for providing me with their fellowships. I would like to thank Ms. Mardelle Susman for her editorial assistance. I also want to thank Drs Victor E. Reyes and Alfredo Torres for their advice and support.

**MECHANISM OF ACTION OF AexU, A NEW TYPE III
SECRETION SYSTEM EFFECTOR FROM AN EMERGING
HUMAN PATHOGEN *Aeromonas hydrophila***

Publication No. _____

Johanna Carolina Sierra, Ph.D.

The University of Texas Medical Branch at Galveston, August 2010

Supervisor: Ashok K. Chopra, Ph.D., C.Sc

Our laboratory first reported the complete sequence of the type III secretion system (T3SS) from a diarrheal isolate SSU of *A. hydrophila*. We identified an effector protein (designated as AexU) of the T3SS, which exhibited ADP-ribosyltransferase (ADPRT) and GTPase-activating protein (GAP) activity. AexU was successfully expressed in the HeLa cell Tet-Off system and I provided evidence that cells expressing and producing the full length AexU showed actin reorganization followed by apoptosis. Earlier, we showed that the $\Delta aexU$ null mutant was attenuated in a mouse model, and I now demonstrated that while the parental *A. hydrophila* strain could be detected in the lung, liver, and spleen of infected mice, the $\Delta aexU$ mutant was rapidly cleared from these organs resulting in increased survivability of animals. The GAP activity of AexU was mainly responsible for host cell apoptosis and disruption of actin filaments. Further, AexU prevented phosphorylation of c-Jun, JNK and I κ B α and inhibited IL-6 and IL-8 secretion from HeLa cells. Our data indicated that AexU operated by inhibiting NF- κ B and inactivating Rho GTPases. Importantly, however, when the $\Delta aexU$ null mutant was complemented with the mutated *aexU* gene devoid of ADPRT and GAP activities, a higher mortality rate in mice with concomitant increase in the production of proinflammatory cytokines/chemokines was noted. These data indicated that either such a mutated AexU is a potent inducer of them or that AexU possesses yet another unknown activity that is modulated by ADPRT and GAP activities and results in this aberrant cytokine/chemokine production responsible for increased animal death.

Table of Contents

List of Figures	ix
List of Tables	iv
Introduction.....	1
Chapter 1: Literature Review.....	3
The genus <i>Aeromonas</i>	3
Clinical infections associated with <i>Aeromonas</i>	4
Gastroenteritis	4
Septicemia.....	5
Hemolytic Uremic Syndrome (HUS).....	6
Skin and soft tissue infection	6
Peritonitis	7
Respiratory tract infections	8
Virulence factors produced by <i>Aeromonas</i>	8
Enterotoxins	8
Quorum sensing	10
Other virulence factors.....	11
secretion systems in gram-negative bacteria.....	11
Type 3 secretion system (T3SS)	14
Identification of the <i>aexU</i> gene in <i>Aeromonas hydrophila</i> SSU.....	17
Cloning of the <i>aexU</i> gene from <i>A. hydrophila</i> SSU	17
AexU is secreted and translocated via T3SS	19
Effects of AexU on cytotoxicity and phagocytosis.....	24
AexU contributes to the virulence of <i>A. hydrophila</i> SSU in mice.....	25
Chapter 2: Materials and Methods.....	28
Cell lines and transfections	28
Bacterial cultures and vectors	29
Electroporation.....	30

Site-directed mutagenesis of the <i>aexU</i> gene	30
Complementation of the <i>A. hydrophila</i> SSU $\Delta act/\Delta aexU$ isogenic mutant <i>in trans</i> with the native <i>aexU</i> or <i>aexU</i> devoid of ADPRT or GAP and/or both activities	32
Recombinant protein purification	32
Antibody production	33
ADP-ribosyltransferase Assays	34
Western Blot analysis	36
Intracellular staining	37
Host cell morphology.....	38
Transmission electron microscopy	38
Host cell apoptosis	39
Host cell viability	39
<i>In vitro</i> GTP-ase Activating protein activity (GAP) assay	40
Phospho-protein detection	40
Cytokine/chemokine detection.....	41
Animal infections and detection of bacteria in peripheral tissues	41
Histopathology	42
Statistics	42
 Chapter 3: Biological Characterization of a New Type III Secretion System Effector from a Clinical Isolate of <i>Aeromonas hydrophila</i>	43
Introduction.....	43
Results.....	45
Purification of rAexU full length and its NH ₂ -terminal and COOH-terminal domains and antibody production.....	45
Purified rAexU possesses ADP-ribosyltransferase activity.....	47
Expression of the <i>aexU</i> gene in HeLa Tet-Off cells	49
Cell morphology and actin filament evaluation in HeLa Tet-Off cells transfected with the <i>aexU</i> gene	53
AexU induces apoptosis in transfected HeLa Tet-Off cells.....	55
Discussion	59

Chapter 4: Unraveling the mechanism of action of a new type III secretion system effector AexU from <i>Aeromonas hydrophila</i>	65
Introduction.....	65
Results.....	67
AexU functions as a GTPase-activating protein (GAP) for RhoA, Rac1 and Cdc42, and this activity is dependent on the arginine residue located at position 145	67
Alterations in actin cytoskeleton of HeLa Tet-Off cells transfected with the <i>aexU</i> gene are associated with GAP activity	68
Induction of apoptosis by AexU in transfected HeLa Tet-Off cells is dependent on GAP activity	71
AexU interferes with the phosphorylation of c-Jun and I κ B α in normal HeLa cells co-cultured with <i>A. hydrophila</i> SSU.....	72
AexU inhibits secretion of IL-6 and IL-8 by HeLa cells co-cultured with <i>A. hydrophila</i> SSU	75
Detection of <i>A. hydrophila</i> SSU in peripheral organs of mice resulting in tissue injury is mediated by AexU	76
<i>A. hydrophila</i> $\Delta act/\Delta aexU$ isogenic mutant complemented with the ADPRT ⁻ /GAP ⁻ mutated version of the <i>aexU</i> gene is more virulent than the one producing the native form of the <i>aexU</i> gene	78
Discussion	81
Conclusions.....	88
Future Directions	90
References.....	91

List of Figures

Figure 1.1: Overview of secretion systems in Gram negative bacteria.	12
Figure 1.2: Architecture of the T3SS.	15
Figure 1.3: Genetic organization of the 4150 bp DNA fragment of <i>A. hydrophila</i> cloned in the plasmid pBlue-aexU.	17
Figure 1.4: Amino acid sequence comparison between AexU and AexT.	18
Figure 1.5: Translocation of AexU from <i>A. hydrophila</i> SSU.	21
Figure 1.6: Translocation of GSK-tagged AexU (AexU::GSK) from <i>A. hydrophila</i> SSU.	22
Figure 1.7: AexU-associated cytotoxicity.	23
Figure 1.8: Anti-phagocytic activity of AexU.	25
Figure 1.9: The role of AexU during <i>A. hydrophila</i> infection in a septicemic mouse model.	26
Figure 1.10: Immunization of mice with rAexU.	27
Figure 3.1: Amino acid sequence alignment of AexT from <i>A. salmonicida</i> and AexU from <i>A. hydrophila</i> SSU.	46
Figure 3.2: Schematic representation of AexU.	47
Figure 3.3: Recombinant purified AexU.	48
Figure 3.4: ADP-ribosyltransferase activity of AexU as evidenced by hydrolysis of [¹⁴ C]NAD.	49
Figure 3.5: Expression and production of AexU in transfected HeLa Tet-Off cells.	50
Figure 3.6: Fluorescent staining of HeLa Tet-Off cells transfected with plasmids encoding the <i>aexU</i> gene.	52
Figure 3.7: Phalloidin staining of HeLa Tet-Off cells transfected with plasmids encoding the <i>aexU</i> gene.	54
Figure 3.8: Transmission electron microscopy of HeLa Tet-Off cells transfected with plasmids encoding the <i>aexU</i> gene.	55

Figure 3.9: Induction of apoptosis in HeLa Tet-Off cells transfected with <i>aexU</i> gene.	57
Figure 3.10: Caspase 3 and 9 detection in HeLa Tet-Off cells transfected with <i>aexU</i> gene for 48 h.	59
Figure 4.1: <i>In vitro</i> GAP activity of AexU.	68
Figure 4.2: Assessment of the actin cytoskeleton by phalloidin staining in HeLa Tet-Off cells expressing the genes encoding native AexU or its GAP ⁻ mutated version.	70
Figure 4.3: Assessment of the apoptotic rate in HeLa Tet-Off cells expressing the genes encoding native and mutated version (GAP ⁻) of AexU.	71
Figure 4.4: Phosphorylation of c-jun, IκBα, and JNK in HeLa cells co-cultured with WT <i>A. hydrophila</i> SSU or its $\Delta aexU$ mutant.	72
Figure 4.5: Phosphoprotein detection in HeLa cells by Western blot analysis.	74
Figure 4.6: Secretion of IL-6 and IL-8 was evaluated in supernatants of HeLa cells co-cultured with either the Δact mutant of <i>A. hydrophila</i> SSU or its $\Delta act/\Delta aexU$ mutant.	75
Figure 4.7: Detection of either the Δact mutant of <i>A. hydrophila</i> SSU (parental strain) or its $\Delta act/\Delta aexU$ mutant in mice after 48 h of i.p. injection with 8×10^5 cfu.	76
Figure 4.8: Histopathological analysis of tissues.	77
Figure 4.9: Survival curve and bacterial counts from mice infected with <i>A. hydrophila</i> $\Delta act/\Delta aexU$ mutant strains complemented with native, ADPRT123 ⁻ , GAP ⁻ or ADPRT123 ⁻ /GAP ⁻ versions of AexU.	79
Figure 4.10: Cytokine/chemokine profile from the spleens of mice infected with <i>A. hydrophila</i> $\Delta act/\Delta aexU$ mutant complemented with the native or ADPRT123 ⁻ /GAP ⁻ mutant form of AexU	81

List of Tables

Table 1: Primers used for cloning and site-directed mutagenesis of AexU.....	31
--	----

Introduction

Aeromonas hydrophila is a Gram-negative bacterium associated with a variety of human diseases, such as gastroenteritis, cellulitis, bacteremia, soft tissue infection, peritonitis and hemolytic-uremic syndrome (19, 78, 83). Human infections can be acquired by contact with contaminated water or soil, and this organism has also been isolated from food samples, which has suggested its importance as a food-borne pathogen (8, 42, 81, 102). In addition to being prevalent in water sources, this bacterial pathogen is highly resistant to water chlorination especially when in biofilms and to multiple antibiotics (102). Consequently, *A. hydrophila* was included on the Environmental Protection Agency's "Contaminant Candidate List" (27).

Numerous virulence factors have been identified in the diarrheal isolate SSU of *A. hydrophila*, including enterotoxins, hemolysins, proteases, and most recently, an effector protein secreted via the type 3 secretion system (T3SS), referred to as AexU (119, 121, 123). The T3SS apparatus allows the translocation of bacterial effectors into the cytoplasm of eukaryotic cells. Once injected into the cytoplasm, these effectors can induce alterations of the cytoskeleton, signaling pathways, apoptosis, and in general, manipulate the host cells to the advantage of the bacteria.

Previous studies showed that mice infected with the $\Delta aexU$ deletion mutant were significantly protected from mortality, indicating that AexU contributed to the virulence of *A. hydrophila* (123). Additionally, immunization of mice with the recombinant AexU protected them from subsequent lethal challenge dose of the WT bacterium (123). Increased phagocytosis was observed in murine macrophages infected with an $\Delta aexU$ mutant of *A. hydrophila* as compared to macrophages infected with the parental strain (123).

After the initial identification of AexU, I started studies to biologically characterize this T3SS effector protein. Sequence analysis of AexU showed that the NH₂-terminal domain has homology with other T3SS effectors, like AexT from *A. salmonicida* and ExoS/T from *Pseudomonas aeruginosa*, but the COOH-terminal domain of AexU was unique, with no homology to any known proteins in the NCBI database. Initial experiments indicated that AexU possessed ADP-ribosyltransferase (ADPRT) activity and once translocated into the host cell cytoplasm, was able to disrupt the actin cytoskeleton and apoptosis by the activation of caspase 3 (126).

In the following study, I provided evidence that AexU also possessed GTPase-activating protein (GAP) activity, prevented the phosphorylation of c-Jun, JNK and I κ B α and inhibited IL-6 and IL-8 secretion from HeLa cells. Earlier, we showed that the $\Delta aexU$ mutant was attenuated in a mouse model, and now I have demonstrated that while the parental *A. hydrophila* strain could be detected in the lung, liver, and spleen of infected mice, the $\Delta aexU$ mutant was rapidly cleared from these organs resulting in increased survival of the animals. Importantly, however, when the $\Delta aexU$ mutant was complemented with the *aexU* gene devoid of ADPRT and GAP activities, a higher mortality rate with a concomitant increase in the production of proinflammatory cytokines was noted. These data indicated that either such a mutated AexU is a potent inducer of them or that AexU possesses yet another unknown activity that is modulated by ADPRT and GAP activities and results in aberrant cytokine production responsible for increased animal death.

Chapter 1: Literature Review

THE GENUS *AEROMONAS*

The genus *Aeromonas* consists of 27 species that are motile Gram-negative rods and produce oxidase, catalase and nitrate reductase. They have the ability to ferment D-glucose and trehalose (1). Initially, the genus *Aeromonas* was included in the family Vibrionaceae together with *Vibrio* and *Pleisomonas*, because of some shared characteristics like the presence in the ecosystems, disease spectra and phenotypic features (76). However, with the availability of new molecular techniques, in particular based on the 16S rRNA gene sequencing, the genus *Aeromonas* now has its own family (Aeromonadaceae) (77).

At first, aeromonads were broken in two distinctive groups: the mesophilic and the psychrophilic group. *Aeromonas hydrophila* typified the mesophilic group, characterized by motile strains that grew well at temperatures between 35 and 37°C and caused human infections (77). The psychrophilic group comprises non-motile strains that grow at temperatures between 22 and 25°C and cause disease in fish (77). Later, there was an effort to redefine the mesophilic group through DNA studies; it was established that multiple hybridization groups existed within this group (106). Each one of these hybridization groups (HG) has numbers for defined species (for example, *A. hydrophila* was classified as HG1) (77).

Aeromonads habitat is very diverse; they can be isolated from multiple aquatic habitats like freshwater bodies, estuarine waters, raw sewage, treated sewage and can also be found in chlorine-treated municipal drinking water (62). Additionally, they have been found in fish, foods, domesticated pets, invertebrate species and soil (77).

A. hydrophila, *A. caviae* and *A. veronii* species have been mainly isolated from clinical samples and are responsible for multiple human infections, including intestinal, extraintestinal and systemic infections (76).

CLINICAL INFECTIONS ASSOCIATED WITH *AEROMONAS*

Gastroenteritis

The most common site for the isolation of aeromonads is the gastrointestinal tract, and diarrhea due to *Aeromonas* is a phenomenon described in both developing and industrialized countries. *Aeromonas* gastroenteritis usually presents as watery and self-limited diarrhea accompanied by low fever, abdominal pain, vomiting and mild to moderate dehydration. This form accounts for 75% to 89% of all cases of *Aeromonas* gastroenteritis (77, 140). On the other hand, a dysenteric form is less common with frequencies between 3% and 22%, the symptoms include cramping abdominal pain together with mucus and blood in the stools (140). *Aeromonas* can also be responsible for subacute or chronic diarrhea, the symptoms are nonspecific and include multiple watery bowel movements per day, leading to a significant weight loss (77). Although not often, cholera-like disease has also been associated with *Aeromonas* characterized by non-bloody rice-water diarrhea (62).

Epidemiological studies have found that cultures from symptomatic and control individuals are positive for the three main species, *A. hydrophila*, *A. caviae* and *A. veronii* (76). The association of *Aeromonas* with traveler's diarrhea was evaluated among Finnish tourist visiting Morocco, and *Aeromonas* spp. were isolated from 8.7% of the samples from the patients with diarrhea and from 1.4% of the non-diarrheal group (69). In the same study, *Aeromonas* was identified as the sole pathogen in 5.5% of the patients. These differences varied widely between studies, for example, 52.4% of Peruvian children with

diarrhea were positive for *Aeromonas* in contrast just 8.7% of the controls tested were positive. However, 50% of the children positive for *Aeromonas* had other enteropathogens present as well (103). In a prospective study of children in Chicago, *Aeromonas* spp. were isolated from 7.3% of the patients with diarrhea and from 2.2% of the controls (25). Recently, a cross-sectional survey in South Africa identified *Aeromonas* spp. as one of the five most common bacterial causes of diarrhea in patients attending public hospitals, with *Aeromonas* spp. isolated from 20.8% of the cases (115).

Septicemia

More than 80% of the cases of *Aeromonas* septicemia occur in immunocompromised individuals. In this group of patients the usual portal of entry is the gastrointestinal tract and those with myeloproliferative disorders or chronic liver disease are at the greatest risk (77). Also less common, *Aeromonas* septicemia could develop as a result of severe wound infection in trauma patients; in this case the infection is acquired from an exogenous source, most commonly by exposure to contaminated water, and the mortality rate is approximately 60% (76). In very rare cases, healthy individuals with no recognized risk factors and without major trauma can develop septicemia by *Aeromonas* and in this group of individuals the mortality rate is less than 20% (77). Also, the occurrence of *Aeromonas*-associated septicemia in burn patients that sustained injuries in 38% to 80% of their body has been reported and in these cases the source of infection could be contaminated soil or water (12, 110). There are four species of *Aeromonas* recognized to cause septicemia, *A. hydrophila*, *A. veronii*, *A. caviae* and *A. jandei*, and from these *A. hydrophila* is responsible for 65% of the mono-microbial infections (76).

Hemolytic Uremic Syndrome (HUS)

A small number of HUS cases have been reported in the literature, the first case was reported in 1988 and *A. sobria* was identified as the causative agent (51). However, the first well documented case occurred in 1991, a 23 month old child developed HUS after an episode of bloody diarrhea caused by *A. hydrophila*. This strain showed cytotoxicity on Vero cells and the patient's serum had high titers of cytotoxin neutralizing antibodies (17). A review of 82 cases of HUS by a Canadian group showed that 2 of these cases were caused by *A. hydrophila*, supporting the fact that *Aeromonas* can cause HUS (113). The latest case was reported in 2007, where a 40 year old male was infected with *A. veronii* and developed HUS after an episode of non-bloody watery diarrhea (51).

Skin and soft tissue infection

After the gastrointestinal tract, the integument and deeper soft tissues underlying the epidermis are the second most common anatomical sites from where *Aeromonas* spp. are isolated (76). The wound infections can range from mild pathologies affecting the subcutaneous surface like cellulitis to more serious illnesses affecting fascia, tendons, muscle, joints and bone (65, 77). Usually individuals are infected with *Aeromonas* after an abrasion or penetrating injury that allows the exposure of the tissue to environmental sources like soil or water. Most of the time, the lesions are located on the extremities. Another category includes individuals that suffer major trauma like airplane, automobile and boating accidents where pronounced tissue damage allows the introduction of soil, wood or metal contaminated with *Aeromonas* (65). Lately, the importance of *Aeromonas* as an emerging pathogen was recognized after natural disasters like the ones in New Orleans after hurricane Katrina and in Thailand after the tsunami in 2004 (73, 108).

Between December 2004 and January 2005, cultures from wounds and/or pus specimens were performed from patients with traumatic injuries that were transferred from 6 provinces of southern Thailand after the tsunami (73). The most commonly isolated pathogen from individuals with skin and soft tissue infections was *Aeromonas* spp. accounting for 22.6% of the infections, and within this group *A. hydrophila* was the predominant species followed by *A. veronii* biovar *sobria* (73). In the same study, the sensitivity to different antibiotics was tested and the data showed that only 21% of *Aeromonas* isolates were susceptible to cefazolin and only 23% were susceptible to amoxicillin-clavulanate. In contrast, those isolates were susceptible to amikacin, gentamicin, cefepime, cefotaxime, ceftazidime, ciprofloxacin, imipenem, and trimethoprim-sulfamethoxazole (73).

In September 2005, environmental samples were collected within New Orleans after hurricane Katrina. The aim of the study was to determine hazards for humans and wildlife from pathogens and toxic materials in the floodwaters (108). Water samples were analyzed for the presence of coliforms as well as members of the genera *Aeromonas* and *Vibrio*. Two sampling locations, the Superdome and Charity Hospital, showed particularly high levels of *Aeromonas* spp. with bacterial densities of 2.6×10^7 and 5.6×10^6 CFU/mL, respectively, and approximately 50% of these isolates corresponded to *A. hydrophila* (108). Due to the high levels of *Aeromonas* in the water samples, the authors indicated the high risk for contact and opportunistic infections after skin abrasions or cuts.

Peritonitis

Aeromonas-associated peritonitis is more frequent in Southeast Asia than in America or Europe (77). This kind of infection is usually found in middle-aged males with an underlying disease. Primary *Aeromonas* peritonitis, which results from the spread

of an infection from the blood or lymph to the peritoneum, is often detected in patients with liver disease (77). A retrospective study from January 1997 to December 2006 of patients with spontaneous bacterial peritonitis due to *Aeromonas* spp. showed that most of the infections were observed during the summer months and diarrheal episodes were more frequent in this group when compared with the subjects with spontaneous bacterial peritonitis caused by other bacteria (28). Within the group with peritonitis caused by *Aeromonas*, 93% had *A. hydrophila* and 7% *A. sobria* infection.

Respiratory tract infections

Respiratory infections caused by *Aeromonas* spp. include epiglottitis, empyema, lung abscesses and pneumonia and these infections have been described both in immunocompetent and immunocompromised individuals. The most common respiratory alteration due to infection with *Aeromonas* is pneumonia. In immunocompetent individuals, the infection usually appears after contact with an aquatic environment involving major trauma, as in near-drowning experiences (98). On the other hand, in patients with a preexisting condition, the respiratory infection appears to come from hematogenous dissemination from the gastrointestinal tract to the respiratory tract (98). For both groups, the patient's condition deteriorates rapidly and rapid demise is common (77).

VIRULENCE FACTORS PRODUCED BY *AEROMONAS*

Enterotoxins

Aeromonas spp. produce multiple enterotoxins, including cytotoxic and cytotoxic. Up to this time, two cytotoxic enterotoxins have been identified in *Aeromonas* isolates, heat-labile (Alt) and heat-stable (Ast), which do not cause degeneration of the crypts and

villi of the small intestine (29). Additionally, a cytotoxic enterotoxin, called Act, also was identified and characterized from a diarrheal isolate SSU of *A. hydrophila* (114).

The heat-labile cytotoxic enterotoxin, Alt, from *A. hydrophila* SSU consists of a single polypeptide chain (33). This toxin was active when tested in *in vivo* and *in vitro* assays. Immunization of mice with purified recombinant Alt induced a significant decrease in the fluid secretory response when animals were challenged with WT *A. hydrophila* (33). Treatment of Chinese Ovary Hamster (CHO) cells with recombinant Alt elevated the levels of Ca^{2+} ; however, pretreatment with a phospholipase C inhibitor blocked this Ca^{2+} release (33). Latter studies showed that prostaglandin (PGE_2) levels in CHO cells treated with Alt were regulated by phospholipase A_2 -activating protein (PLAA) (112).

The heat-stable enterotoxin, Ast, was also identified in the SSU isolate of *A. hydrophila* (31). The recombinant form of Ast was biologically active *in vivo* as determined by the rat ligated ileal loop assay and it induced elongation of CHO cells along with the elevation of cAMP in *in vitro* assays (119).

The cytotoxic enterotoxin (Act) was purified from a diarrheal isolate SSU of *A. hydrophila*. It is produced as a pre-toxin and conversion to active toxin requires the removal of 23 amino acids at the NH_2 -terminal end and the proteolytic cleavage of a 4-5 kDa peptide from the COOH -terminal end (32). Two regions in the protein, amino acid residues 245-274 and 361-405, were identified as important for the biological activity of the toxin. Antibodies generated against these peptides significantly reduced the cytotoxic and hemolytic activity of the native toxin (49). The mechanism of action of Act involves the formation of 1.14-2.8 nm pores in host cells; this allows the entry of water from the external milieu inducing cell swelling and later lysis (50). Act aggregates in the cellular membrane once in contact with erythrocytes, but pre-incubation of the toxin with

cholesterol reduces the hemolytic activity of Act by inducing aggregation of the toxin prior to the binding with the erythrocytes (50). Act plays an important role in the pathogenesis of *Aeromonas* infection because of its ability to induce the infiltration of macrophages and mononuclear cells at the site of infection, and at the same time, in stimulating the production of TNF- α , IL-6, IL-8 and inducible nitric oxide synthase (iNOS) (34). The response of murine macrophages to Act has been evaluated by Affymetrix GeneChips, and multiple immune-related genes were up-regulated, in particular those genes that were associated with inflammation or stress response, like TNF, G-CSF, MIP and Glutaredoxin, among others (57). Act also increased the expression of multiple pro-apoptotic encoding genes, like Bcl-10, BimEL, GADD45 and TDAG51 in murine macrophages (57). The promoter activity of the *act* gene was increased in the presence of Ca²⁺ and inhibited by glucose and iron (121). The search for additional regulatory genes that modulated the expression of the *act* gene in our laboratory lead to the identification of the glucose-inhibited division gene (*gidA*). The *gidA* isogenic mutant of *A. hydrophila* possessed reduced hemolytic and cytotoxic activity associated with Act (120). The DNA adenine methyltransferase (*dam*) gene from *A. hydrophila* was also characterized, showing that Dam altered the levels of Act which was secreted via the type II secretion system (44).

Quorum sensing

The quorum sensing process allows bacteria to act co-operatively by producing and detecting small compounds, inducing or repressing the expression of specific genes when the concentration of the signaling molecule reaches a specific threshold via the LuxR family of transcriptional activators. This process has been described in *Aeromonas* spp. and the principal quorum sensing molecule synthesized by the *ahyI* locus (encoding an auto-inducer) in *A. hydrophila* is N-(butanoyl)-L-homoserine lactone (BHL) (136).

Deletion of the *ahyI* gene in *A. hydrophila* abolishes BHL production resulting in reduced production of two exoproteases (serine protease and metalloprotease), but their production could be restored by the addition of exogenous BHL (136). On the contrary, mutation in the *ahyR* gene (*luxR* homolog) resulted in the loss of these two protease activities, which could not be restored by the addition of BHL (136). Also, it was shown that *ahyI* mutants that could not produce BHL failed to produce a mature biofilm, making bacteria more susceptible to host defenses and antimicrobial agents (89).

Other virulence factors

Recent studies in *A. hydrophila* SSU identified a functional type 6 secretion system (134). Until now, two virulence factors secreted via the T6SS have been identified, Hcp (Haemolysin co-regulated protein) and Vgr (Valine-glycine repeats) G1 family of proteins (132, 134). Hcp is translocated into the cytoplasm of eukaryotic cells and induces apoptosis mediated via caspase 3 activation (134). Additionally, Hcp is secreted into the extracellular media where it is able to interfere with the activation of macrophages, leading to inhibition of *A. hydrophila* phagocytosis (125). Our laboratory also reported the existence of the VgrG1 protein in *A. hydrophila*. This bacterial effector possesses ADPRT activity towards actin and once translocated into the host cells, induces disruption of the actin cytoskeleton and apoptosis (132).

SECRETION SYSTEMS IN GRAM-NEGATIVE BACTERIA

Gram-negative bacteria have evolved multiple pathways to transport proteins across their inner and outer membranes. Six different secretion systems (Type 1 to 6) have been described in these pathogens and this classification is based on the characteristics of the secretion mechanism. **Figure 1.1** shows a representative diagram of different secretion systems in various gram-negative bacteria.

complex that reaches into the periplasm, and a secretion pore in the outer membrane (79). Secretion occurs in two steps; first the proteins are targeted to the Sec machinery by the signal peptide and are transported into the periplasm, the second step includes the removal of the signal peptide and transport of the fully folded protein across the outer membrane (79).

The type 4 secretion system (T4SS) allows the translocation of proteins or complexes of protein and single stranded DNA. The T4SS in gram-negative bacteria is believed to have evolved from bacterial conjugation machineries; the recipients for the transported substrate can be bacteria of the same or different species, or organisms from a different kingdom like fungi, plant or mammalian cells (9). The majority of the complexes transported by the T4SS are not secreted into the extracellular media but directly translocated into the cytoplasm of the host (23).

The type 5 secretion system (T5SS) is also called autotransporter. Its primary structure is modular and possesses three domains: the signal sequence, the passenger domain, and the translocation unit. The signal sequence located at the NH₂-terminal end allows targeting of the protein to the inner membrane. The passenger domain harbors the specific effector function. The translocation unit, located at the COOH-terminal end of the effector, is inserted into the outer membrane and forms a β -barrel secondary structure that allows the secretion of the passenger domain into the extracellular media (61).

The type 6 secretion system (T6SS) has been recently described and its cluster contains between 12-to-25 genes, the composition and organization of which vary among different bacteria (109). Most of the components of the cluster are not secreted and only Hcp and VgrG proteins have been identified in the supernatant of bacteria carrying the T6SS cluster (22). It remains unclear if the secretion process occurs in one or two steps because there are no canonical NH₂-terminal signal sequences identified and the

macromolecular structure of the system has not been resolved. The published data support a model that mimics the mechanism of the T4 bacteriophage (109). One of the hypothetical models proposes that the tail of VgrG is inserted into the outer membrane through the NH₂-terminal domain and punctures the host cell through the needle like structure formed by the central domains, releasing the active domain into the extracellular medium or the cytosol of the host cell (22).

Type 3 secretion system (T3SS)

The T3SS structure and function are conserved among different gram negative bacteria and it consists of more than 20 proteins from which many show homology to the flagellar system components (97). Bioinformatics studies have shown that nearly one billion years ago, bacteria already had genes highly homologous to the modern T3SS (90). The T3SS machinery is designed to translocate bacterial proteins, called effectors, to the cytoplasm of the host cells to modulate the host biochemical functions like cytoskeleton architecture, programmed cell death, cell cycle progression, endocytic trafficking, and gene expression.

The secretion machinery is composed of the basal body, a needle-like projection and the translocon as depicted in **Figure 1.2**. The basal body provides a structural framework for the other components. Studies from *Salmonella*, *Shigella* and *E. coli* showed that this structure consists of only three proteins that assemble into a supramolecular structure forming oligomers of high symmetry (90). A long filamentous structure, the needle-like projection, composed of a single protein, protrudes from the outer membrane and is anchored about halfway through the basal body in the inner ring structure (90). This needle complex is traversed by a channel (~28Å in diameter) that allows transport of the effector proteins (55). The translocon is located at the tip of the

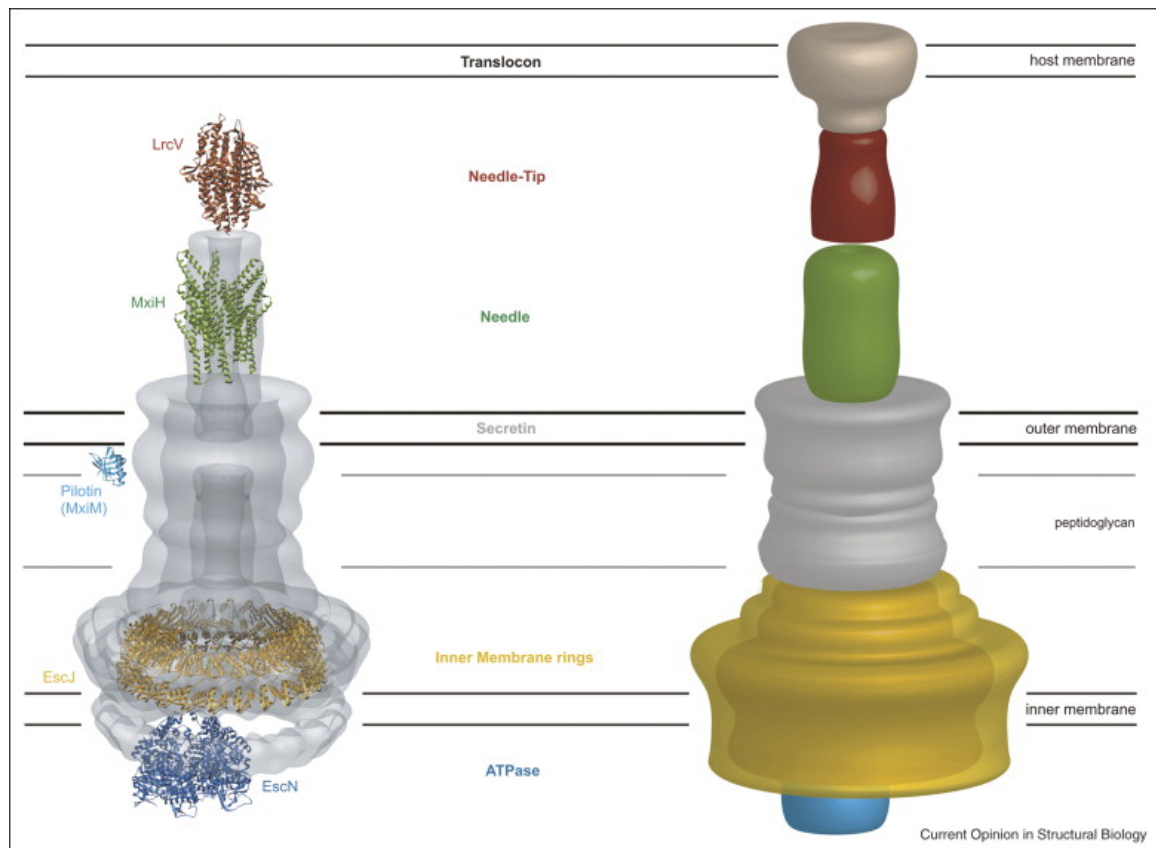


Figure 1.2: Architecture of the T3SS. Left figure, crystal structure of the known protein components docked in a cryo EM map of the *Salmonella typhimurium* apparatus. Right figure, model of the T3SS displaying the main components (basal body, needle-like projection and translocon). “Reprinted from Current Opinion in Structural Biology, Vol 18 (2) , Trevor F. Moraes, Thomas Spreter, and Natalie CJ Strynadka, Piecing together the type III injectisome of bacterial pathogens, Pages 258-266, © Copyright (2008), with permission from Elsevier.”

needle structure and this is a complex of several proteins that forms a pore in the host cell allowing injection of the bacterial effectors (90).

Assembly of the T3SS is a highly regulated process, in which assembly of the base structure leads to the recruitment of a series of highly conserved inner membrane proteins that include an ATPase and a set of more than five integral membrane proteins that are critical for the functioning of the system (90). Once the base is fully assembled, this structure begins the transport of components that are necessary for the assembly of the inner rod and needle-like projection (55). Then the apparatus becomes competent for

the translocation of the effector proteins (55). The bacteria possesses a mechanism to recognize the substrates that will be translocated via the T3SS, most of the effectors have a secretion signal within the first 20-to-30 amino acids but these are not cleaved upon secretion (55). Another layer of specificity may be conferred by cytosolic chaperones that bind some of the T3SS effector proteins. These chaperones interact with a 50-to-100 amino acid domain on the secreted protein that is located downstream of the secretion signal (55). Co-crystal structures of chaperons bound to the secreted protein have showed that the effector protein is in a non-globular conformation but maintains its secondary structure (14, 128). It has been proposed that the chaperons play a dual function, first they may “prime” the effector proteins for unfolding before secretion, and second, they prevent the premature interaction of the effector with other components of the T3SS machinery (129, 141). After the effector protein in complex with the chaperon is targeted to the secretion machinery, the chaperon must be removed from the effector to allow its secretion. *In vitro* studies using highly conserved ATPase associated with the T3SS showed that interaction of the ATPase with the effector-chaperon complex results in the dissociation of the complex and unfolding of the effector (3). The mechanism by which the T3SS delivers the effector protein into the eukaryotic cells is poorly understood. In addition to the needle complex, the bacteria also need a subset of proteins known as translocators that are inserted in the cell membrane and form a channel that allows the transport of the effector protein into the cytosol of the host cell (66, 137). Bacterial strains lacking the translocators are able to secrete effector proteins to the extracellular media but are unable to deliver them into the target cells, indicating that the needle complex is insufficient to mediate translocation (66). It has been proposed that the needle “docks” onto the pore made by the translocators, allowing the delivery of the effector protein into the host cell cytoplasm (55).

The T3SS regulatory mechanism controls the assembly and activation of the machinery; this regulation is mainly transcriptional and occurs in two steps. First, the expression of the genes necessary for the assembly of the apparatus and second the expression of the genes encoding the effector proteins (53). Environmental signals, like temperature, acidity and presence of divalent cations, can control the expression of genes necessary for the assembly of the T3SS. Multiple pathogenic bacteria reside in the environment and once they encounter an animal host, there is an increase in the temperature of their surroundings. For *Shigella* and *Yersinia*, it has been shown that temperature increase leads to the expression of the T3SS genes (91, 107). Studies in *Shigella* showed that an AraC-like transcriptional activator (VirF) responds by activating a regulatory cascade, leading to the activation of genes necessary for the assembly of the T3SS apparatus (139).

IDENTIFICATION OF THE *aexU* GENE IN *AEROMONAS HYDROPHILA* SSU

Cloning of the *aexU* gene from *A. hydrophila* SSU

The T3SS operon of *A. hydrophila* SSU contains 26,855 bp, encoding 35 genes (123). When compared with the T3SS genes of *A. salmonicida* and *Y. enterocolitica*,



Figure 1.3: Genetic organization of the 4150 bp DNA fragment of *A. hydrophila* cloned in the plasmid pBlue-aexU. Diagram of ORFs from a plasmid obtained after screening chromosomal DNA of *A. hydrophila* with the *aexT* gene probe. ORF1: portion of amino acid permease, ORF2: homolog of YopE chaperon SycE, ORF3: AexT homolog of AexU, ORF4: a hypothetical protein. ORFs are not drawn to scale.

conservation was observed in some genes of *A. hydrophila* SSU, however, the sequences differed significantly in certain genes.

Based on Southern blot analysis using *A. salmonicida aexT* (encodes a T3SS effector protein) gene probe under low-stringency conditions, a 4.2-kb band was

SSUAexU	MQIQHTHTSGLQAVAQHNDATAEVGRLGQLEARQVATSQDALQLGNRSEPQKGQGLLSRLG	60
HM21AexU	MQIQANTVGTQAVAHSDATTGVGQMGLQLEARQVATGQDAILLGNRSEPQKGQGLSRSE	60
AexT	MQIQANTVGTQAVAHSDATTGVGRMGQMEARQVATGQDAILLGSRSEPQKGQGLLSRLG	60
	**** * * * * *	
SSUAexU	AQLARPFVALKEWIGNLLGARSEAPAHSAAPPADSLSLADQKRLLLQKALPFTLGGLDKAN	120
HM21AexU	SRPARVLAAIKIEWIGNLLGSGKSAAAPKVQTATSP--EDLQRLMKQAAFSSSLGGFAKAD	118
AexT	AQLARPFVAIKIEWISNLLGTDKRAAPKAQTAVSP--EDLQRLMKQAAFSSSLGGFAKAD	118
	** * * * * *	
SSUAexU	ELNNIDAQQQLGQEHARLATGNGALRSLATSLNGIKDGSMRQESQTLAAGLLERPIAGIPL	180
HM21AexU	VLNNIAAEQLGKDHAATLATGNGPLRSLCTALQAVVVGSEQPQLRELAAGLLARPIAGIPL	178
AexT	VLNNITGEQLGKDHASLATGNGPLRSLCTALQAVVIGSQPQLRELATGLLARPIAGIPL	178
	**** * * * * *	
SSUAexU	QQWGTGGKVTIELIANATPEQLQEAMSQLHAVMAEVADLQRAVKAEVAGEPLP-AVTSAE	239
HM21AexU	QQWGTGGKVTIELLASATPELLQEAMSQLHTAMGEVADLQRAVKAIEIAGEPAQSATTKAD	238
AexT	QQWGSVGGKVTIELTSAPPELLKEAMSQLHTAMGEVADLQRAVKAEVAGEPARSATTAAA	238
	**** * * * * *	
SSUAexU	VVAAPHGEAKPAARETVAMARQTEVTGYKQALELISYQASYLLRDQASTEVTLSDDLNA	299
HM21AexU	AAPVQSGESKGAAREQVAMARQTPATGYKLALDLISYQASYLLRDQTSTEVTLSSDDLNA	298
AexT	VAPLQSGESE--VNVEPADKALAEGLQEQLGEAEQYLGEQPHGTYSDAEVMALGLYTNG	296
	** * * * *	
SSUAexU	LHQHIADGSINGSHMAKLQTRGDLQILRTLALSLASGSDANGASLGNALDSLASARPNQR	359
HM21AexU	LHQHIADGSINSSHMAKLQTRGDLQTLRTLALSLASGSDAKGSSSLGHALDSLASVRPNQR	358
AexT	EYQHLNRSRLRQEKQLDAGQALIDQGMSTAFKSTPTEQLIKTFRGTHGGDAFNEVAEQV	356
	** * * * *	
SSUAexU	LVLGGLMQFAGQTDQAWADQTAGKP-EDRLDAGARLRFDTGHMKAELARLDDSAARQVLQ	418
HM21AexU	LVLGGLMQFAGQTEQAWVDHTALKPREERLDAGARLRFDTGHMKAELGRLGDSEARQVLQ	418
AexT	GHDVAYLSTSRDPKVATNFGSGSISTIFGRSGIDVSDISVEGDEQEILYNKETDMRVLL	416
	* * *	
SSUAexU	QLEGDFGDRAKAVCDFAVAQVSTFADSESSPEAVLVSRLTRMGNLVGSGLTDELKVRLQLP	478
HM21AexU	QLEGAFGDRAAICDFAVAQVSGFADSESSPEAVLVSRLTRMGNLVGSGLTALKERLQLP	478
AexT	SAKDERGVTRRVLEEASLGEQSGHSGKGLLDG-----LDLARG	453
	* * *	
SSUAexU	ESARGEPTMIDSVSQLTPLELAALAHIGVGADYL	512
HM21AexU	ESARGEPTMIDSVSQLTPLELAALAHIGVDESYL	512
AexT	AGGADKPQEQRIRLKMRLDLA-----	475
	* * * *	

Figure 1.4: Amino acid sequence comparison between AexU and AexT. Comparison of amino acid sequence of AexU from *A. hydrophila* SSU, AexU from *A. veronii* HM21 and AexT from *A. salmonicida*. * Denotes fully conserved amino acid residues.

visualized when the chromosomal DNA of *A. hydrophila* SSU was digested with *Xma*I restriction enzyme. Subsequently, DNA fragments were recovered in the size range of 3.8 to 4.6 kb, and ligated into a pBluescript vector at the *Xma*I site to generate a plasmid library in *Escherichia coli* DH5 α (123).

By screening this library with the *aexT* gene probe, 5 positive clones were obtained from a total of 350 colonies screened. The DNA sequence from one of this recombinant plasmid (designated as pBlueaexU) contained a 4,150-bp DNA fragment with 4 opening read frames (ORFs). The ORF1 (position 1 to 818 bp) represented a portion of the amino acid permease gene; the ORF2 (position 1414 to 1770 bp), which was on the complementary DNA strand, encoded a protein that had 38% homology with the YopE chaperone SycE of *Yersinia*; the ORF3 (position 1969 to 3507 bp) revealed a 39% identity with the *aexT* gene from *A. salmonicida*, and the ORF4 (position 3605 to 4081 bp) on the complementary DNA strand encoded a hypothetical protein (**Figure 1.3**) (123).

The ORF3 (designated as AexU) encoded a protein of 512 aa residues. The NH₂-terminus of AexU (aa residues 1-231) shared 24%, 67%, and 54% homology with the YopE of *Y. enterocolitica*, the NH₂-terminus of AexT from *A. salmonicida*, and the NH₂-terminus of ExoT from *P. aeruginosa*, respectively. However, the COOH-terminus of this protein (aa residues 232-512) differed entirely from that of AexT of *A. salmonicida* (**Figure 1.4**) and had no sequence similarity to any known protein in the database.

AexU is secreted and translocated via T3SS

Based on DNA sequence analysis, several pieces of evidence suggested that the expression and secretion of AexU were coupled to the T3SS. First, the T3SS effectors usually are genetically linked with their chaperones (38, 63). In *A. hydrophila* SSU, the ORF2, which was only 200 bp upstream of the *aexU* gene, encoded a protein that had homology with the YopE chaperone SycE (**Figure 1.3**). Second, a DNA consensus sequence (TGCAAAAA) which is required for binding of the master T3SS transcriptional activator ExsA of *P. aeruginosa*, was identified upstream of the *aexU*

gene (18, 54), and finally ExsA homolog AscA was identified in the T3SS operon of *A. hydrophila* (122).

To confirm that AexU was indeed secreted through the T3SS, human colonic epithelial cells (HT-29) were exposed to the WT *A. hydrophila* and its various mutants. After 2 h infection, the HT-29 cells were osmotically lysed with water and fractionated into soluble and insoluble fractions. As shown in **Figure 1.5** Panel I, AexU was detected in the bacterial cell pellet fraction (lanes 1-7) from all of the tested strains except for the $\Delta aexU$ mutant (lane 5). The secreted form of AexU (lanes 8-14) was detected in the tissue culture supernatant of HT-29 cells infected with only the $\Delta acrV$ mutant (lane 11), and the translocated form of AexU (lanes 15-21) was observed from the WT (lane 15), $\Delta aopB$ (lane 17), $\Delta acrV$ (lane 18), and $\Delta aexU/C$ (lane 20), but not from the $\Delta ascV$ (lane 16) and $\Delta aexU$ (lane 19)-infected host cells. The *ascV* gene of *A. hydrophila* represents an *yscV* homolog of *Yersinia* spp, which encodes an inner-membrane component of the T3SS channel, and deletion of the *ascV* gene blocked the entire T3SS secretion channel (20). Therefore, the inability of AexU to be translocated in the $\Delta ascV$ mutant (lane 16) indicated that this effector was secreted and translocated via the T3SS.

Antibodies to calnexin (CNX), β -actin, and DnaK were used as fractionation controls. The CNX is a 90-kDa integral protein of the endoplasmic reticulum and linked to the membrane fraction of eukaryotic cells, while the non-polymerized actin (45 kDa) is associated with the cytoplasmic fraction. However, the polymerized actin forms filament that is attached to the membrane fraction. The DnaK is a 70 kDa heat shock protein which is conserved among many bacteria and was used to show how intact the bacterial cells were (37, 43). As shown in **Figure 1.5** Panel II, CNX was only detected in the insoluble fraction (lanes 1-7), while actin was primarily associated with the soluble fraction (lanes 15-21). Only a small amount of actin was detected in the insoluble fraction

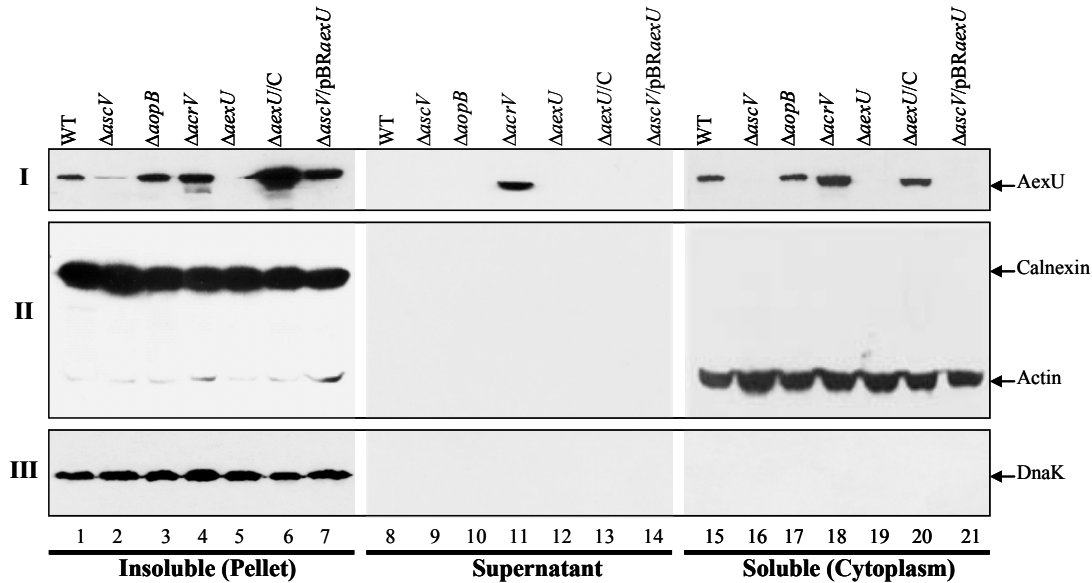


Figure 1.5: Translocation of AexU from *A. hydrophila* SSU. HT-29 human colonic epithelial cells were infected with different *A. hydrophila* strains (MOI of 10) for 2 h at 37°C. The culture supernatants were collected, filtered and TCA precipitated (supernatant). The infected host cells were osmotically lysed with water and centrifuged to separate soluble (cytoplasm) and insoluble (pellet) fractions. The collected samples were run on an SDS-10% PAGE and subjected to Western blot analyses using antibodies to AexU (Panel I), Calnexin and actin (Panel II), and to DnaK (Panel III). Lanes 1, 8 and 15: WT *A. hydrophila*; Lanes 2, 9 and 16: $\Delta ascV$ mutant; Lanes 3, 10 and 17: $\Delta aopB$ mutant; Lanes 4, 11 and 18: $\Delta acrV$ mutant; Lanes 5, 12 and 19: $\Delta aexU$ mutant; Lanes 6, 13 and 20: $\Delta aexU/C$ complemented strain; Lanes 7, 14 and 21: $\Delta ascV/pBRaexU$. “Reprinted from Microbial Pathogenesis, Vol 43 (4), Sha J, Wang SF, Suarez G, Sierra JC, Fadl AA, Erova TE, Foltz SM, Khajanchi BK, Silver A, Graf J, Schein CH, Chopra AK., Further characterization of a type III secretion system (T3SS) and of a new effector protein from a clinical isolate of *Aeromonas hydrophila*--part I., Pages 127-146, © Copyright (2007), with permission from Elsevier.”

(lanes 1-7). Further, DnaK could only be detected in the fraction associated with bacterial cells (Panel III, lanes 1-7) but not in the supernatant and soluble fractions (Panel III, lanes 8-21). These data indicated that CNX, actin, and DnaK were fractionated into their expected locations in the experiment.

To further study translocation of AexU in different bacterial mutant strains, the COOH-terminus of full length AexU was fused in-frame with a 13-aa residue glycogen synthase kinase (GSK) tag (60). The GSK-tagged protein is not phosphorylated when inside the bacteria; however, translocation of a GSK-tagged protein into eukaryotic cells resulted in host cell protein kinase-dependent phosphorylation of the tag at a specific serine residue, which could subsequently be detected with phosphospecific GSK antibodies (60).

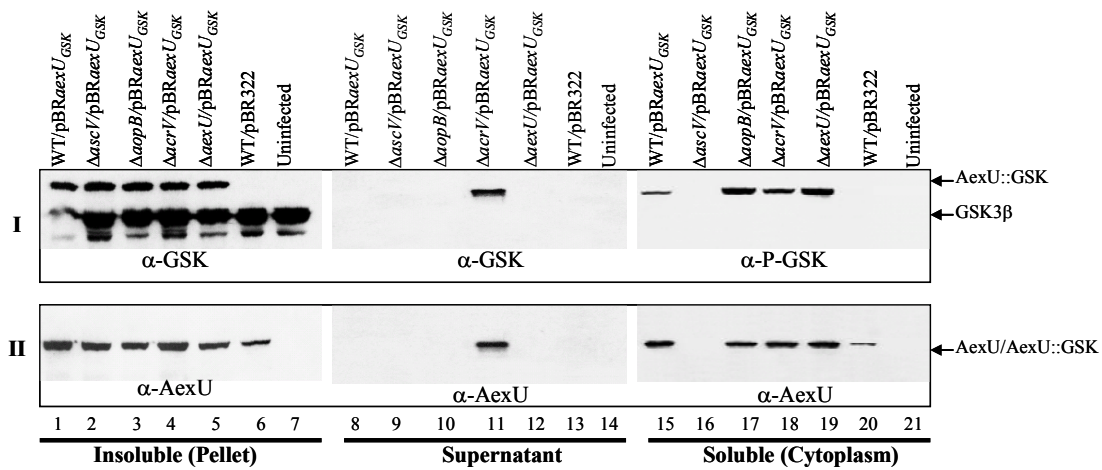


Figure 1.6: Translocation of GSK-tagged AexU (AexU::GSK) from *A. hydrophila* SSU. HT-29 human colonic epithelial cells were infected with different *A. hydrophila* strains transformed with the plasmid pBRaexUGSK (MOI of 10) for 2 h at 37°C. The culture supernatants were collected, filtered and TCA precipitated (supernatant). The infected host cells were osmotically lysed with water and centrifuged to separate soluble (cytoplasm) and insoluble (pellet) fractions. The collected samples were run on an SDS-10% PAGE and subjected to Western blot analyses with antibodies to GSK-3β (Panel I, lanes 1-14), phosphospecific GSK-3β (Panel I, lanes 15-21) and AexU (Panel II), the latter detected both native and GSK-tagged AexU. Lanes 1, 8 and 15: WT/pBRaexUGSK; Lanes 2, 9 and 16: ΔascV/pBRaexUGSK; Lanes 3, 10 and 17: ΔaopB/pBRaexUGSK; Lanes 4, 11 and 18: ΔacrV/pBRaexUGSK; Lanes 5, 12 and 19: ΔaexU/pBRaexUGSK; Lanes 6, 13 and 20: WT/pBR322; Lanes 7, 14 and 21: Uninfected cells. The GSK-3β from HT-29 cells was shown as a control to demonstrate specificity of the GSK antibodies. “Reprinted from Microbial Pathogenesis, Vol 43 (4), Sha J, Wang SF, Suarez G, Sierra JC, Fadl AA, Erova TE, Foltz SM, Khajanchi BK, Silver A, Graf J, Schein CH, Chopra AK., Further characterization of a type III secretion system (T3SS) and of a new effector protein from a clinical isolate of *Aeromonas hydrophila*—part I., Pages 127-146, © Copyright (2007), with permission from Elsevier.”

As shown in **Figure 1.6 Panel I**, non-phosphorylated and/or phosphorylated forms of GSK-tagged AexU (AexU::GSK) were detected from the WT/pBRaexUGSK (lanes 1 and 15), ΔaopB/pBRaexUGSK (lanes 3 and 17), ΔacrV/pBRaexUGSK (lanes 4 and 18), and ΔaexU/pBRaexUGSK (lanes 5 and 19) infected groups of HT-29 cells. The ability to detect phosphorylated AexU::GSK suggested translocation of AexU::GSK in these groups of host cells infected with the designated mutants. As noted, only the non-phosphorylated form of AexU::GSK was detected from the ΔascV/pBRaexUGSK infected HT-29 cells (Panel I, lanes 2 and 16), indicating the translocation of AexU::GSK was

blocked in the $\Delta ascV$ mutant. The secretion of AexU::GSK was detected only in the supernatant of $\Delta acrV$ /pBRAexU_{GSK} infected HT-29 cells (lane 11). These data are in agreement with the results shown in **Figure 1.5**. The AexU::GSK was not detected from the control groups in which HT-29 cells were either infected with the WT/pBR322 or were not infected (lanes 6, 7, 20 and 21). Anti-AexU antibodies were also employed to probe the blots (panel II), and a similar pattern as shown in panel I was obtained except that the native form of AexU was detected in the insoluble and soluble fractions from the WT/pBR322 infected HT-29 cells (Panel II, lanes 6 and 20). The GSK-3 β from HT-29 cells reacted with anti-GSK antibodies (panel I, lanes 1-7) but not with its phosphospecific antibodies (panel I, lanes 15-21), indicating specificity of the GSK

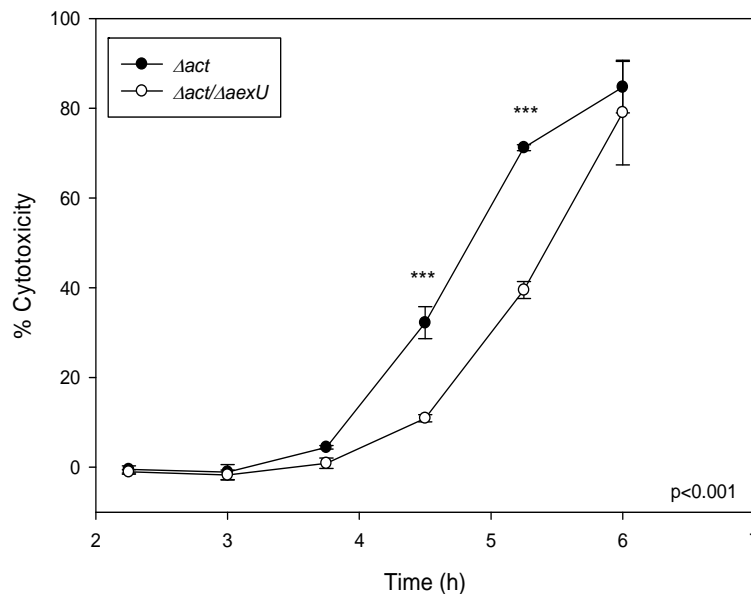


Figure 1.7: AexU-associated cytotoxicity. HeLa cells were infected with the $\Delta act/\Delta aexU$ double-knockout mutant (open circles) and its parent strain Δact (solid circles) at an MOI of 0.5 for about 6 h. At various time points during the infection, cytotoxicity was measured by the lactate dehydrogenase (LDH) enzyme release assay. “***” Denotes statistically significant values ($p \leq 0.001$) compared to the parental strain Δact using Student's t test. Three independent experiments in duplicate wells were performed. “Reprinted from Microbial Pathogenesis, Vol 43 (4), Sha J, Wang SF, Suarez G, Sierra JC, Fadl AA, Erova TE, Foltz SM, Khajanchi BK, Silver A, Graf J, Schein CH, Chopra AK., Further characterization of a type III secretion system (T3SS) and of a new effector protein from a clinical isolate of *Aeromonas hydrophila*--part I., Pages 127-146, © Copyright (2007), with permission from Elsevier.”

antibodies.

Effects of AexU on cytotoxicity and phagocytosis

To test for cytotoxicity associated with AexU, RAW264.7 murine macrophages, along with both HT-29 and HeLa cells were infected with various *Aeromonas* strains at a MOI of 0.5. There were not apparent differences between the WT bacterium and its $\Delta aexU$ mutant in terms of their ability to induce cell morphological changes and cytotoxicity in host cells as measured by the release of lactate dehydrogenase (LDH) enzyme (data not shown). However, compared to its parental Δact strain (142), the double knockout mutant $\Delta act/\Delta aexU$ was significantly less cytotoxic to the HeLa cells, a finding that was most pronounced up to 5.5 h of infection (**Figure 1.7**). These data indicated a masking effect caused by the cytotoxic nature of Act (122, 142).

In the phagocytosis assay, macrophages engulfed approximately 11% and 10.4% of bacteria in $\Delta ascV$ - and $\Delta aopB/\Delta aexU$ -infected cells, while only 2.8% and 2.9% of the $\Delta aopB$ mutant and $\Delta aopB/\Delta aexU$ -complemented strain, respectively, were taken up by the phagocytes (**Figure 1.8**). These data indicated that AexU had an anti-phagocytic activity. Importantly, as T3SS effectors only exhibited their biological functions when they were translocated into eukaryotic cells (38, 104, 135), the phagocytosis data were in agreement with the findings that the $\Delta aopB$ mutant was still able to translocate AexU into eukaryotic cells (**Figures 1.5 and 1.6**). As no difference was observed between the T3SS secretion channel negative mutant $\Delta ascV$ and the double-knockout mutant $\Delta aopB/\Delta aexU$, in term of phagocytosis (**Figure 1.8**), it appeared that AexU was mainly responsible for anti-phagocytic activity.

AexU contributes to the virulence of *A. hydrophila* SSU in mice

To assess the role of AexU during *A. hydrophila* infections, mice were infected with WT *A. hydrophila*, with and without the pBR322 vector, the $\Delta aexU$ toxin mutant and its complemented strain $\Delta aexU/C$. Between 90 to 100% of the animals infected with the WT *A. hydrophila* SSU died at a 2-3 LD₅₀s dose within 48 h. However, mice infected with the $\Delta aexU$ mutant revealed a 60% survival rate (**Figure 1.9**), indicating AexU contributed to the virulence of *A. hydrophila*. Then, mice were immunized with rAexU for one month and challenged with a 2-3 LD₅₀ dose of WT *A. hydrophila*. As shown in

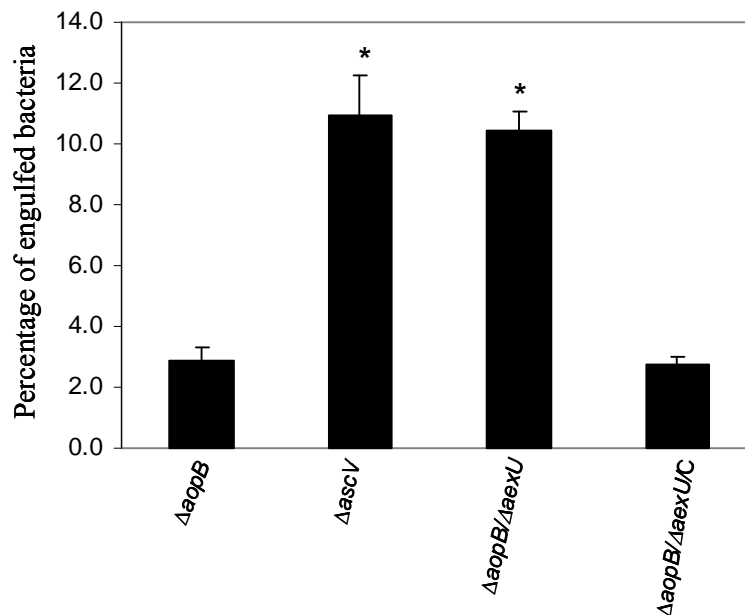


Figure 1.8: Anti-phagocytic activity of AexU. RAW264.7 murine macrophages were infected with different *A. hydrophila* strains (MOI of 0.5): the single- knockout mutants $\Delta aopB$ and $\Delta ascV$, the double-knockout mutant $\Delta aopB/\Delta aexU$ and its complemented strain $\Delta aopB/\Delta aexU/C$. Three hours after infection, the infected phagocytes were washed and treated with 200 μ g/ml of gentamicin for 1 h. Subsequently, the macrophages were washed with PBS and lysed with 1% TX-100 to release intracellular bacteria. The bacteria were titrated, and the percentage of phagocytosis was calculated by dividing the viable bacterial count after gentamicin treatment by the initial bacterial count. The values are the arithmetic means \pm S.D. from three independent experiments (shown as percentage of engulfed bacteria). “*” Denotes statistically significant values ($p \leq 0.05$) when compared with the $\Delta aopB$ mutant using the Student’s t test. “Reprinted from Microbial Pathogenesis, Vol 43 (4), Sha J, Wang SF, Suarez G, Sierra JC, Fadl AA, Erova TE, Foltz SM, Khajanchi BK, Silver A, Graf J, Schein CH, Chopra AK., Further characterization of a type III secretion system (T3SS) and of a new effector protein from a clinical isolate of *Aeromonas hydrophila*--part I., Pages 127-146, © Copyright (2007), with permission from Elsevier.”

Figure 1.10, mice immunized with rAexU were 100% protected. In contrast, 90% of the mice died in the unimmunized group (**Figure 1.10**).

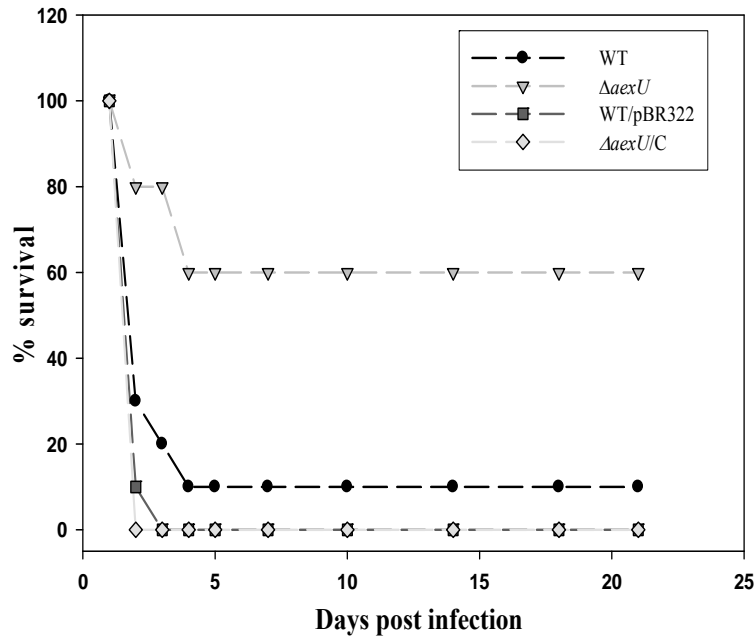


Figure 1.9: The role of AexU during *A. hydrophila* infection in a septicemic mouse model. Groups of 10 Swiss Webster mice were infected i.p. with WT *A. hydrophila* (solid dots), WT *A. hydrophila* transformed with plasmid pBR322 alone (square), $\Delta aexU$ mutant (triangle), and its complemented strain $\Delta aexU/C$ (diamond). Deaths were recorded for 3 weeks post-infection. The bacterial doses used represented approximately 2-3 LD50s of WT *A. hydrophila*. “*” Denotes statistically significant values ($p \leq 0.05$) compared to the WT bacterium using Fisher’s exact test. Three independent experiments were performed, and data from a typical experiment are shown. “Reprinted from Microbial Pathogenesis, Vol 43 (4), Sha J, Wang SF, Suarez G, Sierra JC, Fadl AA, Erova TE, Foltz SM, Khajanchi BK, Silver A, Graf J, Schein CH, Chopra AK., Further characterization of a type III secretion system (T3SS) and of a new effector protein from a clinical isolate of *Aeromonas hydrophila*--part I., Pages 127-146, © Copyright (2007), with permission from Elsevier.”

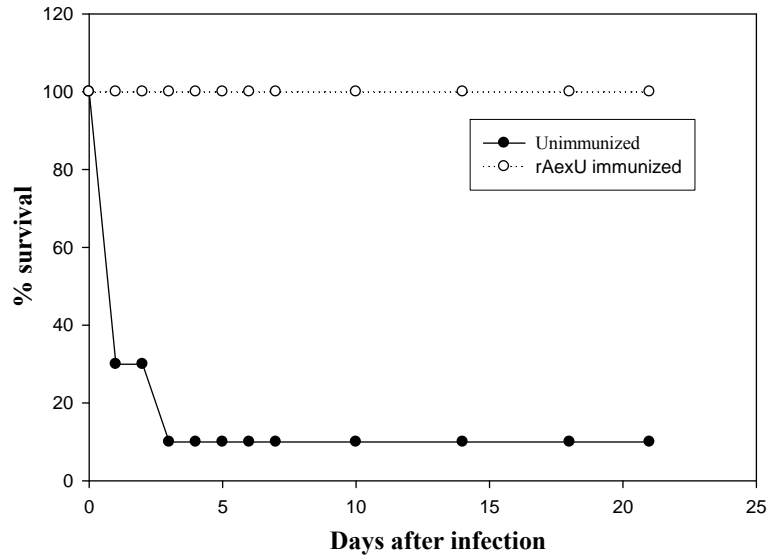


Figure 1.10: Immunization of mice with rAexU. 10 Swiss Webster mice were immunized i.p. with 10 μ g of purified rAexU (open circle) before challenge with the WT *A. hydrophila* at a dose of 2-3 LD₅₀s. A group of 10 unimmunized mice that were given the adjuvant alone were used as a control (solid circle) before challenge with the WT bacterium. Deaths were recorded for 3 weeks post-infection. “*” Denotes statistically significant values ($p \leq 0.05$) compared to unimmunized group of mice using the Fisher’s exact test. Three independent experiments were performed, and data from a typical experiment are shown. “Reprinted from Microbial Pathogenesis, Vol 43 (4), Sha J, Wang SF, Suarez G, Sierra JC, Fadl AA, Erova TE, Foltz SM, Khajanchi BK, Silver A, Graf J, Schein CH, Chopra AK., Further characterization of a type III secretion system (T3SS) and of a new effector protein from a clinical isolate of *Aeromonas hydrophila*--part I., Pages 127-146, © Copyright (2007), with permission from Elsevier.”

Chapter 2: Materials and Methods

CELL LINES AND TRANSFECTIONS

HT-29, a human colonic intestinal epithelial cell line, was obtained from American Type Culture Collection (Manassas, VA). HeLa Tet-OffTM, a human cervical epithelial cell line, was obtained from Clontech (Mountain View, CA). Cells were grown in Dulbecco's modified eagle medium (DMEM) with high glucose (Invitrogen-Gibco, Carlsbad, CA), supplemented with 10% fetal bovine serum (FBS) Tet approved (Clontech) and 100 µg/ml of G-418 (Cellgro, Herndon, VA) under standard tissue culture conditions at 37°C and 5% CO₂ in a humid atmosphere.

HeLa Tet-offTM cells were stably transfected with a plasmid containing tetracycline-controlled transactivator (tTA) (Clontech). The cells were subsequently transfected by electroporation with a pBI-EGFP plasmid (Clontech) containing a bidirectional promoter (Tetracycline Response Element, TRE) that separately controls expression of the gene encoding EGFP (enhanced green fluorescent protein) and the gene of interest. In the HeLa Tet-OffTM system, addition of tetracycline or doxycycline prevents the binding of tTA to TRE, thus inhibiting any expression of the gene of interest and that of EGFP. The DNA fragments encoding the full-length (512 aa residues), NH₂-terminus (aa residues 1-231), COOH-terminal domain (aa residues 232-512), and the mutated versions [ADPRT123⁻ (with no ADP Ribosyltransferase activity) or GAP⁻ (with no GTPase activating protein activity)] of AexU were cloned at the *NheI* and *MluI* restriction enzyme sites of the vector pBI-EGFP. The efficiency of transfection was determined as the percentage of cells expressing the gene coding for EGFP by fluorescent microscopy (Axiovert 200M, Carl Zeiss, Thornwood, NY) and flow cytometry (FACScan, Becton Dickinson, San Diego, CA). HeLa Tet-Off cells transfected with the

pBI-EGFP vector alone (without any insert) served as a negative control. Western blot analysis and flow cytometry, as well as confocal microscopy after intracellular staining using specific antibodies, were also performed to examine the production of the various forms of AexU in HeLa Tet-Off cells.

BACTERIAL CULTURES AND VECTORS

Escherichia coli HMS174-DE3 cells (with IPTG-inducible *lac* promoter-based bacteriophage T7 RNA polymerase gene on the chromosome) were obtained from Novagen (Madison, WI). These cells were grown, after transformation with appropriate recombinant plasmid DNA (in pET-30a vector with the bacteriophage T7 promoter gene), in Luria Bertani (LB) medium supplemented with 100 µg/ml of kanamycin (Sigma St. Louis, MO) at 37°C with continuous shaking (180 rpm). The plasmid DNA was isolated from *E. coli* DH5α clones transformed with pBI-EGFP recombinant plasmids, which were grown in LB medium supplemented with ampicillin (100 µg/ml) at 37°C with continuous shaking (180 rpm). The genes encoding the full-length, NH₂-terminus, or COOH-terminus of AexU were cloned into a bacteriophage T7 RNA polymerase/promoter-based pET-30a vector for hyper-expression and purification purposes. Briefly, the appropriate DNA fragments were cloned at the *Xho*I and *Bgl*II restriction enzyme sites of the vector pET-30a, resulting in fusion of the various forms of AexU at the NH₂-terminal end with the histidine (His)-tag.

A. hydrophila SSU, a diarrheal isolate, was grown in LB medium supplemented with 100 µg/ml rifamicin (a spontaneous antibiotic-resistant strain) (123). The single deletion isogenic mutant strains, namely Δact and $\Delta aexU$, were grown in the presence of 100 µg/ml kanamycin, while the $\Delta act/\Delta aexU$ double isogenic mutant was cultivated in the presence of both kanamycin and 40 µg/ml each of spectinomycin and streptomycin (123).

ELECTROPORATION

For electroporation of *E. coli* cells with various plasmids, 1 ml of bacterial cultures in LB medium was washed 3 times in chilled, sterile water followed by 1 wash in chilled 10% glycerol. The cells were resuspended in 10% glycerol, mixed with 100 ng of appropriate plasmids and electroporated in a Gene Pulser Xcell (BioRad, Hercules, CA) using an exponential protocol at 3000 V, capacitance of 25 μ F, and resistance of 200 Ω in 2 mm cuvettes (BioRad). After electroporation, the cells were allowed to recover in 2 ml of LB medium without antibiotics for 1 h. Subsequently, the cells were plated on LB agar plates containing appropriate antibiotics and grown overnight. Well-isolated colonies were then selected and grown in LB medium with appropriate antibiotics. The plasmid DNA was isolated using QIAprep® Miniprep Kit (Qiagen, Inc., Valencia, CA) and subjected to restriction enzyme analysis and DNA sequencing at the Biomolecular Resource Facility at UTMB to confirm target gene sequences.

For electroporation of HeLa Tet-Off cells, they were grown in T75 flasks to ~70-80% confluency. The cells were detached using 0.25% trypsin-EDTA (Invitrogen-Gibco) and washed 3 times in chilled DMEM without serum, before resuspending in chilled serum-free DMEM at a density of 5×10^6 cells/ml. The various plasmids (100 ng) were then transfected by electroporation using an exponential protocol at a voltage of 350, capacitance of 950 μ F and unlimited resistance ($\infty \Omega$) in 4 mm cuvettes (BioRad). The cells were then recovered in complete medium (DMEM/10% FBS/G-418), plated, and grown under standard tissue culture conditions.

SITE-DIRECTED MUTAGENESIS OF THE *aexU* GENE

To obtain different mutated versions of the *aexU* gene, I used the Altered Sites *in vitro* Mutagenesis System (Promega, Madison, WI). The encoding region of the gene for native AexU was amplified by polymerase chain reaction (PCR) and by using the primers

listed in **Table 1**. This gene was then cloned into the pALTER-1 vector, which is tetracycline resistant (Tc^R) and ampicillin sensitive (Ap^S), and used to transform *E. coli* JM109 cells, which subsequently were infected with the R408 helper phage. The phagemic, single-stranded DNA was isolated by following the manufacturer's instructions. This DNA was used as a template for the mutagenesis reaction with different mutagenic primers (**Table 1**). For generating the ADPRT123⁻ mutated version of AexU, consecutive rounds of mutations were performed using the three mutagenic primers. Each mutagenesis reaction generated a different mutated form of the *aexU* gene in pALTER-1, which was then transformed into *E. coli* ES1301 *mutS*-competent cells. Plasmid DNA was isolated from *E. coli* ES1301 cells and then transformed into *E. coli* JM109 cells which were screened for Tc^S and Ap^R phenotype. All of the mutations were confirmed by DNA sequence analysis. In the ADPRT123⁻ mutated AexU, following mutations were made E30A, E263A, and E421A (**Figure 3.2**).

Table 1: Primers used for cloning and site-directed mutagenesis of AexU.

Primer name	Sequence	Purpose
<i>aexU</i> -EcoRI <i>aexU</i> -BamHI	5'-CCGGAATTCATGCAGATTCAAACACATACCAGC-3' 5'-CGCGGATCCTTACAGATAGTCAGCCCCGACACCG-3'	PCR amplification of the full length <i>aexU</i> gene for cloning in pALTER
<i>aexU</i> -E30A	5'-GGCCAGCTG <u>gcc</u> GCTCGTCAGG -3'	Mutagenic oligonucleotide to replace glutamate at position 30 by alanine
<i>aexU</i> -E263A	5'-GCGCCAGACC <u>gcc</u> GTCACCGGTT-3'	Mutagenic oligonucleotide to replace glutamate at position 263 by alanine
<i>aexU</i> -E421A	5'-GCAACAGCTG <u>gcc</u> GGGGATTTTG -3'	Mutagenic oligonucleotide to replace glutamate at position 421 by alanine
<i>aexU</i> -R145A	5'-TGGCGCCCTG <u>gcc</u> TCGCTGGCA -3'	Mutagenic oligonucleotide to replace arginine at position 145 by alanine
<i>aexU</i> -NheI <i>aexU</i> -SalI	5'-GGTCGCTAGCATGCAGATTCAAACACATACCAGC-3' 5'-GGTCGTCGACTTACAGATAGTCAGCCCCGACACCG-3'	PCR amplification of the full length <i>aexU</i> gene for cloning in pBR322
<i>aexU</i> -MluI <i>aexU</i> -NheI	5'-TCACACGCGTATGCAGATTCAAACACATACCAGC-3' 5'-GGTCGCTAGCTTACAGATAGTCAGCCCCGACACCG-3'	PCR amplification of the full length <i>aexU</i> gene for cloning in pBI-EGFP

Underlining indicates restriction enzyme sites in the primers. Lower case and underlining indicate the codon used to replace glutamate by alanine or arginine by alanine.

COMPLEMENTATION OF THE *A. HYDROPHILA* SSU $\Delta act/\Delta aexU$ ISOGENIC MUTANT *IN TRANS* WITH THE NATIVE *aexU* OR *aexU* DEVOID OF ADPRT OR GAP AND/OR BOTH ACTIVITIES

The genes encoding the native and mutated versions of AexU (e.g., ADPRT123⁻, GAP⁻ and ADPRT123⁻/GAP⁻) were PCR amplified from the pALTER plasmids prepared for the site directed mutagenesis using primers listed in Table 1. These DNA fragments were cloned in the pBR322 vector at *SalI* and *EcoRI* sites and transformed into *E. coli* DH5 α cells. The pBR322-*aexU*_{native}, pBR322-*aexU*_{ADPRT123⁻}, pBR322-*aexU*_{GAP⁻}, and pBR322-*aexU*_{ADPRT123⁻/GAP⁻} recombinant plasmids (Tc^s and Ap^r) were isolated from the corresponding *E. coli* strains and electroporated in *A. hydrophila* $\Delta act/\Delta aexU$ isogenic mutant. The presence of different plasmids in *A. hydrophila* $\Delta act/\Delta aexU$ isogenic mutant was confirmed by digestion of the isolated plasmid DNA using appropriate restriction endonucleases. The production of various forms of AexU from the pBR322 vector in *A. hydrophila* $\Delta act/\Delta aexU$ isogenic mutant was confirmed by Western blot analysis by using antibodies to AexU, which were previously developed in the laboratory (123).

RECOMBINANT PROTEIN PURIFICATION

Both the full length and COOH-terminus of the *aexU* toxin gene, expressed in *E. coli* from the pET-30a system, were used for purification of the toxin (as a His-tag) and subsequent antibody production. Purification of the toxins was achieved using the Probond™ purification system (Invitrogen-Gibco) following the hybrid protocol as described by the manufacturer. Briefly, after induction with 1 mM IPTG for 4 h, *E. coli* cells (in 100 ml volume) were washed twice in phosphate-buffered saline (PBS). The cells were lysed in binding buffer containing 4 M urea, pH 7.8, overnight at 4°C. The suspension was centrifuged at 7000 rpm for 10 min, and the supernatant was incubated for 30 min to 1 h with nickel resin that was previously stabilized under denaturing

conditions. The resin was washed twice with denaturing binding buffer-4 M urea, pH 7.8, twice with denaturing wash buffer-4 M urea, pH 6.0, and four times with native wash buffer, pH 8.0. The proteins from the column were eluted with 250 mM imidazole. Fractions (1 ml) were collected, and an aliquot (20 μ l) of each fraction, was subjected to sodium dodecyl sulfate (SDS)-10% polyacrylamide gel electrophoresis (PAGE) to verify identity of hyper-produced AexU (full length and its COOH-terminal domain) by performing Coomassie blue staining of the gels. Fractions containing the toxins were mixed and dialyzed against PBS overnight at 4°C. The protein concentration was measured by Bradford Assay (BioRad) and the samples stored at -20°C.

The native full length AexU, its NH₂- and COOH-terminal domains and the mutated versions (ADPRT123⁻ or GAP⁻) were purified for the ADP ribosyltransferase assay following the non-denaturing protocol for the Probond™ purification system (Invitrogen-Gibco). Briefly, cells prepared as described above were sonicated and centrifuged, and the supernatant was incubated with nickel resin that had previously been stabilized for native conditions. The resin was washed four times with native wash buffer, pH 8.0, containing 0.1% Triton X-100, and the proteins were eluted with a gradient of imidazole from 100 mM to 1 M. Fractions were collected and the presence of the various domains of AexU verified by SDS-PAGE and Coomassie blue staining. Fractions containing purified rAexU were mixed and dialyzed against 10 mM phosphate buffer, pH 7.4, overnight at 4°C. The proteins were concentrated using 10 kDa cutoff centricons (Millipore, Bedford, MA) to 1 mg/ml and used immediately for the ADP-ribosylation assay.

ANTIBODY PRODUCTION.

Swiss Webster mice (Taconic Farms, Germantown, NY) were immunized intraperitoneally (i.p.) with 10 μ g of rAexU (10 mice each for full length and its COOH

terminal domain) mixed with a synthetic adjuvant derived from *Salmonella minnesota* monophosphoryl-lipid A (MPL)/ trehalose dicorynomycolate (TDM)/ tubercule bacillus cell wall skeleton (CWS) (Sigma) in 2% Tween 80 at day 0, with a booster dose of respective antigens (10 µg) on day 15. Sera were obtained from mice after bleeding them *via* the retro-orbital route at weeks 2 and 4 after immunization, and the antibody titers were determined by enzyme-linked immunosorbent assay (ELISA) using appropriate rAexU as the source of the antigens.

Briefly, ELISA plates were coated with 100 µl of rAexU (10 ng/mL) in carbonate buffer, pH 9.0, overnight at 4°C. The plates were washed 5X with 300 µl of PBS/0.05% Tween 20, pH 7.6, and then the plates were blocked with 250 µl of 1% bovine serum albumin (BSA) in PBS for 1 h. The sera were diluted in PBS/0.1% BSA in a range from 1:5 to 1:10240 and incubated with the antigen for 1 h at room temperature. Next, the plates were washed 5X, followed by 1 h incubation with horse-radish peroxidase (HRP)-conjugated goat α-mouse IgG (Southern Biotechnology Associates, Inc., Birmingham, AL) at a dilution of 1:5000, and 100 µl of 3,3',5,5'-tetramethyl-benzidine (TMB, Sigma) was used as the substrate. The reaction was stopped with 50 µl of 1 N H₂SO₄ and the plates were read at 450 nm in a VERSAmax tunable microplate reader (Molecular Devices Corporation, Sunnyvale, CA). Dilutions of the sera that were in the middle of the logarithmic portion (~1:1000) of the ELISA titration curves were tested for their reactivity to the respective antigens by performing Western blot analysis.

ADP-RIBOSYLTRANSFERASE ASSAYS

The reaction mixture for each sample contained 100 µM of nicotinamide [U-¹⁴C] adenine dinucleotide (specific activity 265 mCi/mmol) (GE Healthcare, Piscataway, NJ) and 0.2 M sodium acetate buffer, pH 6.0, in a total volume of 20 µl. HT-29 cells (5 x 10⁷ cells/ml) were sonicated for 4 cycles of 10 sec each on ice at 80 W in sodium acetate

buffer, pH 6.0, and 4 μ l was added to the reaction mixture for each sample. The reaction was started by the addition of whole cell lysates from *E. coli* hyper-producing the full-length, NH₂-terminus, or COOH-terminal domain of AexU or 4 μ g of their respective purified protein. After incubation at room temperature for 1 h, the reaction was stopped with trichloroacetic acid (TCA, final concentration 10%) in 0.2 M sodium acetate, pH 6.0, and the mixture blotted onto nitrocellulose membranes and allowed to dry. The membranes were washed 5X with 10% TCA and again air-dried before adding 5 ml of scintillation liquid (ScintiVerse, Fisher Scientific, Pittsburgh, PA) and the radioactivity measured as counts per minute using a liquid scintillation counter (LS 6500, Beckman Coulter, Inc. Fullerton, CA). Background radioactive counts from the reaction mixture without the rAexU toxins were subtracted from the experimental values to evaluate ADPRT activity of the various forms of the toxin.

Normal HeLa cells were washed twice with ice cold PBS and resuspended in 20 mM Tris-HCl (pH 7.5) containing 1 mM EDTA, 1 mM dithiothreitol (DTT), and 5 mM MgCl₂. HeLa cells were sonicated for 3 cycles of 10 sec each on ice and then centrifuged at 14,000 rpm for 10 min. Protein concentration of the supernatant was measured by the Bradford assay. An aliquot (25 μ g) of the lysates was incubated with 2 μ g of rAexU and 10 μ M of biotinylated NAD (R&D Systems, Minneapolis, MN) for 30 min at 37°C. Additionally, as a positive control, I used 2 μ g of rVegetative Insecticidal Protein (VIP)-2 domain of VgrG1 from *A. hydrophila* ATCC 7966, which is a T6SS effector and recently characterized in our laboratory (132). The reaction mixture without the addition of rAexU served as a negative control in our assays. The reaction was stopped by adding SDS sample buffer, and the samples were subjected to SDS-PAGE and then transferred to a nitrocellulose membrane. After blocking non-specific sites with TBS and 1% bovine serum albumin (BSA), I incubated the membrane with streptavidin-horseradish

peroxidase (HRP), followed by three washes with TBS + 0.1% Tween-20 and substrate addition (ECL Western Blotting Detection, GE Healthcare).

WESTERN BLOT ANALYSIS

For assessment of antibody reactivity in sera, rAexU (2 µg/lane of full length or its COOH terminal domain) was subjected to SDS-10% PAGE and transferred to Hybond™-ECL™ nitrocellulose membranes (GE Healthcare) following the standard Western blot procedure (36). Membranes were cut into strips corresponding to the lanes of the gel, blocked with 1% BSA/5% skim milk, and were subsequently incubated with anti-AexU sera from individual mice (1:1000) diluted in Tris-buffered saline (TBS), pH 7.6, and 0.5% skim milk for 1 h with constant shaking at room temperature. The strips were then incubated for 1 h with secondary antibody (Goat α-mouse IgG [diluted 1:10000] conjugated with HRP [Southern Biotechnology Associates, Inc.]). Five washes of strips were performed between various steps using TBS/0.05% Tween 20 for 10 min each. The blots were developed with Super Signal® West Pico Chemiluminescent substrate (Pierce, Rockford, IL) followed by X-ray film exposure.

Likewise, HeLa cells were lysed in SDS-Tris-Glycine buffer (36) after 24 h of transfection and subjected to electrophoresis and Western blot analysis as described above. Subsequent to blocking of the membranes, they were incubated for 1 h with α-AexU antibodies (a mixture of antibodies [equal amounts] to the full length and COOH-terminal domain; diluted 1:1000). This was followed by incubation with the secondary antibodies and substrate before X-ray film exposure as described above.

The phosphorylation status of c-Jun and IκBα degradation was also confirmed by Western blot analysis. Briefly, HeLa cells were infected (multiplicity of infection [MOI] of 2) with either the Δact or the $\Delta act/\Delta aexU$ mutant strain of *A. hydrophila* SSU for different time points. Cells were washed with PBS and then resuspended in RIPA buffer

(Pierce, Rockford, IL). Samples were subjected to SDS-4-20% PAGE and Western blot analysis. Specific antibodies to β -tubulin, c-Jun, phospho c-Jun (Ser63), and I κ B α were used in these assays.

INTRACELLULAR STAINING

HeLa Tet-Off cells after 24 h of transfection were washed twice in PBS, pH 7.6, and then permeabilized using CytoFixTM/CytoPermTM (Becton Dickinson) for 20 min on ice in the dark. The α -AexU antibody containing hyper-immune serum (diluted 1:100), as well as the pre-immune serum (diluted 1:100), was used as the source of primary antibodies. The antibodies against both the full length and COOH-terminus of AexU were mixed in equal proportion for intracellular staining. After incubation with the cells at room temperature for 2 h, various forms of AexU in HeLa cells were visualized using phycoerythrin (PE)-conjugated α -mouse IgG antibody (Santa Cruz, Santa Cruz, CA) for 1 h. Between steps, the cells were washed 3X with PermwashTM (Becton Dickinson) and centrifuged between washes at 400 x g for 5 min. Finally, the cells were fixed with 2% paraformaldehyde and stored at 4°C in the dark until analyzed. The samples were acquired in a FACScanTM (Becton Dickinson) and analyzed using CellQuestTM (Becton Dickinson) software and WinMDI[®].

For confocal microscopy, cells that were stained for flow cytometric analysis were placed on glass slides and centrifuged, using a Shandon Cytospin cytocentrifuge (Thermo Scientific, Waltham, MA) at 1500 rpm for 5 min. The cover slips were mounted with mounting medium containing DAPI for fluorescence (Vector, Burlingame, CA) and the images acquired in a 1.0 Zeiss LSM 510 UV Meta laser scanning confocal microscope system (Carl Zeiss). For fluorescence microscopy, the cells were placed on glass slides and the images were acquired in a fluorescence microscope (Olympus BX51/DPManager v.1.2.1.107/DPCController v.1.2.1.108, Olympus Optical CO. LTD).

HOST CELL MORPHOLOGY

Changes in the morphology of HeLa cells were visualized under light microscopy, as well as by confocal microscopy using phalloidin staining. Cells electroporated with various constructs expressing different forms of *aexU* gene were grown in a chambered cover glass system (Nalge-Nunc™, Naperville, IL) and stained with Alexa-fluor® 568 phalloidin (Invitrogen-Gibco) following the manufacturer's instructions. Briefly, the cells were fixed with 3.7% buffered formaldehyde for 10 min, followed by incubation with 0.1% Triton X-100 in PBS for 5 min. Then, the samples were incubated with Alexa-fluor® 568 phalloidin (diluted 1:40) for 30 min. Finally, the cells were kept in PBS in the dark at 4°C. Each step was followed by 3 PBS washes. The images were acquired in a 1.0 Zeiss LSM 510 UV Meta laser scanning confocal microscope system.

TRANSMISSION ELECTRON MICROSCOPY

HeLa cell monolayers, after 30 h of transfection with various constructs as described above, were fixed in a mixture of 2.5% formaldehyde and 0.1% glutaraldehyde in 0.05 M of cacodylate buffer, pH 7.2, containing 0.03% trinitrophenol and 0.03% CaCl₂ for 1 h at room temperature. After washing in 0.1 M cacodylate buffer, the cells were scraped and pelleted. The pellets were post-fixed in 1% OsO₄ in 0.1 cacodylate buffer, *en bloc* stained with 2% aqueous uranyl acetate, dehydrated in graded series of ethanol and embedded in Poly/Bed 812 (Polysciences, Warrington, PE). Ultrathin sections were cut on a Reichert-Leica Ultracut S ultramicrotome (Leica, Wetzlar, Germany), stained with lead citrate and examined in a Philips 201 electron microscope (Philips, Eindhoven, The Netherlands) at 60 kV.

HOST CELL APOPTOSIS

Induction of apoptosis in HeLa Tet-Off cells expressing the native or the mutated version of the *aexU* gene was evaluated by detection of cytoplasmic nucleosomes and caspase 3 activation. HeLa Tet-Off cells transfected with the empty vector were treated overnight with 10 μ M camptothecin as a positive control for both the assays. For the detection of nucleosomes, I used the cell death detection ELISA kit (Roche, Indianapolis, IN). Lysates (1×10^5 cells) from the HeLa cells were prepared after 24 h of transfection by following the manufacturer's instructions. The color reaction was measured in a microplate reader at 405 nm.

The caspase 3 activation was evaluated with a colorimetric assay from BioVision Inc. Mountain View, CA). After 24 h of transfection, whole lysates (200 μ g) of HeLa Tet-Off cells were incubated with 50 μ l of 2X reaction buffer containing 10 mM DTT and 5 μ l of peptide substrate (*N*-acetyl-Asp-Glu-Val-Asp-7-amino-4-*p*-nitroalanine [DEVD-pNA]) for 2-24 h at 37°C and read at 405 nm in a microplate reader.

HOST CELL VIABILITY

To determine host cell viability, incorporation of 7-amino actinomycin D (7-AAD) and colorimetric MTT [3-(4,5-dimethylthiazol-2-yl)-2,5-diphenyl tetrasodium bromide] assay for cell survival were performed. For 7-AAD assays, electroporated HeLa cells with various constructs at different time points were detached from the tissue culture plates with 0.25% trypsin-EDTA, washed, and then incubated for 10 min with 7-AAD (5 μ l per tube) (Becton Dickinson). Flow cytometry acquisition was performed immediately after the incubation, and the percentage of positive cells was determined using CellQuest™ software. For MTT assays, HeLa cells at a concentration of 3×10^5 cells/ml were plated in 96-well plates, after transfection with various constructs, and grown under normal tissue culture conditions. After 24 h, 10 μ l (5 mg/ml) of MTT (Chemicon-

Millipore, Billerica, MA) was added and the plates incubated for 3 h at 37°C. Any crystals that formed were dissolved by adding 100 µl of 0.04 N HCl in isopropanol. The color reaction was acquired with a microplate reader at 570 nm.

***IN VITRO* GTP-ASE ACTIVATING PROTEIN ACTIVITY (GAP) ASSAY**

GAP activity of purified native and mutated rAexU was evaluated by using the RhoGAP Assay Biochem Kit (Cytoskeleton, Denver, CO). Small GTPase proteins (Ras, RhoA, Rac1 and Cdc42) were incubated with either 4 µg of rAexU (native and GAP mutant) or 6 µg of p50 Rho GAP as a positive control, reaction buffer, and 200 µM of GTP in a 96-well plate. Additionally, I evaluated the intrinsic activity of the small GTPase proteins and did not detect any significant increase in the absorbance in these samples (absorbance in the range of 0.01). The reaction was incubated for 20 min at 37°C, and then 120 µl of the CytoPhos reagent was added to each well. The color reaction was measured at 650 nm in a microplate reader.

PHOSPHO-PROTEIN DETECTION

Bio-Plex Phosphoprotein Testing Assay (BioRad) was employed for the detection of phosphorylated proteins in HeLa cells infected with various strains of *A. hydrophila*. Briefly, HeLa cells were infected with the WT *A. hydrophila* SSU and its $\Delta aexU$ isogenic mutant strain at a multiplicity of infection (MOI) of 2 for 30, 60 and 90 min. At these time points, the monolayers were intact with minimal number of floating cells. After centrifugation to recover cells in suspension, the supernatants were aspirated. Then the host cells (including the ones in the culture supernatant) were washed with cell wash buffer (BioRad), resuspended in lysis buffer, and processed as described by the manufacturer. The protein concentration of each sample was measured by Lowry's

method (36) and same concentration of proteins (25 μ L of a 500 μ g/mL cell lysate) was used for each sample in the assay.

The phosphorylation status of c-Jun and I κ B α degradation was confirmed by Western blot analysis. HeLa cells were infected (MOI of 2) with either the Δact or the $\Delta act/\Delta aexU$ isogenic mutant strain of *A. hydrophila* SSU for 15, 30, 60 and 120 min. Cells were washed with PBS and then resuspended in RIPA buffer (Pierce, Rockford, IL). Samples were subjected to SDS-4-20% PAGE and Western blot analysis as described earlier. Specific antibodies to c-Jun, phospho c-Jun (Ser63), and I κ B α were used in these assays.

CYTOKINE/CHEMOKINE DETECTION

Normal HeLa cells were infected with either the Δact or the $\Delta act/\Delta aexU$ isogenic mutant strain of *A. hydrophila* SSU at an MOI of 2 at 37°C. After 1 h of incubation, 100 μ g/ml of gentamicin (Cellgro, Manassas, VA) was added to the culture, and the supernatants recovered at 4, 6 and 24 h after the initial infection. IL-6 and IL-8 secretion was measured with a BioPlex Cytokine detection kit (BioRad).

ANIMAL INFECTIONS AND DETECTION OF BACTERIA IN PERIPHERAL TISSUES

Groups of 15 Swiss Webster mice were infected *via* the i.p. route with either the Δact or the $\Delta act/\Delta aexU$ isogenic mutant strain of *A. hydrophila* SSU at a dose of 8×10^5 (representing approximately 1 LD₅₀) colony forming units (cfu) (142). After 24 h and 48 h of infection, five mice from each group were euthanized and a portion of the lungs, livers and the spleens were weighed and homogenized in 1 mL of sterile water for evaluating bacterial load. Serial dilutions of the homogenized tissues were plated on LB agar plates, and after overnight incubation at 37°C, bacteria were enumerated and the results presented as cfu per gram of tissue.

For the animal survival experiments, groups of 10 mice were infected *via* the i.p. route with 3×10^7 cfu of *A. hydrophila* $\Delta act/\Delta aexU$ isogenic mutant complemented *in trans* with either pBR322-*aexU*_{native}, pBR322-*aexU*_{ADPRT123⁻}, pBR322-*aexU*_{GAP⁻} or pBR322-*aexU*_{ADPRT123⁻/GAP⁻} plasmids. Deaths were recorded for 15 days post-infection. In another experiment, animals (n=15) were infected with 3×10^7 cfu of *A. hydrophila* $\Delta act/\Delta aexU$ isogenic mutant complemented with either the native or the ADPRT123⁻/GAP⁻ mutant of AexU. After 48 h of infection, mice were euthanized and a portion of the spleen was weighed and homogenized in 1 mL of sterile water for evaluating bacterial load. An aliquot of the homogenate was also used for the detection of cytokines/chemokines by a multiplex bead array (Millipore).

HISTOPATHOLOGY

In parallel with the detection of the Δact or the $\Delta act/\Delta aexU$ isogenic mutant strain of *A. hydrophila* SSU in peripheral tissues, portions of the tissues were fixed in 10% buffered formalin, mounted on glass slides and stained with hematoxylin and eosin for light microscopic analysis. The lesions were scored based on a scale correlating with the extent of lesion severity: minimal (2-10%), mild (>10-20%), moderate (>20-50%), and severe (>50%).

STATISTICS

The Tukey's multiple comparison test and Bonferroni post-test were used for statistical analyses of the data by using GraphPad Prism (Software MacKiev, San Diego, CA). For animal studies, I used Kaplan-Meier survival estimates for data analysis. Three independent experiments were performed unless otherwise stated, and arithmetic means with standard deviations were plotted.

Chapter 3: Biological Characterization of a New Type III Secretion System Effector from a Clinical Isolate of *Aeromonas hydrophila*¹

INTRODUCTION

Aeromonas species produce a wide range of virulence factors, including hemolysins, cytotoxic and cytotoxic enterotoxins, proteases, lipases, adhesins, and an S-layer (30, 92, 93). More recently a T3SS, which allows bacteria to translocate effector proteins into the cytosol of eukaryotic cells through needle-like structures, was identified in fish and human isolates of *Aeromonas* species (20, 21, 46, 122). While in *A. salmonicida*, the T3SS operon is located on a plasmid, its location is on the chromosome in fish and clinical isolates of *A. hydrophila* (122, 131, 143). T3SS-secreted effector proteins have the ability to affect a variety of different host biological functions, including alteration of intracellular signaling pathways and disruption of the cytoskeleton (46, 122). For example, ExoT/S from *Pseudomonas aeruginosa* and AexT, a homolog of ExoT, in *A. salmonicida*, have been shown to possess ADPRT activity (18, 59). AexT from *A. salmonicida* has also been shown to induce morphological changes in fish cells, including cell rounding and subsequent lysis (18).

Toxin-mediated ADP-ribosylation involves hydrolysis of the substrate nicotinamide adenine dinucleotide (NAD) to nicotinamide and ADP-ribose, and then selective linking of the ADP-ribose to a target protein(s) of the eukaryotic cell (74). In most cases, toxins ADP-ribosylate key regulators of cellular functions and interfere with vital processes that can sometimes lead to host cell death. Some examples include cholera toxin from *Vibrio cholerae*, which ADP-ribosylates small G-proteins in host cells leading

¹ 126. Sierra, J. C., G. Suarez, J. Sha, S. M. Foltz, V. L. Popov, C. L. Galindo, H. R. Garner, and A. K. Chopra. 2007. Biological characterization of a new type III secretion system effector from a clinical isolate of *Aeromonas hydrophila*-part II. *Microb Pathog* 43:147-160.

to alteration in cyclic AMP-associated signaling, ExoS from *P. aeruginosa* that ADP-ribosylates Ras and vimentin leading to cell toxicity, and Iota toxin from *Clostridium perfringens*, which prevents actin polymerization due to actin ADP-ribosylation (5, 74, 130). A common characteristic of ADP-ribosylating toxins is the presence of a conserved glutamate/glutamine residue (E/Q) located two residues upstream of the catalytic glutamate (74). In both EXE and QXE motifs, for instance, the catalytic residue is the C-terminally located glutamate (E) EXE or glutamine (Q) QXE situated two positions upstream of the glutamate (E/Q)XE (74). These specific motifs have been shown to be associated with the ADP ribosyltransferase activity of *C. limosum* exoenzyme C3 and *C. botulinum* C2 toxin (74).

So far, four T3SS effector proteins (AexT, AopP, AopH, and AopO) have been described in *A. salmonicida* (21, 40, 48). Interestingly, all of these effector genes, except for *aexT*, are located on plasmids, and the majority of the clinical isolates of *Aeromonas* species do not possess such extra-chromosomal elements (Chopra *et al.*, unpublished data). Our laboratory recently molecularly characterized a T3SS from a diarrheal isolate SSU of *A. hydrophila* (122). We subsequently reported regulation of the T3SS and existence of a new T3SS effector protein in *A. hydrophila* SSU (123). Our laboratory designated this effector toxin AexU, due to its 67% homology with AexT from *A. salmonicida* at the NH₂-terminal portion (amino acid [aa] residues 1-231). The *aexU* gene is 1,539 bp in length and encodes a protein with 512 aa residues (GenBank accession number **DQ837530**). This new effector protein, AexU, differs entirely from AexT in the COOH-terminal region (aa residues 232-512); and this domain has no homology with any known proteins in the NCBI database.

Here I reported initial characterization of the biological effects induced by AexU from *A. hydrophila* SSU. I demonstrate that ADPRT activity was associated with the full

length, NH₂-terminal, and COOH-terminal domains of AexU toxin, with the NH₂-terminal domain exhibiting ADPRT activity similar to that of the full length protein. Accordingly, I observed rounding of HeLa Tet-Off cells expressing and producing the full length or NH₂-terminal domain of AexU from a pBI-EGFP vector. On the contrary, HeLa cells that produced only the COOH-terminal domain of the toxin exhibited minimal cell rounding. These alterations in cell morphology were related to disruption of actin filament organization, as evidenced by phalloidin staining. In addition, I found increased levels of apoptosis in HeLa Tet-Off cells producing the AexU full length toxin or its NH₂-terminal domain, compared to cells that were transfected with the vector alone or a recombinant plasmid expressing the COOH terminal domain-encoding portion of the toxin.

RESULTS

Purification of rAexU full length and its NH₂-terminal and COOH-terminal domains and antibody production

Our laboratory recently reported that the *aexU* gene from *A. hydrophila* SSU had 39% identity with the *aexT* gene of *A. salmonicida* over the entire length of these two genes (**Figure 3.1**) (123). Based on sequence analysis, I divided AexU into two portions; the NH₂-terminal domain was represented by aa residues 1-231, while the COOH-terminal domain consisted of aa residues 232-512 (**Figure 3.2**). The NH₂-terminal domains of AexT and AexU exhibited a homology of 67%, and the COOH-terminal domains had no similarity (**Figure 3.1**). Further, the homology of AexU with ExoT (54%) from *P. aeruginosa* was also restricted to the NH₂-terminal portion (124). Recombinant toxins were over-produced (full length, and its NH₂- and COOH-terminal domains) as His-tag fusion proteins in *E. coli* using the pET-30a system, purified by nickel affinity

chromatography, and verified for the purity of the various domains by Coomassie blue staining (Figure 3.3 Panel A).

Initially, the rAexU full length toxin was used to generate antibodies in mice. Serum from individual animals was analyzed for antibody titers by performing ELISA and Western blot analysis against rAexU antigen, and pooled sera from mice with high antibody titers were used for all further assays. However, when these antibodies were

```

AexT      MQIQANTVGTQAVAHSDATTTGVGRMSQMEARQVATGQDAILLGSRSSEPQKGQGLLSRLG  60
AexU      MQIQHTTSGLQAVAQHNDATAEVGRLQLEARQVATSQDALQLGNRSEPQKGQGLLSRLG  60
          **** * * * * * * * * * * * * * * * * * * * * * * * * * * * * * * * *
AexT      AQLARPFVAIKEWISNLLGTDKRAAAPKAQTAVSP-EDLQRLMKQAAFSSSLGGFAKAD  118
AexU      AQLARPFVALKEWIGNLLGARSEAPAHSAAPPADSLSLADQKRLLQKALPFTLGGLDKAN  120
          **** * * * * * * * * * * * * * * * * * * * * * * * * * * * * * *
AexT      VLNNITGEQLGKDHASLATGNGPLRSLCTALQAVVIGSQQPQLRELATGLLARPIAGIPL  178
AexU      ELNNIDAQQLGQEHARLATGNGALRSLATSLNGIKDGSMRQESQTLAAGLLERPIAGIPL  180
          **** * * * * * * * * * * * * * * * * * * * * * * * * * * * * * *
AexT      QQWGSVGGKVTELLTSAPPELLKEAMSQLHTAMGEVADLQRAVKAEVAGEPARSATTAAA  238
AexU      QQWGTVGKVTIELIANATPEQLQEAMSQLHAVMAEVADLQRAVKAEVAGEPLPAVTSAEV  240
          **** * * * * * * * * * * * * * * * * * * * * * * * * * * * * * *
AexT      VAPLQ-SGESEVNVEPADKALAEGLQEFGLEAEQYLGEQPHGTYSDAEVMALGLYTNGE  297
AexU      VAAPHGEAKPAARETVAMARQTEVTGYKQALELISYQASYLLRDQASTEVTLSSDDLNAL  300
          ** * * * * * * * * * * * * * * * * * * * * * * * * * * * * * *
AexT      YQHLNRSRLRQEKQLDAGQALIDQGMSTAFEKSTPTEQLIKTFRGTHGGDAFNEVAEGQVG  357
AexU      HQHIADGSINGSHMAKLQTRGDLQILRTLALSLASGSDANGASLGNALDSLASARPNQRL  360
          ** * * * * * * * * * * * * * * * * * * * * * * * * * * * * * *
AexT      HDVAYLSTSRDPKVATNFGGSGSISTIFGRSGIDVSDISVEGDEQELYN-----  407
AexU      VLGGLMQFAGQTDQAWADQTAGKPEDRLDAGARLRFDTGHMKAELARLDDSAARQVLQL  420
          * * * * * * * * * * * * * * * * * * * * * * * * * * * * * *
AexT      -----KETDMRVLLSAKDERGVTRRVLEEASLGEQSGHSGKGLLDGLDL  450
AexU      EEDFGDRAKAVCDFAVAQVSTFADSESSPEAVLVSRLTRMGNLVGSLTDELKVRLQLPES  480
          * * * * * * * * * * * * * * * * * * * * * * * * * * * * * *
AexT      ARGAGGADKPQEQDIRLKMRLDLA-----  475
AexU      ARGEPTMIDSVSQTLPLELAALAHIGVGADYL  512
          *** * * *

```

Figure 3.1: Amino acid sequence alignment of AexT from *A. salmonicida* and AexU from *A. hydrophila* SSU. Conserved aa residues are represented by asterisks (*), and ADP-ribosylation motifs are shown in continuous-line open boxes for *A. hydrophila*, and dotted-line open boxes for *A. salmonicida*. Arginine finger motif of RhoGAPs is shown in a gray box. “Reprinted from Microbial Pathogenesis, Vol 43 (4), Sierra JC, Suarez G, Sha J, Foltz SM, Popov VL, Galindo CL, Garner HR, Chopra AK., Biological characterization of a new type III secretion system effector from a clinical isolate of *Aeromonas hydrophila*-part II., Pages 147-160, © Copyright (2007), with permission from Elsevier.”

tested against the purified NH₂-terminal and COOH-terminal domains of AexU by Western blot analysis, the COOH-terminal domain reacted weakly (data not shown). Therefore mice were immunized only with the purified COOH-terminal domain of AexU. The sera from these animals showed much higher specificity for the COOH-terminal domain, as well as to the full length of AexU (data not shown). In all subsequent experiments to evaluate expression of different domains of AexU, an equal mixture of anti-AexU full length and anti-AexU COOH-terminal toxin domain antibodies were used (Figure 3.3 Panel B).

Purified rAexU possesses ADP-ribosyltransferase activity

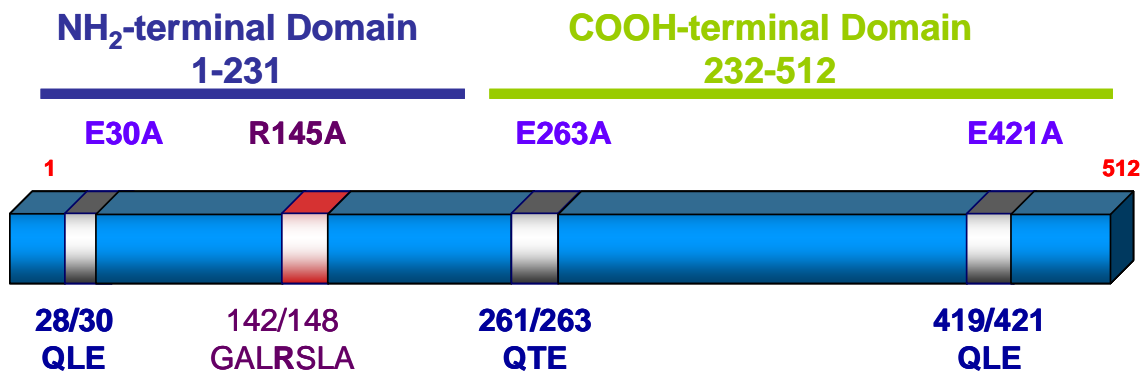


Figure 3.2: Schematic representation of AexU. The schematic representation shows motifs (QXE) associated with ADP-ribosylation (grey boxes) and the arginine finger (red box) with the catalytic arginine residue (R145). The NH₂- (aa residues 1–231), and COOH-(aa residues 232–512) terminal domains of AexU are also shown.

Our previous study indicated that the purified full length AexU possessed ADP ribosyltransferase activity (124), and based on amino acid sequence analysis of the toxin, I identified three QXE motifs, one located within the NH₂-terminal domain (Q28/E30) and the other two (Q261/E263 and Q419/E421) within the COOH-terminal domain of AexU, that might contribute to this ADPRT activity (**Figure 3.2**). I therefore evaluated ADP ribosyltransferase activity of native purified AexU full-length toxin and its NH₂-

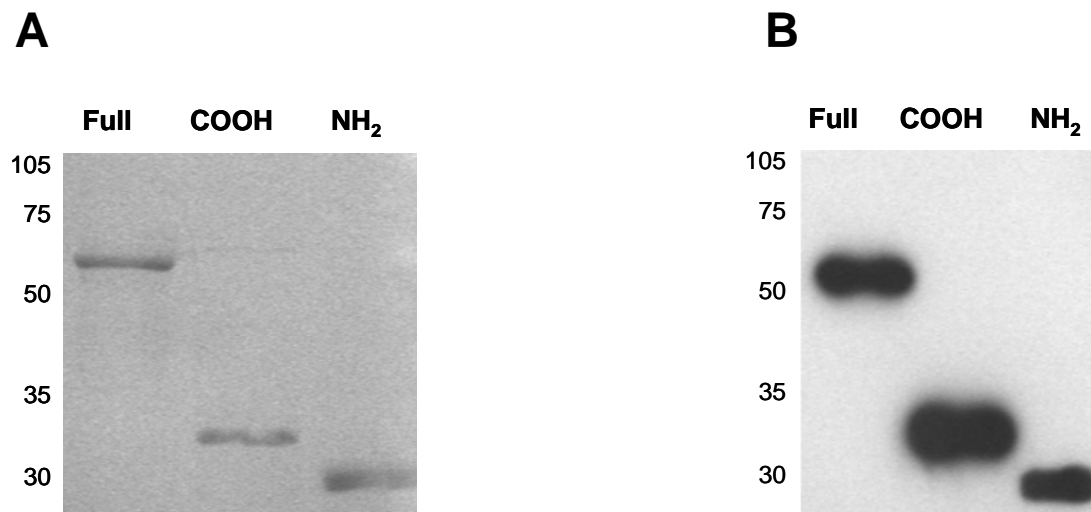


Figure 3.3: Recombinant purified AexU. (A) Coomassie blue staining of SDS–10% polyacrylamide gel containing various forms of purified rAexU. (B) Western blot analysis of purified rAexU toxins. Full=AexU full-length toxin; NH₂=AexU toxin NH₂-terminal domain; COOH=AexU toxin COOH-terminal domain. . “Reprinted from Microbial Pathogenesis, Vol 43 (4), Sierra JC, Suarez G, Sha J, Foltz SM, Popov VL, Galindo CL, Garner HR, Chopra AK., Biological characterization of a new type III secretion system effector from a clinical isolate of *Aeromonas hydrophila*-part II., Pages 147-160, © Copyright (2007), with permission from Elsevier.”

and COOH-terminal domains. As shown in **Figure 3.4**, purified AexU full-length toxin and its NH₂-terminal domain showed much higher ADP-ribosylating activity (~8000 cpm [~40% above control]), compared to the COOH-terminal domain (~3800 cpm [~18% above the control]), and these differences were statistically significant. The purity of various forms of recombinant AexU by Coomassie blue staining is shown in **Figure 3.3 Panel A**, and the identity of the recombinant proteins was verified by Western blot analysis using anti-AexU specific antibodies (**Figure 3.3 Panel B**). The sizes of full-length AexU toxin and its NH₂- and COOH-terminal domains were 58, 26, and 31 kDa, respectively.

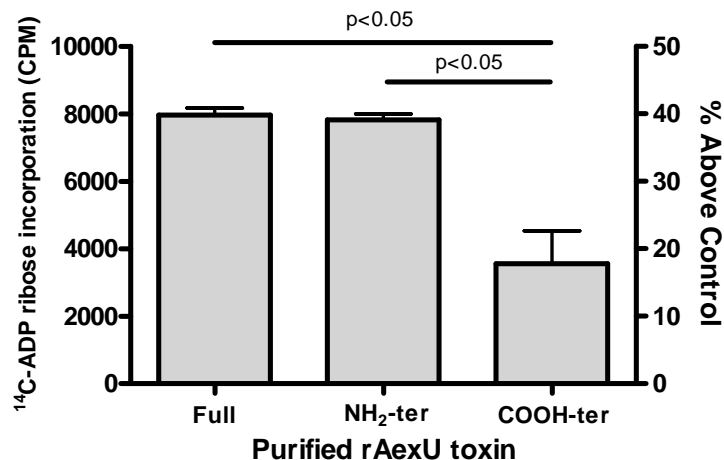


Figure 3.4: ADP-ribosyltransferase activity of AexU as evidenced by hydrolysis of [¹⁴C]NAD. Various domains of affinity purified AexU (4 µg) were incubated with [¹⁴C]NAD and HT-29 whole-cell lysates as a source of target proteins for 1 h at room temperature. The [¹⁴C]ADP-ribose incorporation in the target protein(s) was measured as counts per minute (cpm) in a scintillation counter. The background control contained [¹⁴C]NAD and HT-29 whole cell lysates. The background counts were subtracted from that of the experimental samples. The figure depicts arithmetic means±standard deviations from three independent experiments. The data were analyzed using Tukey's multiple group comparison test. The data were also presented to demonstrate percentage increase in counts by AexU over the control. "Reprinted from Microbial Pathogenesis, Vol 43 (4), Sierra JC, Suarez G, Sha J, Foltz SM, Popov VL, Galindo CL, Garner HR, Chopra AK., Biological characterization of a new type III secretion system effector from a clinical isolate of *Aeromonas hydrophila*-part II., Pages 147-160, © Copyright (2007), with permission from Elsevier."

Expression of the *aexU* gene in HeLa Tet-Off cells

Since it was recently shown that AexU is translocated into eukaryotic cells through the T3SS (124), I decided to mimic translocation by producing the toxin from a pBI-EGFP vector directly into HeLa cells using the Tet-Off system. HeLa Tet-Off cells were transfected by electroporation with a pBI-EGFP vector containing genes for *aexU* full length (1539 bp), the NH₂-terminal domain (1 to 693 bp) or the COOH-terminus (694 to 1539 bp), and transfection efficiency was evaluated by flow cytometry as the percentage of EGFP positive cells over a period of 48 h (data not shown). Within 8 h after transfection, it was possible to observe expression of the gene encoding EGFP in approximately 10% of the cells, which reached a maximum (~53% for the vector control,

~39% for the full length AexU, and ~48% each for its NH₂- and COOH-terminal domains) between 36 and 48 h. After 48 h, the percentages of EGFP positive cells started to decrease (~30% for HeLa cells transfected with the vector alone or the COOH-terminal domain of AexU) by day 5. However cultures transfected with plasmids carrying genes for the full length or NH₂-terminal domain of AexU exhibited a low (~3%) percentage of EGFP positive cells, suggesting a toxic effect caused by the NH₂-terminus of the toxin (data not shown).

Expression and production of the full length and separate domains of AexU at 24

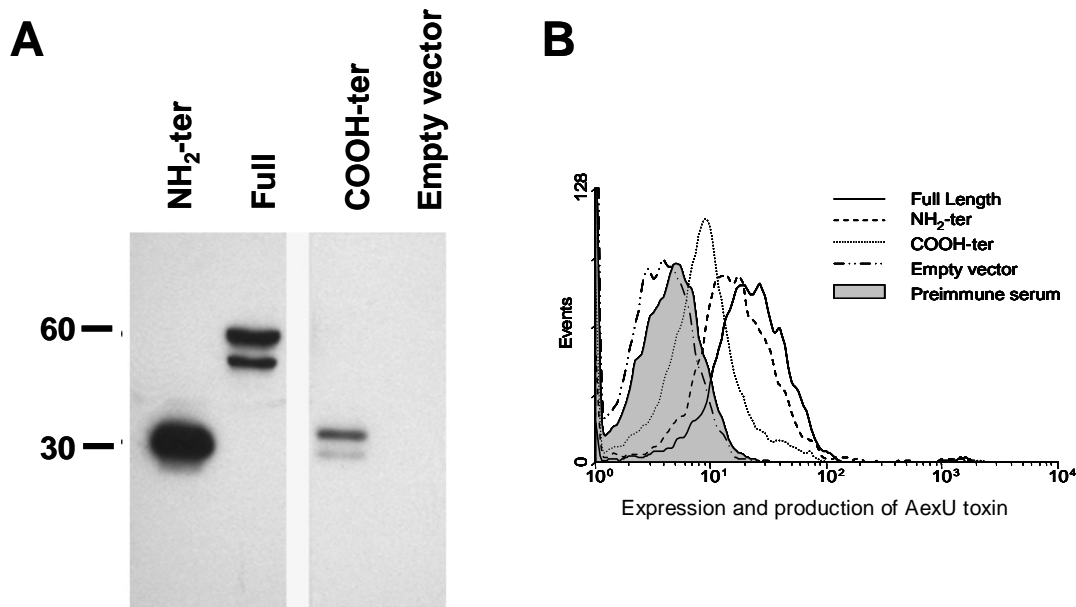


Figure 3.5: Expression and production of AexU in transfected HeLa Tet-Off cells.

(A) Western blot analysis showing production of AexU in whole cell lysates of HeLa Tet-off cells after 24 h of transfection with pBI-EGFP-*aexU* NH₂-terminal (NH₂-ter), full-length (Full), COOH-terminal (COOH-ter) domain encoding region of AexU, or pBI-EGFP empty vector (Empty vector). (B) Expression of three *aexU* gene constructs (recombinant plasmids harboring the full-length, NH₂- or COOH-terminal domain) after permeabilization and intracellular staining using α -AexU full-length toxin and α -AexU COOH-terminal toxin domain specific sera. Mouse pre-immune serum was used as an isotype control. The cells were acquired using a FACScan flow cytometer and analyzed using WinMDI software, gated on EGFP-positive cells. "Reprinted from Microbial Pathogenesis, Vol 43 (4), Sierra JC, Suarez G, Sha J, Foltz SM, Popov VL, Galindo CL, Garner HR, Chopra AK., Biological characterization of a new type III secretion system effector from a clinical isolate of *Aeromonas hydrophila*-part II., Pages 147-160, © Copyright (2007), with permission from Elsevier."

h post-transfection in HeLa Tet-Off cells was confirmed by Western blot analysis (**Figure 3.5 Panel A**). Bands of sizes 58, 26, and 31 kDa corresponded to the full length, NH₂-terminus, and COOH-terminal domain of AexU, respectively. Some degradation of the various domains of AexU was observed. Production of AexU at 24 h post-transfection was also evaluated by flow cytometry using α -AexU-specific antibodies, followed by PE-conjugated anti-mouse IgG. As shown in **Figure 3.5 Panel B**, transfected HeLa Tet-Off cells expressed and produced the full length, as well as the NH₂- and the COOH-terminal domain of AexU, which was evident by shifting in FL2 fluorescence against cells transfected with the vector alone or when pre-immune serum was used instead of hyper-immune serum containing anti-AexU antibodies.

HeLa Tet-Off cells were also evaluated at 24 h post-transfection for the production of AexU by confocal microscopy after immunochemical and DAPI staining. Production of EGFP (green) was detected in HeLa cells that were transfected with the vector alone (**Figure 3.6 Panel A**) and with the different constructs containing either the full-length (**Figure 3.6 Panel B**), the NH₂- (**Figure 3.6 Panel C**) or COOH-terminal (**Figure 3.6 Panel D**) domains of AexU. Each of the various forms of AexU (stained with PE) was clearly visible (red color) (**Figure 3.6 Panels B-D**), except when HeLa cells were transfected with the vector alone (**Figure 3.6 Panel A**). Co-expression of EGFP and AexU was also observed in some HeLa cells (**Figure 3.6, merge, yellow color**). The presence of cells negative for EGFP and the recombinant proteins represented those that were not successfully transfected with the recombinant plasmids, which were visualized by DAPI staining (blue) of the nuclei.

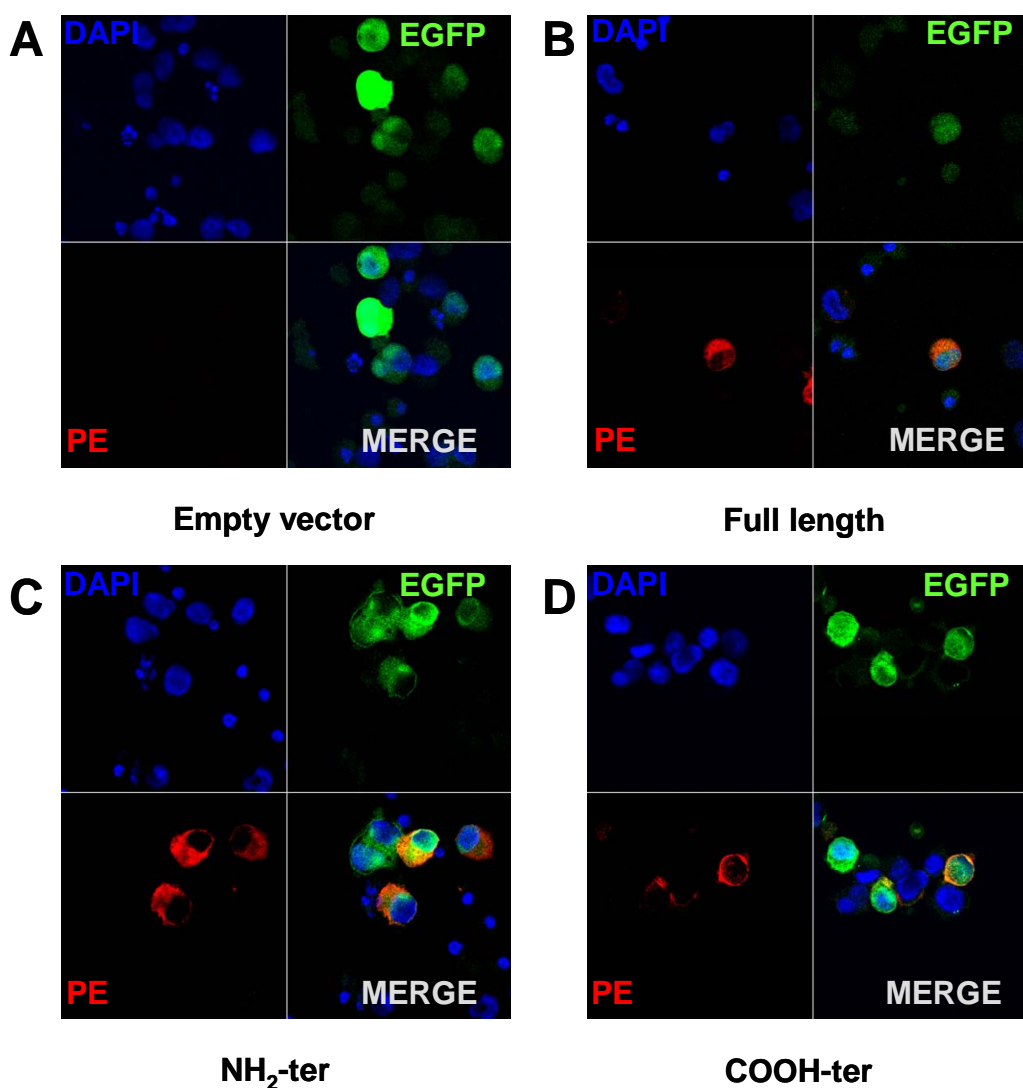


Figure 3.6: Fluorescent staining of HeLa Tet-Off cells transfected with plasmids encoding the *aexU* gene. Expression and production of AexU in HeLa Tet-Off cells as determined by confocal microscopy. After intracellular staining, the cells were bound to glass slides by cytospin/cyocentrifugation and analyzed using a laser scanning confocal microscope. Transfected cells are shown in green (EGFP positive), labeled AexU is shown in red, and nuclei of host cells are in blue (DAPI). HeLa Tet-Off cells transfected with: (A) pBI-EGFP alone (empty vector); (B) pBI-EGFP-*aexU* encoding full-length; (C) pBI-EGFP-*aexU* encoding NH₂-terminal domain; (D) pBI-EGFP-*aexU* encoding COOH-terminal domain. The image shown (magnification 63×) is a representative from three independent experiments. Full-length=AexU full-length; NH₂-ter=AexU NH₂-terminal domain; COOH-ter=AexU COOH-terminal domain; Empty vector=pBI-EGFP (vector alone). “Reprinted from Microbial Pathogenesis, Vol 43 (4), Sierra JC, Suarez G, Sha J, Foltz SM, Popov VL, Galindo CL, Garner HR, Chopra AK., Biological characterization of a new type III secretion system effector from a clinical isolate of *Aeromonas hydrophila*-part II., Pages 147-160, © Copyright (2007), with permission from Elsevier.”

Cell morphology and actin filament evaluation in HeLa Tet-Off cells transfected with the *aexU* gene

ExoS toxin from *P. aeruginosa* induces rounding of the host cells which is characterized by disruption in the polymerization of G-actin into F-actin (104). ExoS and AexU share 31% homology, and HeLa cells transfected with different *aexU* gene constructs exhibited rounded cell morphology with detachment from the tissue culture plates, based on light microscopy observations, after 24 h of transfection. I therefore investigated actin filament architecture by laser confocal microscopy using Alexa-Fluor 568-conjugated phalloidin. Phalloidin binds and stabilizes F-actin molecules, and as a result, cells stained with phalloidin should show only actin filaments and not actin monomers or G-actin. After 24 h of transfection, the rounded cell morphology was more pronounced in HeLa cells transfected with the genes encoding full length AexU (**Figure 3.7 (I) Panel c**) or its NH₂-terminal domain (**Figure 3.7 (I) Panel d**) than those transfected with the DNA fragment encoding the COOH-terminal portion (**Figure 3.7 (I) Panel b**). Cells transfected with the control vector (**Figure 3.7 (I) Panel a**) or the COOH-terminal domain of the gene (**Figure 3.7 (I) Panel b**) exhibited an actin filament network pattern similar to untransfected cells. The actin filament cytoskeleton of cells transfected with the full length or NH₂-terminal domain of the gene encoding AexU, on the other hand, was almost completely disrupted (**Figure 3.7 (I) Panel c and d**). Reorganization of actin by phalloidin staining was quantified by flow cytometry, showing a decrease in the mean fluorescence intensity (MFI) in HeLa cells expressing and producing the full-length and NH₂-terminal domain of AexU, when compared to host cells expressing only the vector alone or the COOH-terminal domain of AexU. These changes were more prominent at 60 h post-transfection (**Figure 3.7 (II)**).

HeLa Tet-off cells transfected with the vector alone or the plasmid containing the *aexU* full length gene were also processed for transmission electron microscopy. At 30 h post-transfection, cells producing AexU showed significant chromatin condensation and fragmentation (**Figure 3.8 Panel B and D**), cytoplasmic vacuolization and separation of the nuclear membrane resulting in expansion of perinuclear space (**Figure 3.8 Panel B**), cellular membrane disruption, and changes in the morphology and density of the mitochondria (**Figure 3.8 Panel B and C**), an overall phenotype most probably associated with late apoptotic events or necrosis. None of these changes were observed in

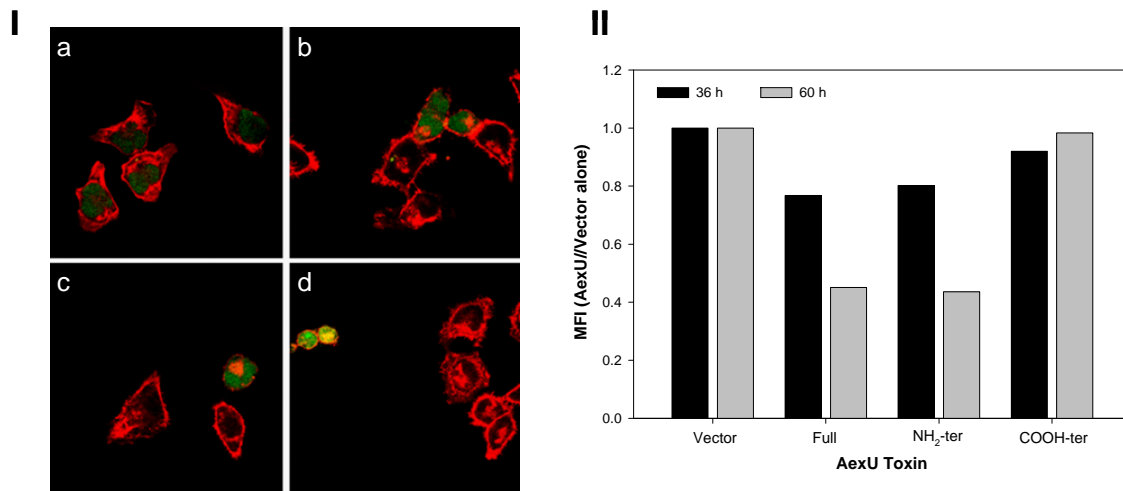


Figure 3.7: Phalloidin staining of HeLa Tet-Off cells transfected with plasmids encoding the *aexU* gene. (I) Evaluation of actin filaments by phalloidin staining in HeLa Tet-Off cells transfected with *aexU* encoding genes. After 24 h, HeLa Tet-Off cells transfected with empty vector (pBI-EGFP, panel a); AexU full-length (panel c); NH₂-(panel d); and COOH-terminal domains (panel b) were stained with Alexa-Fluor 568 phalloidin to visualize F-actin molecules and analyzed by laser confocal microscopy. The actin filaments (red) were intact in cells transfected with the empty vector or aexU encoding the COOH-terminal domain. In contrast, cells transfected with aexU full-length or its NH₂-terminal domain showed a drastic alteration in actin filament network. Transfected cells were distinguishable from un-transfected ones by EGFP production (green). The images shown (magnification 63×) are representative of three independent experiments. (II) Quantification by flow cytometry of the phalloidin staining in HeLa cells transfected with empty vector, and the AexU full-length, NH₂- and COOH-terminal domains of AexU. Ratio of mean fluorescence intensity (MFI) between each sample (pBI-EGFP vector with the *aexU* gene) and the empty vector was calculated. The figure shows a representative experiment from two different assays. “Reprinted from Microbial Pathogenesis, Vol 43 (4), Sierra JC, Suarez G, Sha J, Foltz SM, Popov VL, Galindo CL, Garner HR, Chopra AK., Biological characterization of a new type III secretion system effector from a clinical isolate of *Aeromonas hydrophila*-part II., Pages 147-160, © Copyright (2007), with permission from Elsevier.”

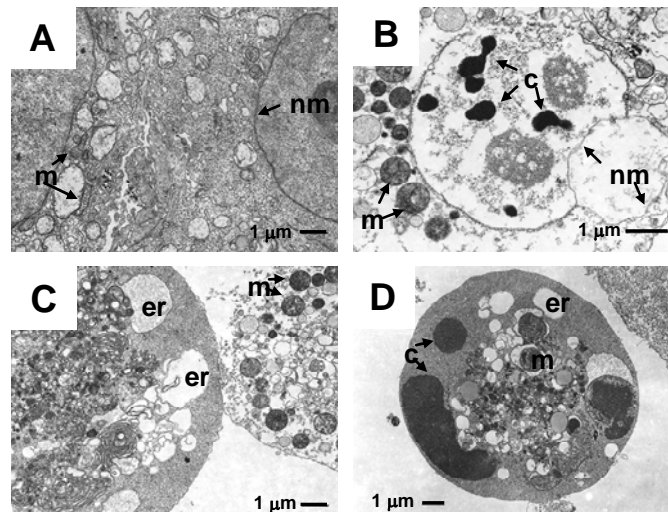


Figure 3.8: Transmission electron microscopy of HeLa Tet-Off cells transfected with plasmids encoding the *aexU* gene. HeLa Tet-Off cells were transfected with vector alone (panel A) or with plasmids encoding *aexU* full-length (panels B–D). HeLa Tet-Off cells transfected with *aexU* gene showed a dramatic cytotoxic effect caused by production of the toxin, including chromatin condensation and fragmentation (panels B and D), changes in mitochondrial density and morphology (panels B and C), separation of the perinuclear membrane (panel B), and expanded endoplasmic reticulum (panel C and D). c=chromatin; m=mitochondria; nm=nuclear membranes; er=endoplasmic reticulum. The images shown are representative of multiple fields. “Reprinted from Microbial Pathogenesis, Vol 43 (4), Sierra JC, Suarez G, Sha J, Foltz SM, Popov VL, Galindo CL, Garner HR, Chopra AK., Biological characterization of a new type III secretion system effector from a clinical isolate of *Aeromonas hydrophila*-part II., Pages 147-160, © Copyright (2007), with permission from Elsevier.”

HeLa cells transfected with the vector alone (**Figure 3.8 Panel A**).

AexU induces apoptosis in transfected HeLa Tet-Off cells

I analyzed cell viability, the rate of apoptosis, and cytotoxicity levels in HeLa cells transfected with the various gene constructs. The incorporation of 7-amino actinomycin D (7-AAD) which permeates the membranes of dead and dying cells and stains their DNA (100, 117), was assessed by flow cytometry. After 24 h of transfection, double positive EGFP/7-AAD HeLa Tet-Off cells were much higher in number (~40%) when the full length or NH₂-terminal domain of AexU was expressed and produced, compared to HeLa cells that expressed and produced the COOH-terminal portion of AexU (~28%) or HeLa cells expressing the vector alone (~23%) (**Figure 3.9 Panel A**). I

also performed colorimetric MTT assays to measure cytotoxicity and mitochondrial activity in cells transfected with the various *aexU* gene constructs or the vector alone. Results of this assay showed that HeLa Tet-Off cells transfected with plasmids containing *aexU* full length toxin or its NH₂-terminal domain genes had less mitochondrial activity than cells transfected with the vector alone ($p<0.001$) or pBI-EGFP plasmid containing the COOH-terminal domain of the toxin gene ($p<0.001$ and $p<0.01$, respectively) (**Figure 3.9 Panel B**). Importantly, the differences in cell cytotoxicity as determined by the MTT assay was statistically significant ($p<0.01$) between HeLa cells transfected with the vector alone and those transfected with the plasmid harboring the gene for the COOH-terminus of AexU.

In order to further confirm the cytotoxic effect of AexU and evaluate the apoptotic rate, I measured the cytoplasmic histone-associated DNA fragments (nucleosomes) by ELISA in HeLa Tet-Off cell lysates after 24 h of transfection with pBI-EGFP plasmids harboring the genes encoding the full length, NH₂-terminus, or COOH-terminal domain of the toxin. As shown in **Figure 3.9 Panel C**, cells producing the AexU-full length or its NH₂-terminal domain had higher rates of apoptosis compared to HeLa cells transfected with the vector alone ($p<0.01$ and $p<0.001$, respectively). The apoptotic rates of HeLa cells expressing and producing full length versus COOH-terminal ($p<0.01$) and NH₂-terminal versus COOH-terminus of AexU ($p<0.001$) were also statistically significant. On the other hand, HeLa cells transfected with the plasmid that contained the COOH-terminal portion of the toxin had apoptotic levels similar to those transfected with the vector alone ($p>0.05$).

Based on the increased rate of apoptosis evidenced by nucleosome detection in HeLa cells expressing and producing AexU, I decided to evaluate the caspase activity in these cells. Caspase 3 is a key mediator of apoptosis in mammalian cells; this effector

caspase is downstream of the activator caspases 8 and 9 (41). Activation of caspase 3 was

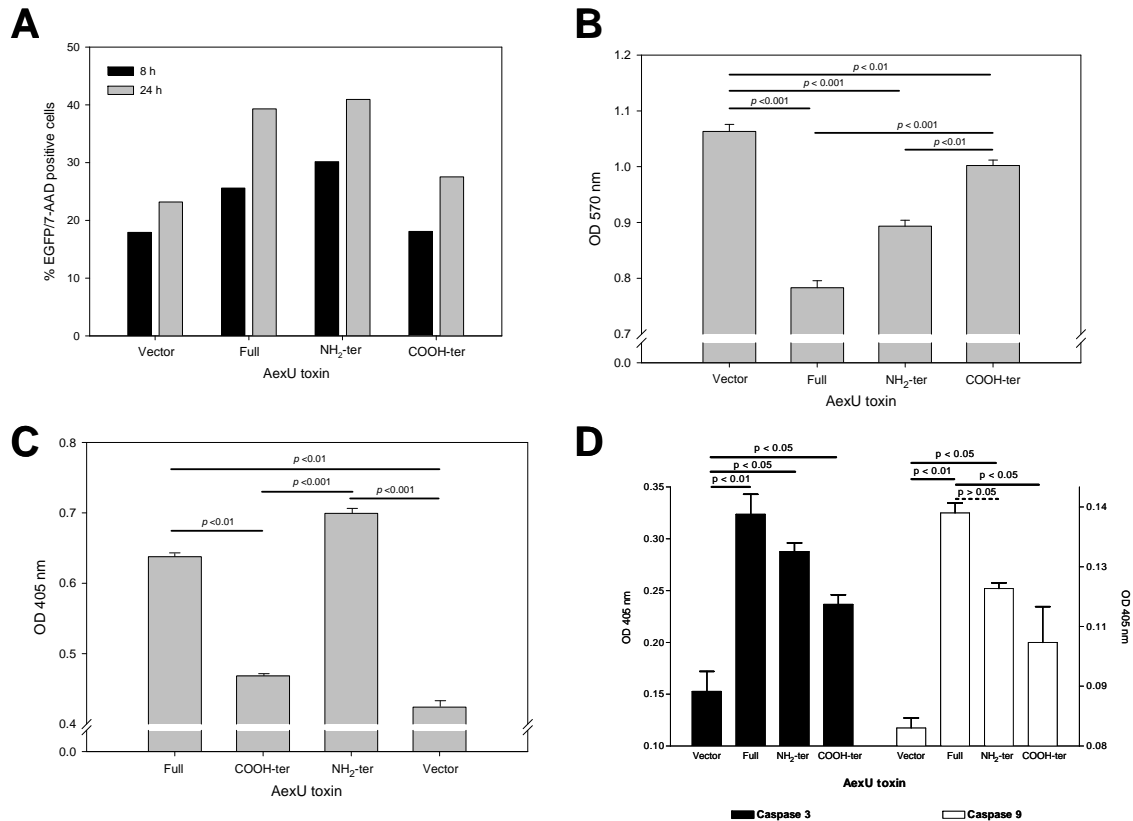


Figure 3.9: Induction of apoptosis in HeLa Tet-Off cells transfected with *aexU* gene. (A) Incorporation of 7-amino actinomycin D (7-AAD) as measured by flow cytometry in HeLa cells after 8 and 24 h of transfection with empty vector and the *aexU* gene constructs. A representative experiment from a total of three is shown in the figure. (B) Cytotoxicity associated with the expression and production of AexU was evaluated by the MTT assay. Mitochondrial activity was reduced in cells transfected with genes encoding the full-length or NH₂-terminal domain of AexU. In contrast, cells transfected with the DNA fragment encoding the COOH-terminal domain of AexU or with the empty vector had higher levels of mitochondrial activity. (C) Detection by ELISA of cytoplasmic nucleosomes in HeLa Tet-Off cell lysates transfected with genes encoding full-length, NH₂- or COOH-terminal domains of AexU after 24 h. An increased rate of apoptosis was evident in cells producing the full-length or NH₂-terminal domain of AexU compared to cells transfected with the empty vector or the COOH-terminal domain. (D) Colorimetric caspase 3 (Black bars) and 9 (white bars) detection in total lysates of HeLa cells transfected with different *aexU* constructs after 24 h. Caspase 3 and 9 activity was increased in HeLa cells producing full-length, NH₂-terminal or COOH-terminal domain of AexU, compared to HeLa cells expressing the vector alone. For caspase 3, significant differences are evident for all of the three constructs (full-length, NH₂- and COOH-terminal domain of AexU), when compared to HeLa cells transfected with the vector alone. An increase in caspase 9 activation was statistically significant in cells producing full-length and NH₂-terminal domain of AexU but not in cells producing the COOH-terminal fragment of AexU when compared to HeLa cells transfected with the vector alone. Figures are representative of three independent experiments. Standard deviations were calculated from duplicate assays from one experiment. "Reprinted from Microbial Pathogenesis, Vol 43 (4), Sierra JC, Suarez G, Sha J, Foltz SM, Popov VL, Galindo CL, Garner HR, Chopra AK., Biological characterization of a new type III secretion system effector from a clinical isolate of *Aeromonas hydrophila*-part II., Pages 147-160, © Copyright (2007), with permission from Elsevier."

significantly increased after 24 h in HeLa cells producing AexU full length toxin ($p<0.01$), its NH₂-terminus ($p<0.05$), or the COOH-terminal domain ($p<0.05$) when compared to HeLa cells transfected with the vector alone (**Figure 3.9 Panel D**). Likewise, after 48 h of transfection with different plasmid constructs, there was a significant increase in active caspase 3 in HeLa cells. Additionally, the increased activation of caspase 3 in HeLa cells producing AexU full length after 48 h of transfection was statistically significant when compared with cells producing the NH₂-terminal ($p<0.01$) or the COOH-terminal ($p<0.001$) domain of AexU. I also detected significant differences in caspase 3 activation in cells producing the NH₂-terminal and COOH-terminal domains of AexU ($p<0.001$) (**Figure 3.10**).

Caspase 3 can be activated by caspase 9 in cells undergoing apoptosis by the mitochondrial stress pathway (2, 41). Induction of apoptosis in this case could be mediated by perturbation of the mitochondria resulting in caspase 9 activation. I assessed activation of caspase 9 in HeLa cells transfected with the various forms of AexU. Activation of caspase 9 was evident 24 and 48 h after transfection with the different AexU constructs. Significant differences after 24 h were observed in HeLa cells producing AexU full length toxin ($p<0.01$) or its NH₂-terminal domain ($p<0.05$), compared to HeLa cells expressing vector alone (**Figure 3.9 Panel D**). A significant difference was also detected between HeLa cells producing AexU full length ($p<0.05$) and cells producing the COOH-terminal domain of the toxin (**Figure 3.9 Panel D**). However, caspase 9 levels were barely statistically significant ($p=0.053$) when comparisons were made between HeLa Tet-Off cells expressing the full length when compared to the NH₂-terminal domain of AexU encoding gene.

Similarly, after 48 h of transfection, increased activation of caspase 9 was evident in cells producing full length ($p<0.001$), NH₂-terminal ($p<0.001$) and COOH-terminal

($p < 0.05$) domains of AexU, compared to HeLa cells transfected with the vector alone (**Figure 3.10**). In addition, significant differences in caspase 9 activation were observed between cells producing full length ($p < 0.01$) or the NH₂-terminal ($p < 0.01$) domain of AexU when compared to cells producing the COOH-terminal domain of the toxin. At 48 h, I also noted statistically significant differences ($p < 0.05$) in caspase 9 production in HeLa cells producing COOH-terminal portion of AexU toxin compared to host cells expressing only the vector (**Figure 3.10**).

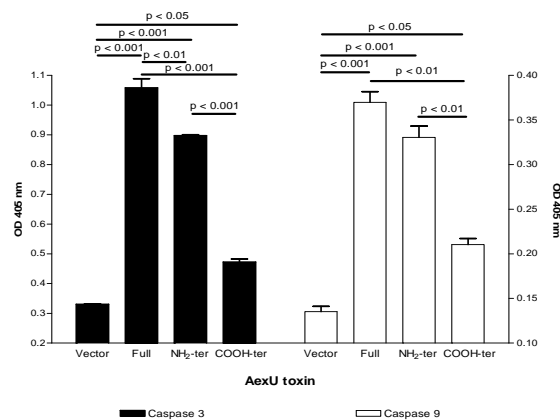


Figure 3.10: Caspase 3 and 9 detection in HeLa Tet-Off cells transfected with *aexU* gene for 48 h. Colorimetric caspase 3 (Black bars) and 9 (white bars) detection in total lysates of HeLa cells transfected with different *aexU* constructs after 48 h. Caspase 3 and 9 activity was increased in HeLa cells producing full-length, NH₂-terminal or COOH-terminal domain of AexU, compared to HeLa cells expressing the vector alone. For caspase 3 and 9, significant differences are evident for all of the three constructs (full-length, NH₂- and COOH-terminal domain of AexU), when compared to HeLa cells transfected with the vector alone. Figure is representative of three independent experiments. Standard deviations were calculated from duplicate assays from one experiment.

DISCUSSION

Previous studies from our laboratory provided evidence for the production of several virulence factors from diarrheal isolate SSU of *A. hydrophila* (44, 46, 50, 57, 119, 122). More recently, our laboratory described a novel T3SS effector protein, AexU, and

demonstrated that an *A. hydrophila* $\Delta aexU$ mutant strain was avirulent in a mouse model of lethality and that mice immunized with rAexU were resistant to infection with wild type *A. hydrophila* (124). In this study, I investigated the biological effects associated with AexU and presented an initial characterization of this toxin in eukaryotic cells. We provided evidence that the NH₂-terminal domain of AexU had more ADPRT activity than its COOH-terminus, even though the COOH-terminal domain possessed two QXE motifs. This could possibly be attributed to the tertiary structure of the recombinant protein making those motifs inaccessible, if these motifs indeed contributed to the enzymatic activity. On the other hand, amino acid sequence analysis search for ADP-ribosylation motifs ([Q/E]XE) in other toxins with ADPRT activity showed the presence of more than one motif that could be associated with this enzymatic activity. For example, AexT has three QXE motifs (**Figure 3.1**), ExoS has five motifs (three QXE and two EXE), ExoT has four motifs (three EXE and one QXE), and Iota toxin has seven motifs (four EXE and three QXE) (data not shown). However the ADP-ribosylating activity in these toxins could be associated with only one of the above-mentioned motifs, or all could contribute to the enzymatic activity. Therefore, structural and functional analysis will be required to confirm which of the AexU QXE motif(s) is associated with the ADP-ribosylation activity.

Microscopic analysis revealed a characteristic rounded morphology of HeLa Tet-Off cells transfected with plasmids containing either the full length or the NH₂-terminal domain of *aexU* gene. Further, most of these cells did not attach to the culture flask and remained in suspension. In contrast, this phenotype was not observed for cells producing the COOH-terminal domain of AexU, which resembled cells producing EGFP alone (control vector) or those that were not transfected. These results suggested that AexU exerted a cytotoxic effect involving disruption of host cell cytoskeletal activities, which

was attributed mainly to the NH₂-terminal portion of the toxin. Indeed, direct assessment of the actin filament network (based on phalloidin staining) confirmed a dramatic disruption of actin polymerization only when the NH₂-terminus of AexU was produced, alone or as part of the full-length protein.

In addition to the induction of cell rounding and alterations in the actin filament network, ADPRT activity was much more pronounced for the full length and NH₂-terminal domain of AexU, compared to the COOH-terminus. ADPRT activity associated with *C. perfringens* iota toxin, botulinum C2 toxin, and the *Salmonella* plasmid virulence protein (SpvB) has been reported to lead to cell rounding by targeting actin, which after ADP-ribosylation, is unable to form filaments (7, 84). Such morphological changes were clearly evident in eukaryotic cell lines, such as Vero (African green monkey kidney epithelial cells), CHO (Chinese hamster ovary cells), and mouse fibroblastic cells (7, 84, 86). These toxins ADP-ribosylate G-actin, which caps the barbed end of F-actin and hence blocks its further polymerization, leading to cell collapse (7). It is therefore possible that AexU toxin's ADP-ribosyltransferase activity plays a similar role in the induction of rounded cell morphology. Such alterations in the actin cytoskeleton induced by AexU toxin could interfere with important host cell functions, such as motility, phagocytosis, secretion, proliferation, and mitosis, and ultimately lead to cell death (10). Alternatively, ADP-ribosylation of RhoC by C3 from *C. botulinum* has been related to actin cytoskeleton disruption and subsequent morphological changes of host cells (26, 67). Thus, ADP-ribosylating toxins can disrupt the actin cytoskeleton not only by targeting G-actin but also by targeting other proteins related to actin polymerization (26, 67). There is therefore a broad range of possible target protein(s) for AexU that could be ADP-ribosylated, underscoring the importance of identifying such targets in the future in order to elucidate in-depth the mechanism of action of AexU. Recently, GTPase-

activating protein (GAP) activity was described for AexT from *A. salmonicida*, which was associated with alterations in the actin cytoskeleton of host cells (87). Therefore, actin reorganization seen with AexU in HeLa-Tet-Off cells could be related to both GAP and ADP-ribosyltransferase activities. The presence of an arginine finger motif in the NH₂-terminal domain of AexU points to the fact that this domain may have GAP activity (**Figure 3.1**).

In addition to AexU, *A. hydrophila* produces the T2SS-Act toxin, which we previously reported to exert a variety of effects *in vitro* and *in vivo*, including cytotoxicity to intestinal and non intestinal cells, an acute inflammatory response, intestinal fluid secretion, up-regulation of the expression of genes encoding proinflammatory cytokines, activation of MAPK signaling, and classical caspase-associated apoptosis (30, 50, 56, 57, 119). Additionally, an Δact mutant of *A. hydrophila* SSU was less virulent in mice than the wild-type bacteria. However, host cells infected with Δact mutant bacteria exhibited changes in their morphology, such as vacuolation in colonic intestinal epithelial cells (HT-29), rounded cell morphology in murine macrophages (RAW264.7), and detachment of host cells from tissue culture plates (122). These results suggested the presence of an effector protein(s) that was different from Act and could be responsible for this phenotype. Based on the results presented in this study, I suggested that AexU toxin could be one of those effector proteins.

Evaluation by transmission electron microscopy of HeLa Tet-Off cells producing different forms of AexU allowed us to identify morphological changes at the ultra-structural level. I observed alterations such as chromatin condensation and fragmentation, vacuolization, membrane disruption, and changes in mitochondrial morphology associated with the expression and production of AexU in HeLa cells. These cytotoxic changes were characteristic of early and/or late apoptosis, suggesting a role of AexU in

an apoptotic or necrotic process. Increased cell death accompanied by a decrease in mitochondrial activity in cells that were producing the full length or NH₂-terminal domain of AexU was confirmed by 7-ADD staining, detection of cytoplasmic nucleosomes, and MTT assays. AexU toxin-induced cell death was caspase-associated, as demonstrated by colorimetric assays for caspase 3 and 9. These data correlated with the observed morphological changes, cytotoxicity, and DNA fragmentation and indicated that AexU induced apoptosis. Furthermore, induction of apoptosis was higher in response to the NH₂-terminal domain compared to the COOH-terminal portion of AexU, correlating with ADPRT activity, nucleosome detection, actin polymerization disruption and mitochondrial activity. Detection of activated caspase 9, together with alteration in the density and morphology of the mitochondria (evidenced by electron microscopy), suggested that the induction of apoptosis as a result of AexU production was mainly mediated *via* the mitochondrial stress pathway.

In the context of *A. hydrophila* infection, the host cell targets for AexU might include immune and intestinal cells, and/or other cells in the body, depending on the route and progression of infection. It is therefore important to investigate the potential for AexU to affect other cells, such as macrophages, which are known to be important in *Aeromonas*-associated gastroenteritis and wound infections. Our previous studies with Δact mutant bacteria combined with the results of this study make AexU a strong candidate for previously observed host effects, such as cell rounding, apoptosis, and some signaling events evoked by *A. hydrophila*, that are not attributed solely to Act.

In summary, these findings indicated that AexU had ADPRT activity, which is primarily associated with the NH₂-terminal domain. Interestingly, the COOH-terminal domain of AexU also had ADPRT activity, although this domain is quite unique with no homology to any known proteins in the NCBI database. Further, in ExoS/T, ADPRT

activity was associated with the COOH-terminus (18, 111), while in AexU this activity was associated with both the NH₂- and COOH-terminal domains. I observed alterations in the actin cytoskeleton of HeLa cells expressing the *aexU* gene that could be linked to apoptotic processes in the host cells. The discovery and characterization of AexU are initial steps in delineating the mechanism of action of this new virulence factor, and with further studies could allow a better understanding of the pathogenicity of *A. hydrophila* and possibly other bacteria that produce similar toxins.

Chapter 4: Unraveling the mechanism of action of a new type III secretion system effector AexU from *Aeromonas hydrophila*²

INTRODUCTION

Previously, I characterized the T3SS-associated effector AexU (with 512 amino acid [aa] residues), that possessed ADPRT activity (126). AexU inhibited phagocytosis of bacteria by macrophages, and it eventually led to host cell death by apoptosis (123, 126). We also demonstrated that AexU played an important role during the infection process, as 60% of mice infected with the $\Delta aexU$ isogenic mutant survived a minimal lethal challenge dose, which killed 90-100% of animals infected with the wild-type (WT) *A. hydrophila* SSU (123).

Studies on the T3SS-secreted effector proteins (e.g., ExoS/T and AexT) from other bacteria, such as *Pseudomonas aeruginosa* and a fish pathogen *Aeromonas salmonicida*, respectively, indicated that they were bifunctional toxins, with the NH₂-terminal domain having GTPase activating protein (GAP) activity, while the COOH-terminal domain had ADPRT activity (11, 18, 47, 71, 82). Importantly, however, was our finding that although the NH₂-terminal domain of AexU (aa residues 1-231) shared 54-67% homology in the corresponding domains of *P. aeruginosa* ExoS (aa residues 1-233) and *A. salmonicida* AexT (aa residues 1-255), respectively, the COOH-terminal domain of AexU (aa residues 232-512) was unique with no homology to any functional protein in the NCBI database. Because of this novel domain, the overall homology of AexU with ExoT/S and AexT dropped to 31 and 40%, respectively. Further, while AexU is 512 aa

² 125. Sierra, J. C., G. Suarez, J. Sha, W. B. Baze, S. M. Foltz, and A. K. Chopra. 2010. Unraveling the mechanism of action of a new type III secretion system effector AexU from *Aeromonas hydrophila*. *Ibid.* doi:10.1016/j.micpath.2010.05.011

residues in length, ExoS and AexT are comprised of 453 and 475 aa residues, respectively (20, 126, 144).

Within the NH₂-terminal domain of AexU, I identified an arginine-finger motif (GALRSLA), similar to that of ExoS (GALRSLS) and AexT (GPLRSLC). Earlier studies based on site-directed mutagenesis indicated an essential role of an arginine residue in the GAP activity of these bacterial toxins (47, 64); however, whether AexU possesses a similar activity is unknown.

In this study, I evaluated the GAP activity of native and mutated versions of AexU from *A. hydrophila* SSU and examined various signaling pathways mediated by AexU in the host cell. Further, I studied the ability of the $\Delta aexU$ null mutant strain to be detected in the peripheral organs of mice after intraperitoneal (i.p.) infection. Overall, our data indicated that AexU operated by inhibiting the activation of NF- κ B by down-regulating the phosphorylation of I κ B α and, thereby, negatively modulating the production of key cytokines/chemokines.

In addition, I provided the first evidence that AexU devoid of ADPRT and GAP activities when produced *in trans* from *A. hydrophila* SSU $\Delta aexU$ strain, was able to trigger significant production of cytokines/chemokines in spleens of infected mice when compared to animals infected with the $\Delta aexU$ strain expressing the native *aexU* gene with intact ADPRT and GAP activities. These data indicated that AexU devoid of its intrinsic activities was even more potent in activating genes for cytokines and chemokines and their overwhelming production resulted in increased mortality in mice in a septicemic mouse model. To our knowledge, this is the first detailed mechanistic study unraveling the mechanism of action of AexU.

RESULTS

AexU functions as a GTPase-activating protein (GAP) for RhoA, Rac1 and Cdc42, and this activity is dependent on the arginine residue located at position 145

Multiple bacterial toxins target GTP-binding proteins, and a particular subset of toxins mimic the action of eukaryotic GAPs by promoting the hydrolysis of bound GTP (4, 52). Sequence analysis and site-directed mutagenesis studies have shown the importance of an essential arginine residue in all of the bacterial GAPs, and this residue is believed to function as the arginine finger already described for GAP activity of eukaryotic proteins (6). By sequence analysis of AexU, I identified a region in the NH₂-terminal domain that exhibited homology to other bacterial proteins with GAP activity, and this region is referred to as arginine finger sequence motif (116). In particular, the arginine residue located at position 145 in AexU could serve as the catalytic aa residue mediating the GAP activity (**Figure 4.1 Panel A**).

Consequently, I performed an *in vitro* GTP-hydrolysis assay of the small GTPases, such as RhoA, Rac1, Cdc42, and Ras. The GAP activity of native recombinant AexU (rAexU) towards RhoA, Rac1, and Cdc42 was confirmed by this assay (**Figure 4.1 Panel C**); however, no activity was detected towards Ras (data not shown). Additionally, I over-produced and purified the mutated version of rAexU (GAP⁻), and evaluated its GAP activity. Importantly, rAexU_{GAP⁻} showed a significant reduction in its capacity to hydrolyze GTP, when I compared it with the native form of rAexU and the positive control p50 Rho GAP that was used in this assay (**Figure 4.1 Panel C**), using the same substrates. These data confirmed that arginine 145 indeed was responsible for the GAP activity of rAexU. The stability of the mutated versus the native form of rAexU based on Coomassie blue staining of the gel is shown in **Figure 4.1 Panel B**.

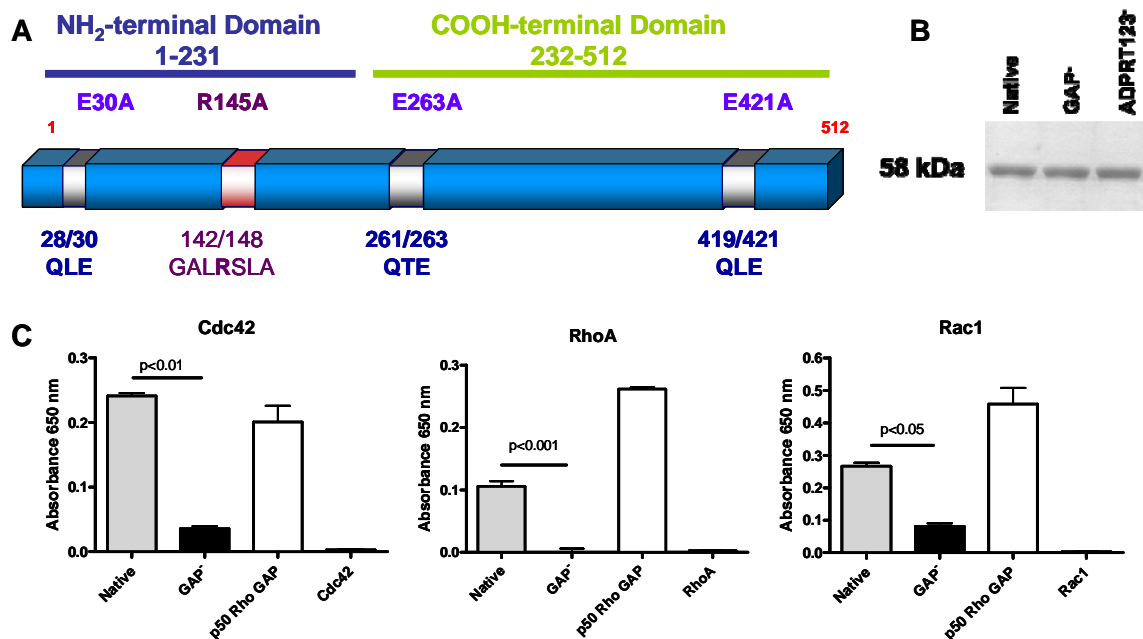


Figure 4.1: *In vitro* GAP activity of AexU. (A) Schematic representation of AexU showing the catalytic arginine residue associated with GAP activity and the potential motifs (QXE) associated with ADPRT activity. (B) Coomassie blue staining of native and different mutated versions of rAexU, with GAP⁻ indicating the mutated version for GAP activity in which arginine residue at position 145 was replaced with alanine and ADPRT123⁻ representing the mutated version for ADPRT activity in which three glutamate residues at positions 30, 263 and 421 were replaced with alanine. (C) *In vitro* GAP activity towards RhoA, Rac1, and Cdc42 by affinity purified rAexU (native and mutated GAP⁻ version). Recombinant RhoA, Rac1, and Cdc42 (25 µg) were incubated with purified rAexU (4 µg) and GTP for 20 min at 37°C. As a positive control, recombinant p50 RhoGAP (6 µg) was added to the reaction instead of rAexU. Additionally, in order to account for the intrinsic GAP activity, each small GTPase (RhoA, Rac1 and Cdc42) was tested in the absence of the GAP protein (last column in each graph). The phosphate groups generated by GAP activity of AexU were quantified by adding the CytoPhos reagent and colorimetric analysis. The values shown are the mean absorbances \pm standard deviations from three independent experiments. ANOVA with Tukey's multiple comparison test was used for statistical analyses of the data. "Reprinted from Microbial Pathogenesis, Sierra JC, Suarez G, Sha J, Baze W., Foltz SM., Chopra AK., Unraveling the mechanism of action of a new type III secretion system effector AexU from *Aeromonas hydrophila*., doi:10.1016/j.micpath.2010.05.011 © Copyright (2010), with permission from Elsevier."

Alterations in actin cytoskeleton of HeLa Tet-Off cells transfected with the *aexU* gene are associated with GAP activity

Several bacterial toxins target GTP-binding proteins to alter host cellular functions, such as chemotaxis, phagocytosis, and secretion and proliferation necessary to eliminate the pathogen from the host (4, 6). One particular strategy is the inhibition of

small GTPases by bacterial toxins having a GAP-like activity. Small GTPases, in particular the Rho GTPases, are involved in regulating host cell polarity, cell adhesion, and the contractile actin/myosin stress fiber formation (4, 52). Since rAexU possesses GAP activity, I investigated whether alterations in the cellular cytoskeleton induced by native AexU were related to GAP activity. The actin filament architecture was evaluated by immunofluorescence and flow cytometry using Alexa-Fluor 568-conjugated phalloidin.

The rounded cell morphology was evident in HeLa Tet-Off cells transfected with the gene encoding native AexU (**Figure 4.2 Panel A-II**); the actin cytoskeleton was almost completely disrupted (**at arrow**). In contrast, HeLa cells transfected with the gene encoding the mutated version of AexU (GAP⁻) (**Figure 4.2 Panel A-III**) exhibited an actin filament network which was much improved compared to in HeLa Tet-Off cells that were transfected with the native *aexU* gene, although not reaching to the level seen in HeLa cells transfected with the vector alone (**Figure 4.2 Panels A-I and 4.2 B & C**). HeLa cells expressing the gene encoding GFP were clearly seen in these three panels. These data indicated that GAP activity contributed to the alteration of the actin cytoskeleton of the host cells.

I then quantified the reorganization of actin by flow cytometry using fluorescently labeled phalloidin, and for this analysis, I used only the GFP⁺ population. The phalloidin mean fluorescence intensity (MFI) of the HeLa Tet-Off cells transfected with the gene encoding GAP⁻AexU was significantly higher (doubled) compared to the MFI of the host cells transfected with the gene encoding native AexU (**Figure 4.2 Panels B & C**). The expression and production of native AexU as well its mutated version after transfection into HeLa Tet-Off cells were evaluated by Western blot analysis that used anti-AexU antibodies to ensure that the effects observed in the actin cytoskeleton were not

Induction of apoptosis by AexU in transfected HeLa Tet-Off cells is dependent on GAP activity

I previously reported an increase in the apoptosis of HeLa Tet-Off cells expressing and producing AexU (126). I measured cytoplasmic histone-associated DNA fragments (nucleosomes) by ELISA in HeLa cells after 24 h of transfection with genes encoding native AexU and the GAP mutant (GAP⁻). The apoptotic rates of HeLa Tet-off cells transfected with genes encoding AexU_{GAP⁻} were significantly lower compared to those in HeLa cells transfected with the gene encoding native AexU (**Figure 4.3 Panel A**). Additionally, I evaluated the activation of caspase 3 in HeLa Tet-Off cells in response to the mutated version of AexU. As shown in **Figure 4.3 Panel B**, there was a significant

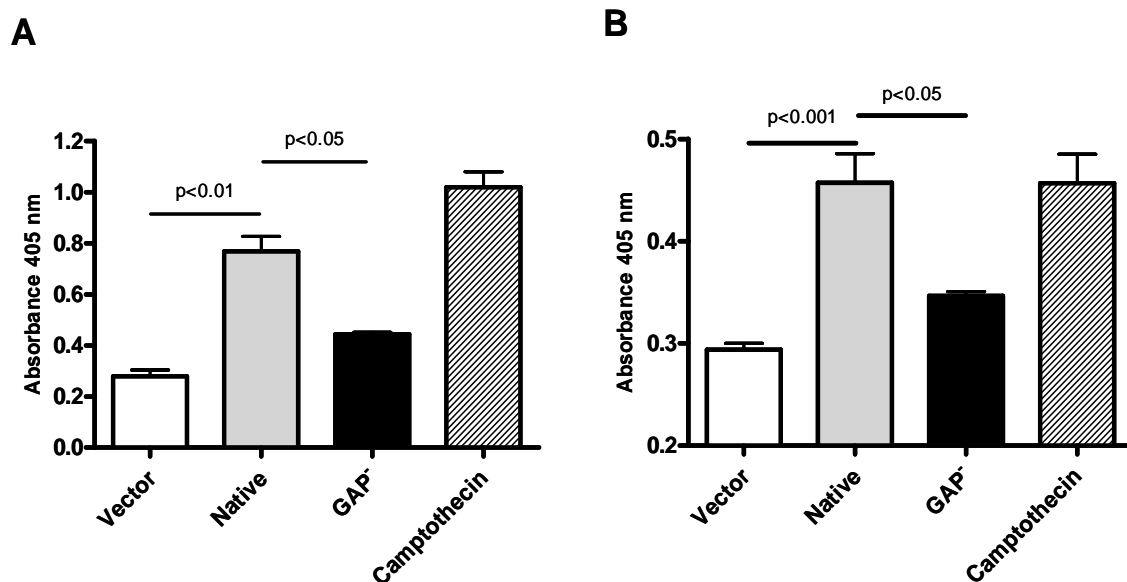


Figure 4.3: Assessment of the apoptotic rate in HeLa Tet-Off cells expressing the genes encoding native and mutated version (GAP⁻) of AexU. (A) Detection of cytoplasmic nucleosomes by ELISA in HeLa Tet-Off cells after 24 h of transfection. (B) Caspase 3 activation measured by colorimetric assay in lysates of transfected HeLa Tet-Off cells. HeLa Tet-Off cells transfected with the empty vector and then treated with Camptothecin were used as a positive control for both assays. The values shown are mean absorbances \pm standard deviations from three independent experiments. ANOVA with Tukey's multiple comparison test was used for statistical analyses of the data. "Reprinted from Microbial Pathogenesis, Sierra JC, Suarez G, Sha J, Baze W., Foltz SM, Chopra AK., Unraveling the mechanism of action of a new type III secretion system effector AexU from *Aeromonas hydrophila*, doi:10.1016/j.micpath.2010.05.011 © Copyright (2010), with permission from Elsevier."

decrease in the activation of caspase 3 in the HeLa cells transfected with gene encoding AexU_{GAP}⁻ compared to HeLa cells transfected with the native version of AexU. As a positive control, I used HeLa Tet-Off cells transfected with vector alone and treated with camptothecin and it showed similar levels of cytoplasmic nucleosomes and caspase 3 activation as in HeLa Tet-Off cells transfected with the native *aexU* gene.

AexU interferes with the phosphorylation of c-Jun and IκBα in normal HeLa cells co-cultured with *A. hydrophila* SSU

In addition to controlling the assembly and disassembly of the host actin cytoskeleton, members of the Rho family of small GTPases activate nuclear factor κB (NF-κB) (95, 105). There is evidence that constitutively activated forms of Rac1 and Cdc42 are able to induce the activation of c-Jun N-terminal kinase/stress-activated protein kinase (JNK/SAPK) (39, 94). Given that AexU possesses GAP activity towards RhoA, Rac1, and Cdc42, I evaluated the effects of either WT *A. hydrophila* or its *ΔaexU* null mutant on the signaling cascades leading to the activation of transcription factors c-Jun and NF-κB.

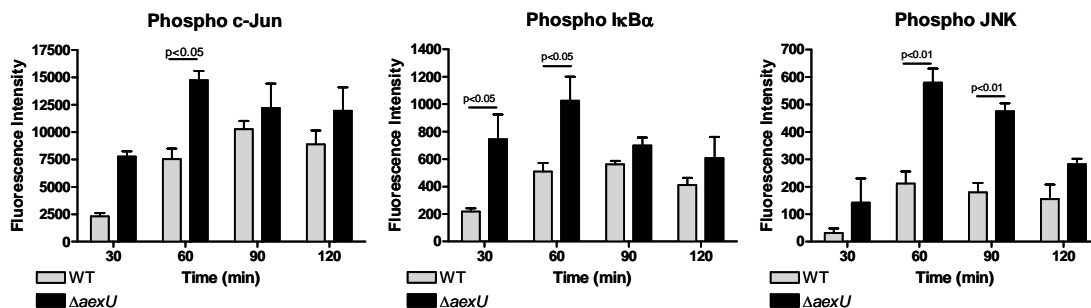


Figure 4.4: Phosphorylation of c-jun, IκBα, and JNK in HeLa cells co-cultured with WT *A. hydrophila* SSU or its *ΔaexU* mutant. HeLa cells were co-cultured with with WT *A. hydrophila* SSU (Grey bars) or its *ΔaexU* mutant (Black bars) and phosphorylation status of c-jun, IκBα, and JNK was determined by using a BioPlex phosphoprotein assay. Cell lysates were obtained at different indicated time points. The values shown are the mean fluorescence intensities ± standard deviations from two independent experiments. ANOVA with Bonferroni post-test was used for statistical analyses of the data. “Reprinted from Microbial Pathogenesis, Sierra JC, Suarez G, Sha J, Baze W., Foltz SM., Chopra AK., Unraveling the mechanism of action of a new type III secretion system effector AexU from *Aeromonas hydrophila*., doi:10.1016/j.micpath.2010.05.011 © Copyright (2010), with permission from Elsevier.”

I observed an increase in the phosphorylation of c-Jun, I κ B α , and JNK in HeLa cells infected with the $\Delta aexU$ mutant of *A. hydrophila* at different time points when compared to HeLa cells infected with the WT strain (**Figure 4.4**), with statistically significant differences observed at 60 min for phospho c-Jun, at 30 and 60 min for phospho I κ B α , and at 60 and 90 min for phospho JNK. These results were confirmed by Western blot analysis using antibodies specific for the phosphorylated form of c-Jun and densitometric analysis of the Western blot (**Figure 4.5 Panels A & B**). For data presented in Figure 4.5, I used *A. hydrophila* with an Δact background to eliminate the strong biological effects associated with this toxin. As shown in **Figure 4.5 Panel B**, the intensity value of the bands (represented as fold increase) for phosphorylated c-Jun was lower in HeLa cells infected with the Δact mutant of *A. hydrophila*, when compared with findings in HeLa cells infected with the $\Delta act/\Delta aexU$ double mutant. Specifically between time points 30-120 min (approximately 4-5 fold increase), I observed statistically significant increases in phosphorylation of c-Jun when the *aexU* gene was deleted from *A. hydrophila*. These results supported our earlier observation (**Figure 4.4**) of AexU's involvement in down regulation of the JNK pathway.

Additionally, I measured I κ B α degradation pattern in HeLa cells infected with the Δact and $\Delta act/\Delta aexU$ mutant strains of *A. hydrophila* SSU (**Figure 4.5 Panels C & D**). After 40-80 min of co-culture, the intensity of the bands (represented as fold change and % decrease) for I κ B α was approximately 70-80% lower in HeLa cells infected with the $\Delta act/\Delta aexU$ mutant compared to that in host cells infected with the parental strain ($p < 0.01$). These data indicated higher degradation of I κ B α in $\Delta act/\Delta aexU$ mutant-infected HeLa cells and therefore correlating with a higher activation of NF- κ B (**Figure 4.5 Panel D**).

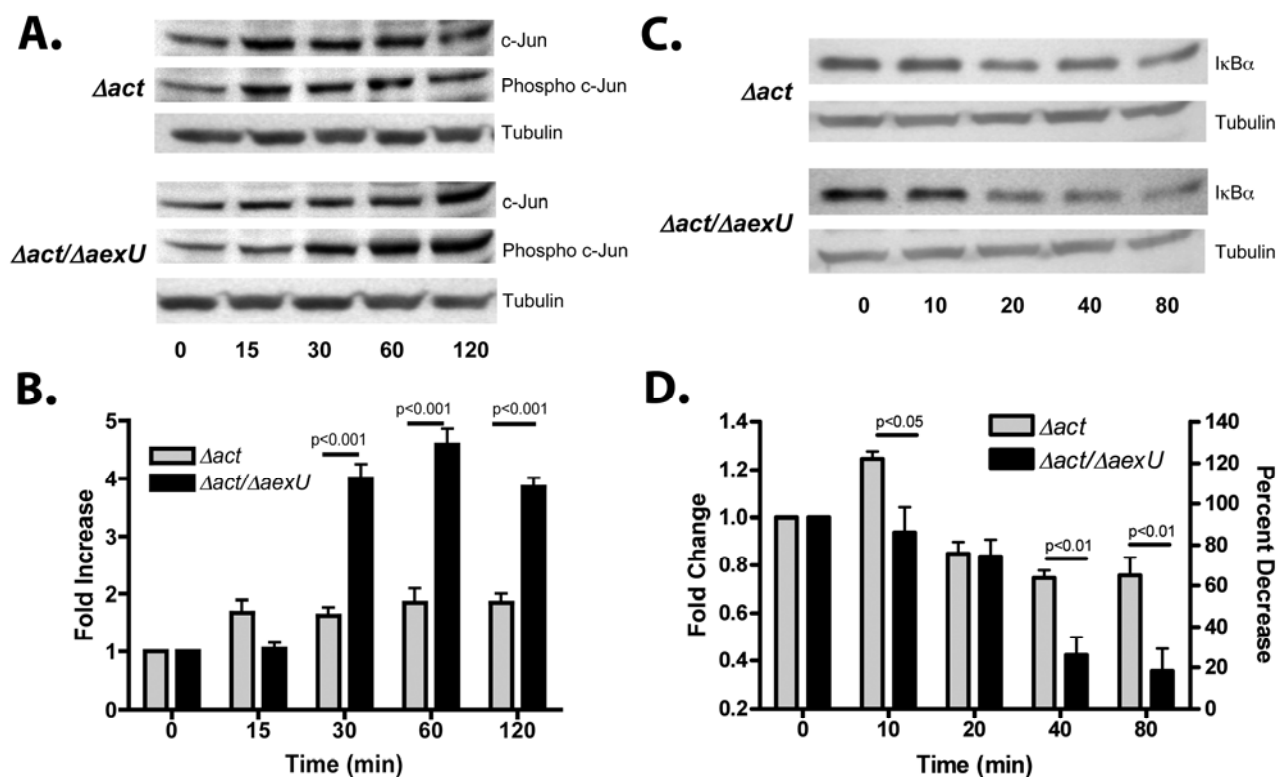


Figure 4.5: Phosphoprotein detection in HeLa cells by Western blot analysis. (A) Phosphorylated and total c-Jun was determined by Western blot analysis in lysates (10 μ g) of HeLa cells co-cultured with either the Δact or the $\Delta act/\Delta aexU$ mutant strain of *A. hydrophila* SSU at different time points. Also a Western Blot for β -tubulin is shown as a loading control. (B) The numbers shown on Y-axis represent the fold increase in density values of the bands for the phosphorylated c-Jun, normalized with the density values for the total c-Jun. The grey bars represent HeLa cells co-cultured with the Δact mutant of *A. hydrophila* SSU and the black bars represent cells co-cultured with the $\Delta act/\Delta aexU$ mutant. The figure represents mean fold increases in phospho c-jun \pm standard deviations from three independent experiments. ANOVA with Bonferroni post-test was used for statistical analyses of the data. (C) IκBα degradation was assessed by Western blot analysis using specific antibodies against IκBα. HeLa cells were co-cultured with indicated strains of *A. hydrophila* SSU and lysates (10 μ g) obtained at different time points were subjected to SDS-4–15% PAGE and Western blot analysis. Western blot for β -tubulin was used as a loading control. (D) The density values of the bands for IκBα were normalized with the density for β -tubulin and then 0 min time point was used as a base line to calculate the fold changes. The Y-axis values shown on the left side are the mean fold changes \pm standard deviations from three independent experiments and the Y-axis values on the right side represent percent decrease in IκBα degradation compared to the 0 min time point. ANOVA with Bonferroni post-test was used for statistical analyses of the data. “Reprinted from Microbial Pathogenesis, Sierra JC, Suarez G, Sha J, Baze W., Foltz SM., Chopra AK., Unraveling the mechanism of action of a new type III secretion system effector AexU from *Aeromonas hydrophila*., doi:10.1016/j.micpath.2010.05.011 © Copyright (2010), with permission from Elsevier.”

AexU inhibits secretion of IL-6 and IL-8 by HeLa cells co-cultured with *A. hydrophila* SSU

Non-immune cells, like epithelial cells, produce cytokines/chemokines and are the first line of defense against infections (70, 99). Pathogens have developed strategies to interfere with the NF- κ B signal transduction pathway, thus reducing the secretion of inflammatory cytokines/chemokines, such as IL-6, IL-8 and IL-1 β (99). Based on the ability of AexU to delay the degradation of I κ B α in HeLa cells (**Figure 4.5 Panels C & D**), I decided to measure the secretion of IL-6 and IL-8 by HeLa cells co-cultured with either the Δact or the $\Delta act/\Delta aexU$ mutant strain of *A. hydrophila*. As can be seen from **Figure 4.6**, IL-6 and IL-8 secretion was reduced in the HeLa cells co-cultured with the parental *A. hydrophila* (*act*-minus background) when compared to the secretion of these cytokines/chemokines by host cells infected with the double mutant $\Delta act/\Delta aexU$. These differences were statistically significant at 24 h after addition of the bacteria.

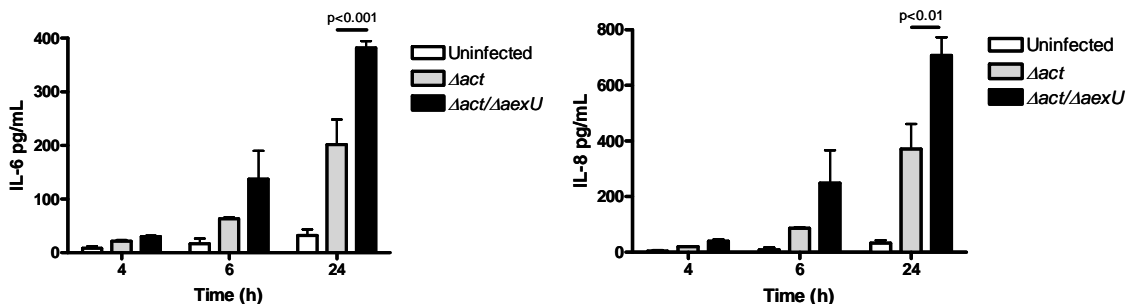


Figure 4.6: Secretion of IL-6 and IL-8 was evaluated in supernatants of HeLa cells co-cultured with either the Δact mutant of *A. hydrophila* SSU or its $\Delta act/\Delta aexU$ mutant. The figure shows mean concentrations in pg/mL of each of the cytokines/chemokines from three independent experiments \pm standard deviations. ANOVA with Bonferroni post-test was used for statistical analyses of the data. “Reprinted from Microbial Pathogenesis, Sierra JC, Suarez G, Sha J, Baze W., Foltz SM., Chopra AK., Unraveling the mechanism of action of a new type III secretion system effector AexU from *Aeromonas hydrophila*., doi:10.1016/j.micpath.2010.05.011 © Copyright (2010), with permission from Elsevier.”

Detection of *A. hydrophila* SSU in peripheral organs of mice resulting in tissue injury is mediated by AexU

To evaluate the role of AexU during *in vivo* infection, I challenged mice with a sub-lethal dose of either the Δact or the $\Delta act/\Delta aexU$ double mutant of *A. hydrophila*. Additionally, a group of mice that did not receive any bacteria (but given phosphate buffered saline [PBS]) was used as a negative control. Our earlier data indicated that the LD₅₀ of the Δact mutant bacteria was almost two logarithmic doses higher than the LD₅₀ of WT *A. hydrophila* (142). After 24 h and 48 h of infection, lungs, livers and spleens were collected, homogenized, and plated to measure the bacterial load. As seen in **Figure 4.7**, at the 48 h time point, there were no bacteria present in the organs of the animals infected with the $\Delta act/\Delta aexU$ mutant of *A. hydrophila*. In contrast, I recovered bacteria from the lungs, livers and spleens of mice infected with the parental strain. The number of parental strain bacteria recovered from different organs at 48 h was higher than the ones detected at 24 h post infection (data not shown).

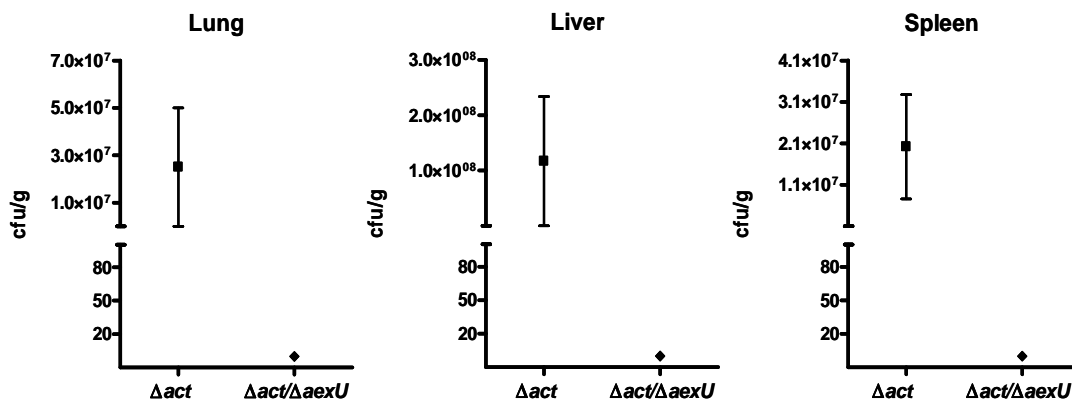


Figure 4.7: Detection of either the Δact mutant of *A. hydrophila* SSU (parental strain) or its $\Delta act/\Delta aexU$ mutant in mice after 48 h of i.p. injection with 8×10^5 cfu. The tissues from five animals per group were weighed and homogenized in water, and the serial dilutions were prepared and plated on LB agar plates. After overnight incubation at 37°C, the number of bacteria was quantified and the cfu per gram of tissue calculated. The data shown represent means with error bars from 5 animals. “Reprinted from Microbial Pathogenesis, Sierra JC, Suarez G, Sha J, Baze W., Foltz SM., Chopra AK., Unraveling the mechanism of action of a new type III secretion system effector AexU from *Aeromonas hydrophila*., doi:10.1016/j.micpath.2010.05.011 © Copyright (2010), with permission from Elsevier.”

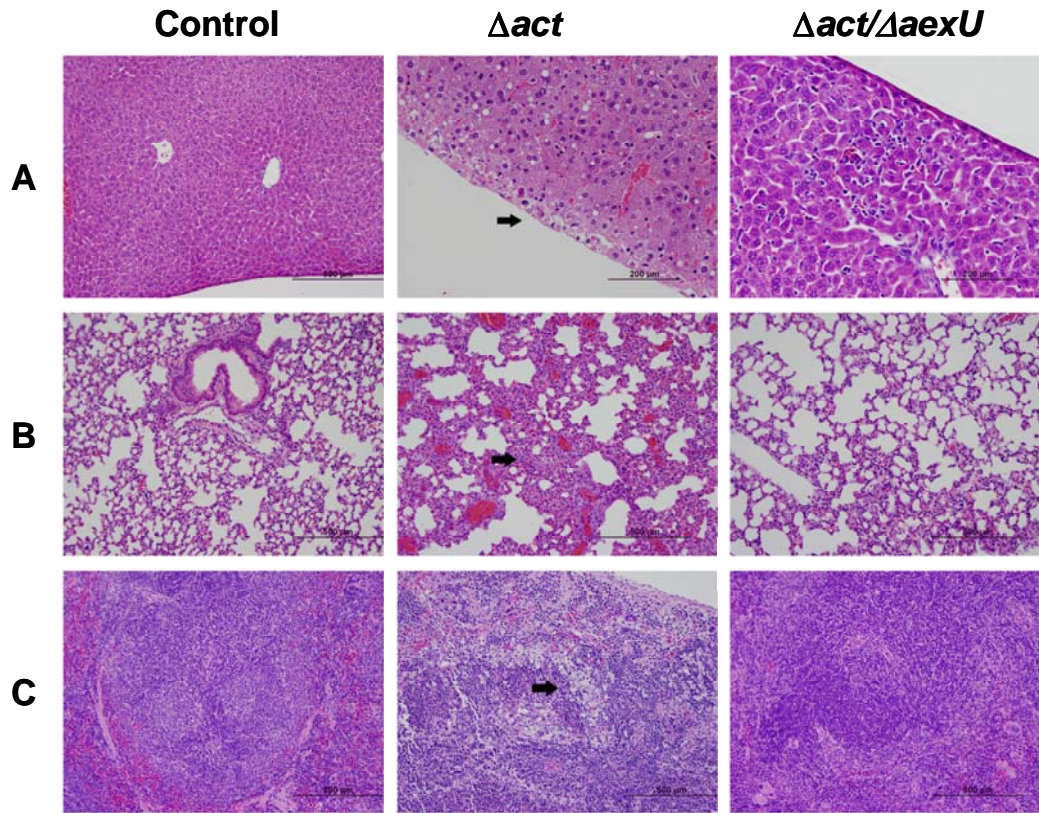


Figure 4.8: Histopathological analysis of tissues. Histopathological analysis of tissues from mice infected with 8×10^5 cfu of either the Δact mutant of *A. hydrophila* SSU (parental strain) or its $\Delta act/\Delta aexU$ mutant strain. Panel A shows tissue section from the liver, and the arrow indicates subcapsular necrosis (middle panel) present in animals infected with the Δact mutant strain. Panel B shows tissue section from the lung, and the expanded interstitium due to acute inflammatory infiltrates of mostly polymorphonuclear cells is indicated with the arrow (middle panel) in animal infected with the Δact mutant bacteria. Panel C shows tissue sections of the spleen, and lymphoid necrosis is indicated by the arrow in mice infected with the Δact mutant strain. No significant alterations were observed in the control group or the $\Delta act/\Delta aexU$ -infected animals. Magnification is represented by the bars (200 and 500 μm). “Reprinted from Microbial Pathogenesis, Sierra JC, Suarez G, Sha J, Baze W., Foltz SM., Chopra AK., Unraveling the mechanism of action of a new type III secretion system effector AexU from *Aeromonas hydrophila*., doi:10.1016/j.micpath.2010.05.011 © Copyright (2010), with permission from Elsevier.”

Tissues from the animals infected with either the parental or the $\Delta act/\Delta aexU$ mutant of *A. hydrophila* were also collected for histopathological analysis. The control group of mice (uninfected) exhibited normal pathology of liver, lung, and spleen (**Figure 4.8 A-C**). Various manifestations of tissue pathology were noted in the livers of mice infected with the parental (Δact) strain including minimal necrosis (**Figure 4.8 A, middle**

panel arrow) or inflammation of the capsule, minimal parenchymal inflammation and granuloma formation. In the lungs of mice infected with the parental strain, the most predominant findings were minimal to mild inflammation in the interstitium with infiltrates of polymorphonuclear cells (**Figure 4.8 middle panel arrow**). Bacteria were also observed in the perivascular region of the lungs. In the spleens, mild to moderate lymphoid necrosis of the white pulp and mild myeloid hyperplasia in the red pulp was noted in mice infected with the parental *A. hydrophila* strain (**Figure 4.8 C middle panel arrow**). The group of mice infected with the $\Delta act/\Delta aexU$ mutant presented significantly much reduced histopathological lesions in the liver, lung, and spleen when compared with the tissues from animals infected with the parental strain.

***A. hydrophila* $\Delta act/\Delta aexU$ isogenic mutant complemented with the ADPRT⁻/GAP⁻ mutated version of the *aexU* gene is more virulent than the one producing the native form of the *aexU* gene**

Previously, I reported the ability of AexU to ADP ribosylate eukaryotic proteins (126). One of the key structural features of ADPRTs is the Q/E-X-E motif, in which the catalytic glutamate (E) is located two residues downstream of a conserved glutamine (Q) or glutamate (E) residue (68, 74). It was shown that substituting catalytic glutamate to alanine significantly reduced the activity of multiple ADPRTs (47, 88). However, our studies with AexU indicated the presence of three Q-X-E motifs, one in the NH₂-terminal domain (aa residues 28-30) and two in the COOH-terminal domain (aa residues 261-263 and 419-421) (**Figure 4.1 Panel A**) (126). Based on this sequence analysis, I generated by site directed mutagenesis a mutated version of AexU in which all of the three glutamates were replaced by alanine. The recombinant protein with these three substitutions (AexU ADPRT123⁻) was tested by an *in vitro* ADPRT assay, as I previously described (133). No ADPRT activity was found to be associated with this mutated version of rAexU (data not shown). The stability of the mutated rAexU devoid of

ADPRT activity compared to that of the native protein was confirmed by Coomassie blue staining of the gel (**Figure 4.1 Panel B**).

In order to assess the contribution of ADPRT and GAP activity of AexU to the virulence of *A. hydrophila* *in vivo*, I expressed and produced the native and mutated versions of AexU *in trans* from *A. hydrophila* $\Delta act/\Delta aexU$ mutant by using the pBR322 vector. Mice were infected *via* the i.p. route with different strains of parental *A. hydrophila* that were complemented with either the native or the mutated form of AexU. As can be seen from **Figure 4.9 Panel A**, infection with bacteria producing the native

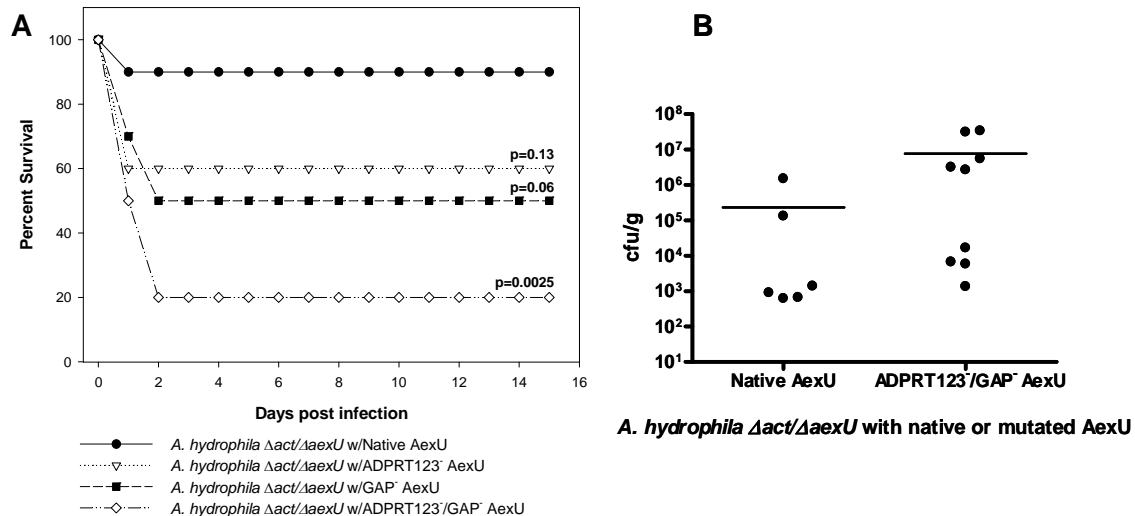


Figure 4.9: Survival curve and bacterial counts from mice infected with *A. hydrophila* $\Delta act/\Delta aexU$ mutant strains complemented with native, ADPRT123⁻, GAP⁻ or ADPRT123⁻/GAP⁻ versions of AexU. (A) Survival curves for mice infected with *A. hydrophila* $\Delta act/\Delta aexU$ mutant strains complemented with native, ADPRT123⁻, GAP⁻ or ADPRT123⁻/GAP⁻ versions of AexU. Deaths were recorded for 15 days. For statistical analysis, survival curves for each of the mutated version of AexU complemented strain was compared with *A. hydrophila* $\Delta act/\Delta aexU$ mutant complemented with the native version of AexU using the Kaplan–Meier survival estimates. These experiments were repeated three times with $n = 10$ in each group and a representative experiment is shown here. (B) Bacterial counts from the spleens of mice infected with *A. hydrophila* $\Delta act/\Delta aexU$ mutant strains complemented with the native or ADPRT123⁻/GAP⁻ mutant form of AexU. The tissues were homogenized, serial dilutions plated, the number of bacteria was quantified and the cfu per gram of tissue calculated. The bacterial counts in individual mouse spleen are shown and a horizontal line represents mean cfu. “Reprinted from Microbial Pathogenesis, Sierra JC, Suarez G, Sha J, Baze W., Foltz SM., Chopra AK., Unraveling the mechanism of action of a new type III secretion system effector AexU from *Aeromonas hydrophila*., doi:10.1016/j.micpath.2010.05.011 © Copyright (2010), with permission from Elsevier.”

form of AexU resulted in 90% survival of mice at a dose of 3×10^7 cfu. In contrast, only 20% ($p=0.0025$) survival of mice was observed in the group infected with *A. hydrophila* expressing the *aexU* gene that was devoid of ADPRT and GAP activities. Mice infected with the *A. hydrophila* strain producing AexU without ADPRT or GAP activity exhibited 60% ($p=0.13$) and 50% ($p=0.06$) survival, respectively. Although these percentages did not reach statistical significance, increased virulence of both ADPRT⁻ and GAP⁻ mutants compared to that of the parental bacteria was noted in at least three independent experiments with 10 animals per group.

Since our results in **Figure 4.7** indicated that AexU mediated spreading of *A. hydrophila* to peripheral organs (possibly by inhibiting bacterial phagocytosis and killing) (123), I decided to investigate the ability of *A. hydrophila* $\Delta act/\Delta aexU$ mutant producing the mutated form of AexU (ADPRT123⁻/GAP⁻) to be detected in the spleens of infected mice. After 48 h of infection, $\Delta act/\Delta aexU$ parental strain producing either the native or the mutated form of AexU could be detected in the spleen with latter in more numbers than the former, although the data did not reach statistical significance (**Figure 4.9 Panel B**).

Finally, I assessed cytokine/chemokine profiles in the spleens of mice infected with $\Delta act/\Delta aexU$ strain of *A. hydrophila* expressing gene for the native or mutated version of AexU (ADPRT123⁻/GAP⁻) by a multiplex bead array. As shown in **Figure 4.10**, I detected significant increases in amounts of IL-6, KC (human equivalent of IL-8), macrophage-inflammatory protein (MIP-2), IL-1 α , macrophage-colony stimulating factor (M-CSF), regulated upon activation, normal T cell expressed and secreted (RANTES), macrophage-chemoattractant protein (MCP-1), and MIP-1 α in spleens of animals infected with *A. hydrophila* $\Delta act/\Delta aexU$ mutant that produced AexU from pBR322 but devoid of ADPRT and GAP activities compared to animals that were

infected with the $\Delta act/\Delta aexU$ strain producing the native version of AexU from the vector pBR322. The levels of cytokines/chemokines in the latter group of animals were minimal and similar to the levels detected in animals which were uninfected and served as a negative control (data not shown). These data indicated that AexU devoid of intrinsic ADPRT and GAP activities triggered expression of several cytokine/chemokine genes.

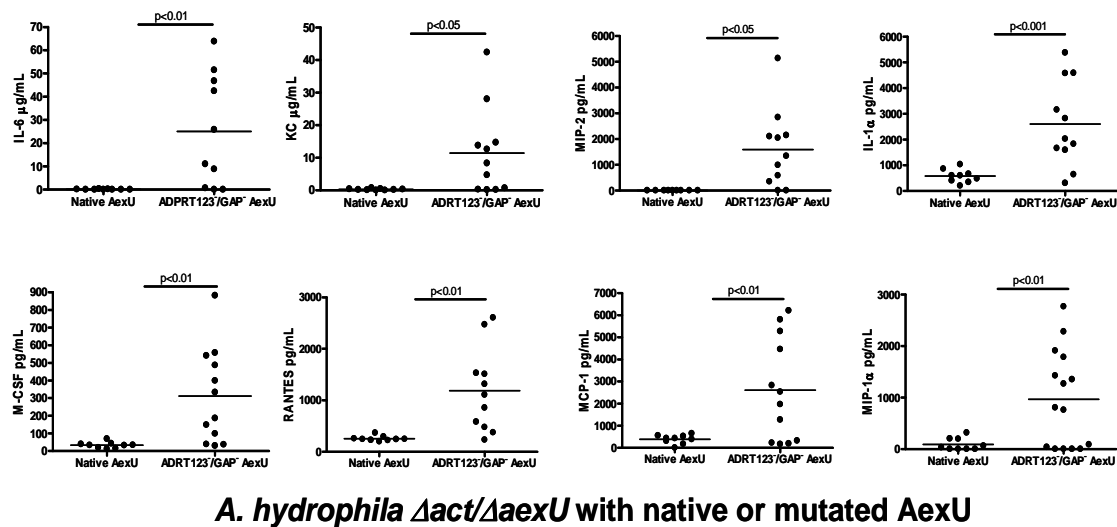


Figure 4.10: Cytokine/chemokine profile from the spleens of mice infected with *A. hydrophila* $\Delta act/\Delta aexU$ mutant complemented with the native or ADPRT123⁻/GAP⁻ mutant form of AexU. Spleen homogenates were analyzed by a multiplex bead array for mouse cytokines/chemokines. The concentration of each cytokine/chemokine was normalized based on the weight of the tissue for each animal. All of the values are expressed as pg/mL except for IL-6 and KC that are expressed as μg/mL. Minimal cytokine production was observed in tissues from uninfected mice (data not shown). The data for each mouse was plotted and the horizontal line represents mean values. Two-way ANOVA was used for statistical analyses of the data. “Reprinted from Microbial Pathogenesis, Sierra JC, Suarez G, Sha J, Baze W., Foltz SM., Chopra AK., Unraveling the mechanism of action of a new type III secretion system effector AexU from *Aeromonas hydrophila*., doi:10.1016/j.micpath.2010.05.011 © Copyright (2010), with permission from Elsevier.”

DISCUSSION

In this study, I showed that the T3SS effector AexU from *A. hydrophila* SSU has GAP activity towards RhoA, Rac1, and Cdc42, and that this activity was dependent on the arginine residue 145 located in a conserved motif shared by multiple GAPs.

Bacteria have developed strategies to alter the activation of host Rho GTPases, and, in the case of toxins with GAP activity, the inhibition of the small GTPases lead to alterations in the assembly and disassembly of the host actin cytoskeleton that is necessary for cell migration, phagocytosis or cell contraction (67, 75). Additionally, it has been reported that Rho GTPases control other cellular functions, such as JNK and p38 MAPK cascades and the transcription factors NF- κ B and SRF (serum-response factor) (75). Our data indicated that the down-regulation in the activity of this GTPase led to alterations in the actin cytoskeleton of HeLa Tet-Off cells transfected with the gene for AexU (**Figure 4.2**). These cells were rounded and detached from the culture plates.

When the HeLa Tet-Off cells were transfected with the plasmid encoding a mutated AexU_{GAP⁻}, the disruption of the actin cytoskeleton was significantly reduced, indicating that the GAP activity of AexU mediated the alterations in cell morphology. However, the MFI of the phalloidin staining did not reach the same level of the cells transfected with the empty vector (**Figure 4.2**), suggesting that AexU devoid of GAP activity possibly could trigger some other cell signaling events (possibly *via* ADPRT or other activity) in the host cells which might be contributing to actin reorganization as well. We will pursue such studies in the future. Indeed studies have shown that although the ADPRT activity associated with ExoS of *P. aeruginosa* contributed to host cell apoptosis (*via* caspase 3 activation) (80), mutant of ExoS devoid of this activity still induced apoptosis in host cells through a different pathway of IL-1 β maturation and secretion (58).

Our previous studies showed that the expression of the *aexU* gene in HeLa Tet-Off cells led to apoptosis mediated by caspase 3 and 9 (126). Here, I observed that HeLa Tet-Off cells expressing the gene encoding the mutated version of AexU (GAP⁻) had a significant decrease in the cytoplasmic nucleosomes as well as caspase 3 activation

compared to HeLa Tet-Off cells expressing the gene encoding native AexU (**Figure 4.3**). Based on these results, I deduced that GAP activity contributed to the induction of apoptosis, although the residual activity might be contributed by the ADPRT activity or other yet unidentified activity of AexU and will be tested in the future. Indeed, it has been reported that inhibition of the Rho function in different cell types induces apoptosis, as evidenced by the reduced expression of anti-apoptotic Bcl-2, increased levels of proapoptotic Bid, and the activation of caspase 3 (15, 16, 72, 96). Since AexU increases the intrinsic rate of GTP hydrolysis of Rho GTPases, specifically inactivating RhoA, Rac1, and Cdc42, our results supported the correlation between Rho protein inactivation and induction of apoptosis.

In addition to their important roles in the assembly and disassembly of the host actin cytoskeleton, Rho GTPases also regulate multiple biochemical pathways like JNK/SAPK and transcription factors, such as SRF, activator protein 1 (AP-1), and NF- κ B (39, 94, 95, 105). I provided evidence that AexU interfered with the phosphorylation of c-Jun, I κ B α and JNK, increasing them in HeLa cells co-cultured with the $\Delta aexU$ null mutant of *A. hydrophila*, when compared to the phosphorylation levels in host cells co-cultured with the parental bacteria (**Figures 4.4 and 4.5**). The ability to interfere with the degradation of I κ B α is an important strategy used by bacterial pathogens to inhibit the activation of NF- κ B (138). Additionally, alterations in the activation state of RhoA, Rac1, and Cdc42 can also inhibit the activity of NF- κ B (105).

Here I reported the ability of AexU from *A. hydrophila* to inhibit the activation of NF- κ B through inactivation of Rho GTPases, as well as through the inhibition of I κ B α degradation. This is an important tool for bacteria because NF- κ B regulates the transcription of a large number of genes involved in immune and inflammatory responses. In agreement with this, I observed a significant decrease in the secretion of IL-

6 and IL-8 from HeLa cells co-cultured with the parental bacteria, when compared to findings with the mutant strain lacking the *aexU* gene (**Figure 4.6**). One of the functional consequences of this repression in the secretion of proinflammatory cytokines/chemokines could be a delay in the recruitment of phagocytic cells to the infection site and the development of a protective immune response allowing bacteria to multiply and subsequently to invade other tissues. This scenario is supported by our previous studies showing a significant increase in the survival of mice infected with an $\Delta aexU$ isogenic mutant strain of *A. hydrophila*, when compared to that of animals infected with the WT strain (123).

Histopathological analysis and bacterial load of the tissues from mice infected with either the parental or the $\Delta aexU$ mutant of *A. hydrophila* showed significant differences (**Figures 4.7 and 4.8**), with rapid clearing of the mutant from mouse organs and exhibiting minimal histological lesions. On the other hand, organs from the parental bacteria-infected animals showed inflammation of the interstitium of the lungs and necrosis of the spleens and livers, as we reported earlier in mice infected with WT *A. hydrophila* (118, 120). Our findings supported an important role of AexU in bacterial survival during *in vivo* infection with *A. hydrophila*.

By using the $\Delta act/\Delta aexU$ mutant strain of *A. hydrophila* complemented with the native or the mutated form of AexU, I was able to show that elimination of ADPRT and GAP activities from AexU resulted in increased virulence of the bacteria (**Figure 4.9 A**). These data suggested there could be an additional activity(ies) that is modulated by the two known intrinsic activities of AexU (i.e., ADPRT and GAP) and needs to be further studied. We were intrigued by our data showing that animals infected with the $\Delta act/\Delta aexU$ mutant complemented with the *aexU* gene devoid of ADPRT and GAP activities had bacteria present in the spleens (**Figure 4.9 B**).

These were surprising results, considering our earlier data showing that the $\Delta act/\Delta aexU$ mutant of *A. hydrophila* was rapidly cleared from mouse organs (**Figure 4.7**). Generally speaking, this $\Delta act/\Delta aexU$ mutant should behave similar to the complemented strain in which the *aexU* gene devoid of ADPRT and GAP activities was expressed *in trans*. However, it must be kept in mind that in the $\Delta act/\Delta aexU$ null mutant, AexU synthesis is abrogated, while in the complemented strain, AexU, albeit missing ADPRT and GAP activities, was still present. Since, we previously showed that AexU inhibits the phagocytic activity of murine macrophages (123), it is conceivable that mutated AexU without its intrinsic ADPRT and GAP activities still retains its antiphagocytic ability, resulting in spreading of the complemented strain to the spleen (**Figure 4.9 B**).

At the same time, those mice infected with the ADPRT123⁻/GAP⁻ mutant of AexU producing strain of *A. hydrophila* had increased production of IL-1 α , IL-6, KC, MCP-1, M-CSF, MIP-1 α , MIP-2, and RANTES in the spleen when compared to mice infected with the strain expressing and producing the native form of AexU. However, this increased cytokine/chemokine production did not have a beneficial effect during the infection in terms of increasing the survivability of animals but had a detrimental effect resulting in high mortality in mice.

It is known that the pro-inflammatory cytokine IL-1 increases the ability of endothelial cells, macrophages, and fibroblast to secrete chemokines like IL-8 and MCP-1 that enhance the migration of macrophages and granulocytes to the site of infection (45). Likewise, RANTES is a chemoattractant and mediates the trafficking and homing of T cells, granulocytes, NK cells and monocytes, and MIP-1 α promotes the local influx of neutrophils (24, 85). Although, the induction of pro-inflammatory responses mediated by cytokines/chemokines is one of the strategies used by the host to overcome infections,

when this kind of response is excessive and uncontrolled, it could lead to detrimental effects (45).

In particular, the systemic inflammatory syndrome is characterized by excessive production of pro-inflammatory mediators that include IL-6, MIP-2, MCP-1, KC, eotaxin and tumor necrosis factor (101). During sepsis, an increased synthesis and secretion of these mediators can cause an elevated systemic inflammation resulting in tissue injury and multiple organ failure leading to septic shock and finally death (35). As I previously mentioned, AexU is able to down-regulate the secretion of cytokines *in vitro* and also hinders the activation of NF- κ B. Consequently, by eliminating the two known activities associated with AexU (ADPRT and GAP) there is an increased production of pro-inflammatory cytokines/chemokines, resulting in increased mortality of the mice.

Another example of the activation of pro-inflammatory cytokines, like IL-1 β , mediated by the T3SS effector devoid of ADPRT activity is ExoS produced by *P. aeruginosa* (58). It has been shown that ExoS negatively regulates the maturation of IL-1 β mediated by Caspase 1, and this effect is dependent on the presence of its ADPRT activity. Consequently, mature IL-1 β could be detected in the bronchoalveolar lavage fluid (BALF) samples of mice infected with *P. aeruginosa* Δ *exoS* mutant and in samples from mice infected with the Δ *exoS* mutant of *P. aeruginosa* that was complemented with ExoS defective in ADPRT activity (58). In this context, caspase 1 is activated through the Nod-like receptors that are part of a multiprotein complex called “inflammasomes”. Activation of caspase 1 leads to pyroptosis, which is a cell death program characterized by cell membrane permeabilization and IL-1 β secretion (13). Importantly, AexU devoid of ADPRT and GAP activities of *A. hydrophila* behaved differently compared to that of ExoS without the ADPRT activity. The former upregulated the production of several cytokines/chemokines with no effect on IL-1 β secretion.

In summary, I observed a reduction in apoptosis and in the alterations of the actin cytoskeleton of HeLa cells in response to inactivation of GAP activity of AexU. I provided first evidence that loss in ADPRT and GAP activities of AexU resulted in increased virulence of the $\Delta aexU$ mutant of *A. hydrophila* that expressed this mutated version of the *aexU* gene, by triggering production of several cytokines/chemokines in mice.

Conclusions

- Recombinant purified AexU full-length and its NH₂- and COOH-terminal domains possess ADRT activity.
- AexU functions as a GTPase-activating protein for RhoA, Rac1 and Cdc42. Site directed mutagenesis in the arginine finger of AexU showed that arginine residue at position 145 is responsible for the catalytic activity of AexU.
- Microscopic analysis after staining with fluorescent phalloidin showed that HeLa Tet-Off cells expressing and producing AexU had rounded cell morphology. This alteration in the actin cytoskeleton of HeLa Tet-Off cells is associated with the GAP activity because HeLa cells transfected with the gene encoding the mutated version of AexU for GAP activity exhibited an actin filament network similar to the cells transfected with the vector alone.
- Evaluation by transmission electron microscopy indicated cytotoxic changes characteristic of early and/or late apoptosis in HeLa Tet-Off cells producing AexU. In agreement with these changes, there was decreased mitochondrial activity, increased cytoplasmic nucleosomes and increased activation of caspase 3 and caspase 9 as compared to HeLa Tet-Off cells transfected with the empty vector.
- Significant reduction in the cytoplasmic nucleosomes as well as in caspase 3 activation was evident in HeLa Tet-Off cells transfected with the mutated version of AexU for GAP activity when compared with cells transfected with the gene encoding native AexU.
- AexU inhibits the phosphorylation of c-jun and I κ B α in normal HeLa cells co-cultured with *A. hydrophila* SSU. In agreement with the delay in the degradation of I κ B α

mediated by AexU, there was also an inhibition in the secretion of IL-6 and IL-8 from HeLa cells.

- Rapid clearance from lung, liver and spleen was evident in mice infected with the $\Delta aexU$ mutant of *A. hydrophila*. In contrast, there was a high number of bacteria in the organs of mice infected with the parental strain. The organs from mice infected with the parental strain showed inflammation of the interstitium of the lungs and necrosis of the spleens and livers. On the other hand, organs from mice infected with the $\Delta aexU$ mutant exhibited minimal histological lesions.
- *A. hydrophila* $\Delta act/\Delta aexU$ isogenic mutant complemented with the mutated version of the *aexU* gene for ADPRT⁻ and GAP⁻ activities is more virulent in the mice model of infection than the one producing the native form of the *aexU* gene. At the same time, there was a significant increase in the production of multiple cytokines (IL-6, KC, MIP-2, IL-1 α , M-CSF, RANTES, MCP-1 and MIP-1 α) in the spleens of mice infected with *A. hydrophila* $\Delta act/\Delta aexU$ that produced AexU devoid of ADPRT and GAP activities compared with animals infected with the strain producing the native version of AexU. These data indicated that either such a mutated AexU is a potent inducer of them or that AexU possesses yet another unknown activity that is modulated by ADPRT and GAP activities and results in this aberrant cytokine/chemokine production responsible for increased animal death.

Future Directions

- To identify the mechanism of action mediating an increased virulence of *A. hydrophila* producing the mutated form of AexU, which is devoid of ADPRT and GAP activities. This could be the result of a still unidentified activity associated with the toxin.
- To identify the host cell protein target(s) for the ADPRT activity of AexU. Such studies will help us in determining if AexU could selectively target a particular cell type and also if a particular signaling pathway is being altered by the ADPRT activity of AexU.
- To determine the specific intracellular localization of AexU once translocated by the T3SS of *A. hydrophila*. Identification of trafficking pathways used by AexU will allow a better understanding of the biological effects associated with this toxin as well as the target protein(s) in eukaryotic cells with which AexU interacts.

References

1. **Abbott, S. L., W. K. Cheung, and J. M. Janda.** 2003. The genus *Aeromonas*: biochemical characteristics, atypical reactions, and phenotypic identification schemes. *J Clin Microbiol* **41**:2348-2357.
2. **Adrain, C., and S. J. Martin.** 2001. The mitochondrial apoptosome: a killer unleashed by the cytochrome seas. *Trends Biochem Sci* **26**:390-397.
3. **Akeda, Y., and J. E. Galan.** 2005. Chaperone release and unfolding of substrates in type III secretion. *Nature* **437**:911-915.
4. **Aktories, K., and J. T. Barbieri.** 2005. Bacterial cytotoxins: targeting eukaryotic switches. *Nat Rev Microbiol* **3**:397-410.
5. **Aktories, K., M. Barmann, I. Ohishi, S. Tsuyama, K. H. Jakobs, and E. Habermann.** 1986. Botulinum C2 toxin ADP-ribosylates actin. *Nature* **322**:390-392.
6. **Aktories, K., G. Schmidt, and I. Just.** 2000. Rho GTPases as targets of bacterial protein toxins. *Biol Chem* **381**:421-426.
7. **Aktories, K., and A. Wegner.** 1989. ADP-ribosylation of actin by clostridial toxins. *J Cell Biol* **109**:1385-1387.
8. **Altwegg, M., G. Martinetti Lucchini, J. Luthy-Hottenstein, and M. Rohrbach.** 1991. *Aeromonas*-associated gastroenteritis after consumption of contaminated shrimp. *Eur J Clin Microbiol Infect Dis* **10**:44-45.
9. **Backert, S., and M. Selbach.** 2008. Role of type IV secretion in *Helicobacter pylori* pathogenesis. *Cell Microbiol* **10**:1573-1581.
10. **Barbieri, J. T., M. J. Riese, and K. Aktories.** 2002. Bacterial toxins that modify the actin cytoskeleton. *Annu Rev Cell Dev Biol* **18**:315-344.
11. **Barbieri, J. T., and J. Sun.** 2004. *Pseudomonas aeruginosa* ExoS and ExoT. *Rev Physiol Biochem Pharmacol* **152**:79-92.
12. **Barillo, D. J., A. T. McManus, W. G. Cioffi, W. F. McManus, S. H. Kim, and B. A. Pruitt, Jr.** 1996. *Aeromonas* bacteraemia in burn patients. *Burns* **22**:48-52.
13. **Bergsbaken, T., S. L. Fink, and B. T. Cookson.** 2009. Pyroptosis: host cell death and inflammation. *Nat Rev Microbiol* **7**:99-109.
14. **Birtalan, S. C., R. M. Phillips, and P. Ghosh.** 2002. Three-dimensional secretion signals in chaperone-effector complexes of bacterial pathogens. *Mol Cell* **9**:971-980.
15. **Blanco-Colio, L. M., A. Villa, M. Ortego, M. A. Hernandez-Presa, A. Pascual, J. J. Plaza, and J. Egido.** 2002. 3-Hydroxy-3-methyl-glutaryl coenzyme A reductase inhibitors, atorvastatin and simvastatin, induce apoptosis of vascular smooth muscle cells by downregulation of Bcl-2 expression and Rho A prenylation. *Atherosclerosis* **161**:17-26.
16. **Bobak, D. A.** 1999. Clostridial toxins: molecular probes of Rho-dependent signaling and apoptosis. *Mol Cell Biochem* **193**:37-42.

17. **Bogdanovic, R., M. Cobeljic, M. Markovic, V. Nikolic, M. Ognjanovic, L. Sarjanovic, and D. Makic.** 1991. Haemolytic-uraemic syndrome associated with *Aeromonas hydrophila* enterocolitis. *Pediatr Nephrol* **5**:293-295.
18. **Braun, M., K. Stuber, Y. Schlatter, T. Wahli, P. Kuhnert, and J. Frey.** 2002. Characterization of an ADP-ribosyltransferase toxin (AexT) from *Aeromonas salmonicida* subsp. *salmonicida*. *J Bacteriol* **184**:1851-1858.
19. **Brouqui, P., and D. Raoult.** 2001. Endocarditis due to rare and fastidious bacteria. *Clin Microbiol Rev* **14**:177-207.
20. **Burr, S. E., K. Stuber, and J. Frey.** 2003. The ADP-ribosylating toxin, AexT, from *Aeromonas salmonicida* subsp. *salmonicida* is translocated via a type III secretion pathway. *J Bacteriol* **185**:6583-6591.
21. **Burr, S. E., K. Stuber, T. Wahli, and J. Frey.** 2002. Evidence for a type III secretion system in *Aeromonas salmonicida* subsp. *salmonicida*. *J Bacteriol* **184**:5966-5970.
22. **Cascales, E.** 2008. The type VI secretion toolkit. *EMBO Rep* **9**:735-741.
23. **Cascales, E., and P. J. Christie.** 2003. The versatile bacterial type IV secretion systems. *Nat Rev Microbiol* **1**:137-149.
24. **Cavaillon, J. M., M. Adib-Conquy, C. Fitting, C. Adrie, and D. Payen.** 2003. Cytokine cascade in sepsis. *Scand J Infect Dis* **35**:535-544.
25. **Challapalli, M., B. R. Tess, D. G. Cunningham, A. K. Chopra, and C. W. Houston.** 1988. *Aeromonas*-associated diarrhea in children. *Pediatr Infect Dis J* **7**:693-698.
26. **Chardin, P., P. Boquet, P. Madaule, M. R. Popoff, E. J. Rubin, and D. M. Gill.** 1989. The mammalian G protein rhoC is ADP-ribosylated by *Clostridium botulinum* exoenzyme C3 and affects actin microfilaments in Vero cells. *Embo J* **8**:1087-1092.
27. **Chauret, C., C. Volk, R. Creason, J. Jarosh, J. Robinson, and C. Warnes.** 2001. Detection of *Aeromonas hydrophila* in a drinking-water distribution system: a field and pilot study. *Can J Microbiol* **47**:782-786.
28. **Choi, J. P., S. O. Lee, H. H. Kwon, Y. G. Kwak, S. H. Choi, S. K. Lim, M. N. Kim, J. Y. Jeong, S. H. Choi, J. H. Woo, and Y. S. Kim.** 2008. Clinical significance of spontaneous *Aeromonas* bacterial peritonitis in cirrhotic patients: a matched case-control study. *Clin Infect Dis* **47**:66-72.
29. **Chopra, A. K., J. Graf, A. J. Horneman, and J. A. Johnson.** 2009. Virulence factor-activity relationships (VFAR) with specific emphasis on *Aeromonas* species (spp.). *J Water Health* **7 Suppl 1**:S29-54.
30. **Chopra, A. K., and C. W. Houston.** 1999. Enterotoxins in *Aeromonas*-associated gastroenteritis. *Microbes Infect* **1**:1129-1137.
31. **Chopra, A. K., and C. W. Houston.** 1989. Purification and partial characterization of a cytotoxic enterotoxin produced by *Aeromonas hydrophila*. *Can J Microbiol* **35**:719-727.
32. **Chopra, A. K., C. W. Houston, J. W. Peterson, and G. F. Jin.** 1993. Cloning, expression, and sequence analysis of a cytolytic enterotoxin gene from *Aeromonas hydrophila*. *Can J Microbiol* **39**:513-523.

33. **Chopra, A. K., J. W. Peterson, X. J. Xu, D. H. Coppenhaver, and C. W. Houston.** 1996. Molecular and biochemical characterization of a heat-labile cytotoxic enterotoxin from *Aeromonas hydrophila*. *Microb Pathog* **21**:357-377.
34. **Chopra, A. K., X. Xu, D. Ribardo, M. Gonzalez, K. Kuhl, J. W. Peterson, and C. W. Houston.** 2000. The cytotoxic enterotoxin of *Aeromonas hydrophila* induces proinflammatory cytokine production and activates arachidonic acid metabolism in macrophages. *Infect Immun* **68**:2808-2818.
35. **Cohen, J.** 2002. The immunopathogenesis of sepsis. *Nature* **420**:885-891.
36. **Coligan, J. E., B. E. Dunn, D. W. Speicher, and P. T. Wingfield (ed.).** 2002. Current protocols in protein science, vol. 2. John Wiley & Sons, Inc., New York.
37. **Coombes, B. K., M. J. Lowden, J. L. Bishop, M. E. Wickham, N. F. Brown, N. Duong, S. Osborne, O. Gal-Mor, and B. B. Finlay.** 2007. SseL is a salmonella-specific translocated effector integrated into the SsrB-controlled salmonella pathogenicity island 2 type III secretion system. *Infect Immun* **75**:574-580.
38. **Cornelis, G. R., and F. Van Gijsegem.** 2000. Assembly and function of type III secretory systems. *Annu Rev Microbiol* **54**:735-774.
39. **Coso, O. A., M. Chiariello, J. C. Yu, H. Teramoto, P. Crespo, N. Xu, T. Miki, and J. S. Gutkind.** 1995. The small GTP-binding proteins Rac1 and Cdc42 regulate the activity of the JNK/SAPK signaling pathway. *Cell* **81**:1137-1146.
40. **Dacanay, A., L. Knickle, K. S. Solanky, J. M. Boyd, J. A. Walter, L. L. Brown, S. C. Johnson, and M. Reith.** 2006. Contribution of the type III secretion system (TTSS) to virulence of *Aeromonas salmonicida* subsp. *salmonicida*. *Microbiology* **152**:1847-1856.
41. **Earnshaw, W. C., L. M. Martins, and S. H. Kaufmann.** 1999. Mammalian caspases: structure, activation, substrates, and functions during apoptosis. *Annu Rev Biochem* **68**:383-424.
42. **Edberg, S. C., F. A. Browne, and M. J. Allen.** 2007. Issues for microbial regulation: *Aeromonas* as a model. *Crit Rev Microbiol* **33**:89-100.
43. **Eremeeva, M. E., W. M. Ching, Y. Wu, D. J. Silverman, and G. A. Dasch.** 1998. Western blotting analysis of heat shock proteins of Rickettsiales and other eubacteria. *FEMS Microbiol Lett* **167**:229-237.
44. **Erova, T. E., A. A. Fadl, J. Sha, B. K. Khajanchi, L. L. Pillai, E. V. Kozlova, and A. K. Chopra.** 2006. Mutations within the catalytic motif of DNA adenine methyltransferase (Dam) of *Aeromonas hydrophila* cause the virulence of the Dam-overproducing strain to revert to that of the wild-type phenotype. *Infect Immun* **74**:5763-5772.
45. **Esch, T., and G. Stefano.** 2002. Proinflammation: a common denominator or initiator of different pathophysiological disease processes. *Med Sci Monit* **8**:HY1-9.
46. **Fadl, A. A., C. L. Galindo, J. Sha, T. E. Erova, C. W. Houston, J. P. Olano, and A. K. Chopra.** 2006. Deletion of the genes encoding the type III secretion system and cytotoxic enterotoxin alters host responses to *Aeromonas hydrophila* infection. *Microb Pathog* **40**:198-210.

47. **Fehr, D., S. E. Burr, M. Gibert, J. d'Alayer, J. Frey, and M. R. Popoff.** 2007. *Aeromonas* exoenzyme T of *Aeromonas salmonicida* is a bifunctional protein that targets the host cytoskeleton. *J Biol Chem* **282**:28843-28852.
48. **Fehr, D., C. Casanova, A. Liverman, H. Blazkova, K. Orth, D. Dobbelaere, J. Frey, and S. E. Burr.** 2006. AopP, a type III effector protein of *Aeromonas salmonicida*, inhibits the NF-kappaB signalling pathway. *Microbiology* **152**:2809-2818.
49. **Ferguson, M. R., X. J. Xu, C. W. Houston, J. W. Peterson, and A. K. Chopra.** 1995. Amino-acid residues involved in biological functions of the cytolytic enterotoxin from *Aeromonas hydrophila*. *Gene* **156**:79-83.
50. **Ferguson, M. R., X. J. Xu, C. W. Houston, J. W. Peterson, D. H. Coppenhaver, V. L. Popov, and A. K. Chopra.** 1997. Hyperproduction, purification, and mechanism of action of the cytotoxic enterotoxin produced by *Aeromonas hydrophila*. *Infect Immun* **65**:4299-4308.
51. **Figueras, M. J., M. J. Aldea, N. Fernandez, C. Aspiroz, A. Alperi, and J. Guarro.** 2007. *Aeromonas* hemolytic uremic syndrome. A case and a review of the literature. *Diagn Microbiol Infect Dis* **58**:231-234.
52. **Fiorentini, C., L. Falzano, S. Travaglione, and A. Fabbri.** 2003. Hijacking Rho GTPases by protein toxins and apoptosis: molecular strategies of pathogenic bacteria. *Cell Death Differ* **10**:147-152.
53. **Francis, M. S., H. Wolf-Watz, and A. Forsberg.** 2002. Regulation of type III secretion systems. *Curr Opin Microbiol* **5**:166-172.
54. **Frank, D. W.** 1997. The exoenzyme S regulon of *Pseudomonas aeruginosa*. *Mol Microbiol* **26**:621-629.
55. **Galan, J. E., and H. Wolf-Watz.** 2006. Protein delivery into eukaryotic cells by type III secretion machines. *Nature* **444**:567-573.
56. **Galindo, C. L., A. A. Fadl, J. Sha, C. Gutierrez, Jr., V. L. Popov, I. Boldogh, B. B. Aggarwal, and A. K. Chopra.** 2004. *Aeromonas hydrophila* cytotoxic enterotoxin activates mitogen-activated protein kinases and induces apoptosis in murine macrophages and human intestinal epithelial cells. *J Biol Chem* **279**:37597-37612.
57. **Galindo, C. L., J. Sha, D. A. Ribardo, A. A. Fadl, L. Pillai, and A. K. Chopra.** 2003. Identification of *Aeromonas hydrophila* cytotoxic enterotoxin-induced genes in macrophages using microarrays. *J Biol Chem* **278**:40198-40212.
58. **Galle, M., P. Schotte, M. Haegman, A. Wullaert, H. J. Yang, S. Jin, and R. Beyaert.** 2008. The *Pseudomonas aeruginosa* Type III secretion system plays a dual role in the regulation of caspase-1 mediated IL-1beta maturation. *J Cell Mol Med* **12**:1767-1776.
59. **Ganesan, A. K., D. W. Frank, R. P. Misra, G. Schmidt, and J. T. Barbieri.** 1998. *Pseudomonas aeruginosa* exoenzyme S ADP-ribosylates Ras at multiple sites. *J Biol Chem* **273**:7332-7337.
60. **Garcia, J. T., F. Ferracci, M. W. Jackson, S. S. Joseph, I. Pattis, L. R. Plano, W. Fischer, and G. V. Plano.** 2006. Measurement of effector protein injection by type III and type IV secretion systems by using a 13-residue phosphorylatable glycogen synthase kinase tag. *Infect Immun* **74**:5645-5657.

61. **Gerlach, R. G., and M. Hensel.** 2007. Protein secretion systems and adhesins: the molecular armory of Gram-negative pathogens. *Int J Med Microbiol* **297**:401-415.
62. **Ghenghesh, K. S., S. F. Ahmed, R. A. El-Khalek, A. Al-Gendy, and J. Klena.** 2008. *Aeromonas*-associated infections in developing countries. *J Infect Dev Ctries* **2**:81-98.
63. **Ghosh, P.** 2004. Process of protein transport by the type III secretion system. *Microbiol Mol Biol Rev* **68**:771-795.
64. **Goehring, U. M., G. Schmidt, K. J. Pederson, K. Aktories, and J. T. Barbieri.** 1999. The N-terminal domain of *Pseudomonas aeruginosa* exoenzyme S is a GTPase-activating protein for Rho GTPases. *J Biol Chem* **274**:36369-36372.
65. **Gold, W. L., and I. E. Salit.** 1993. *Aeromonas hydrophila* infections of skin and soft tissue: report of 11 cases and review. *Clin Infect Dis* **16**:69-74.
66. **Hakansson, S., K. Schesser, C. Persson, E. E. Galyov, R. Rosqvist, F. Homble, and H. Wolf-Watz.** 1996. The YopB protein of *Yersinia pseudotuberculosis* is essential for the translocation of Yop effector proteins across the target cell plasma membrane and displays a contact-dependent membrane disrupting activity. *Embo J* **15**:5812-5823.
67. **Hall, A.** 1998. Rho GTPases and the actin cytoskeleton. *Science* **279**:509-514.
68. **Han, S., and J. A. Tainer.** 2002. The ARTT motif and a unified structural understanding of substrate recognition in ADP-ribosylating bacterial toxins and eukaryotic ADP-ribosyltransferases. *Int J Med Microbiol* **291**:523-529.
69. **Hanninen, M. L., S. Salmi, L. Mattila, R. Taipainen, and A. Siitonen.** 1995. Association of *Aeromonas* spp. with travellers' diarrhoea in Finland. *J Med Microbiol* **42**:26-31.
70. **Hedges, S. R., W. W. Agace, and C. Svanborg.** 1995. Epithelial cytokine responses and mucosal cytokine networks. *Trends Microbiol* **3**:266-270.
71. **Henriksson, M. L., C. Sundin, A. L. Jansson, A. Forsberg, R. H. Palmer, and B. Hallberg.** 2002. Exoenzyme S shows selective ADP-ribosylation and GTPase-activating protein (GAP) activities towards small GTPases in vivo. *Biochem J* **367**:617-628.
72. **Hippenstiel, S., B. Schmeck, P. D. N'Guessan, J. Seybold, M. Krull, K. Preissner, C. V. Eichel-Streiber, and N. Suttorp.** 2002. Rho protein inactivation induced apoptosis of cultured human endothelial cells. *Am J Physiol Lung Cell Mol Physiol* **283**:L830-838.
73. **Hiransuthikul, N., W. Tantisiriwat, K. Lertutsahakul, A. Vibhagool, and P. Boonma.** 2005. Skin and soft-tissue infections among tsunami survivors in southern Thailand. *Clin Infect Dis* **41**:e93-96.
74. **Holbourn, K. P., C. C. Shone, and K. R. Acharya.** 2006. A family of killer toxins. Exploring the mechanism of ADP-ribosylating toxins. *Febs J* **273**:4579-4593.
75. **Jaffe, A. B., and A. Hall.** 2005. Rho GTPases: biochemistry and biology. *Annu Rev Cell Dev Biol* **21**:247-269.

76. **Janda, J. M., and S. L. Abbott.** 1998. Evolving concepts regarding the genus *Aeromonas*: an expanding Panorama of species, disease presentations, and unanswered questions. *Clin Infect Dis* **27**:332-344.
77. **Janda, J. M., and S. L. Abbott.** 2010. The genus *Aeromonas*: taxonomy, pathogenicity, and infection. *Clin Microbiol Rev* **23**:35-73.
78. **Janda, J. M., L. S. Guthertz, R. P. Kokka, and T. Shimada.** 1994. *Aeromonas* species in septicemia: laboratory characteristics and clinical observations. *Clin Infect Dis* **19**:77-83.
79. **Johnson, T. L., J. Abendroth, W. G. Hol, and M. Sandkvist.** 2006. Type II secretion: from structure to function. *FEMS Microbiol Lett* **255**:175-186.
80. **Kaufman, M. R., J. Jia, L. Zeng, U. Ha, M. Chow, and S. Jin.** 2000. *Pseudomonas aeruginosa* mediated apoptosis requires the ADP-ribosylating activity of exoS. *Microbiology* **146** (Pt 10):2531-2541.
81. **Kirov, S. M.** 1993. The public health significance of *Aeromonas* spp. in foods. *Int J Food Microbiol* **20**:179-198.
82. **Krall, R., G. Schmidt, K. Aktories, and J. T. Barbieri.** 2000. *Pseudomonas aeruginosa* ExoT is a Rho GTPase-activating protein. *Infect Immun* **68**:6066-6068.
83. **Kuhn, I., M. J. Albert, M. Ansaruzzaman, N. A. Bhuiyan, S. A. Alabi, M. S. Islam, P. K. Neogi, G. Huys, P. Janssen, K. Kersters, and R. Mollby.** 1997. Characterization of *Aeromonas* spp. isolated from humans with diarrhea, from healthy controls, and from surface water in Bangladesh. *J Clin Microbiol* **35**:369-373.
84. **Kurita, A., H. Gotoh, M. Eguchi, N. Okada, S. Matsuura, H. Matsui, H. Danbara, and Y. Kikuchi.** 2003. Intracellular expression of the *Salmonella* plasmid virulence protein, SpvB, causes apoptotic cell death in eukaryotic cells. *Microb Pathog* **35**:43-48.
85. **Lee, S. C., M. E. Brummet, S. Shahabuddin, T. G. Woodworth, S. N. Georas, K. M. Leiferman, S. C. Gilman, C. Stellato, R. P. Gladue, R. P. Schleimer, and L. A. Beck.** 2000. Cutaneous injection of human subjects with macrophage inflammatory protein-1 alpha induces significant recruitment of neutrophils and monocytes. *J Immunol* **164**:3392-3401.
86. **Lesnick, M. L., N. E. Reiner, J. Fierer, and D. G. Guiney.** 2001. The *Salmonella* spvB virulence gene encodes an enzyme that ADP-ribosylates actin and destabilizes the cytoskeleton of eukaryotic cells. *Mol Microbiol* **39**:1464-1470.
87. **Litvak, Y., and Z. Selinger.** 2007. *Aeromonas salmonicida* Toxin AexT Has a Rho Family GTPase-Activating Protein Domain. *J Bacteriol* **189**:2558-2560.
88. **Liu, S., S. M. Kulich, and J. T. Barbieri.** 1996. Identification of glutamic acid 381 as a candidate active site residue of *Pseudomonas aeruginosa* exoenzyme S. *Biochemistry* **35**:2754-2758.
89. **Lynch, M. J., S. Swift, D. F. Kirke, C. W. Keevil, C. E. Dodd, and P. Williams.** 2002. The regulation of biofilm development by quorum sensing in *Aeromonas hydrophila*. *Environ Microbiol* **4**:18-28.

90. **Marlovits, T. C., and C. E. Stebbins.** Type III secretion systems shape up as they ship out. *Curr Opin Microbiol* **13**:47-52.
91. **Maurelli, A. T., B. Blackmon, and R. Curtiss, 3rd.** 1984. Temperature-dependent expression of virulence genes in *Shigella* species. *Infect Immun* **43**:195-201.
92. **Merino, S., A. Aguilar, M. M. Noguerras, M. Regue, S. Swift, and J. M. Tomas.** 1999. Cloning, sequencing, and role in virulence of two phospholipases (A1 and C) from mesophilic *Aeromonas* sp. serogroup O:34. *Infect Immun* **67**:4008-4013.
93. **Merino, S., X. Rubires, S. Knochel, and J. M. Tomas.** 1995. Emerging pathogens: *Aeromonas* spp. *Int J Food Microbiol* **28**:157-168.
94. **Minden, A., A. Lin, F. X. Claret, A. Abo, and M. Karin.** 1995. Selective activation of the JNK signaling cascade and c-Jun transcriptional activity by the small GTPases Rac and Cdc42Hs. *Cell* **81**:1147-1157.
95. **Montaner, S., R. Perona, L. Saniger, and J. C. Lacal.** 1998. Multiple signalling pathways lead to the activation of the nuclear factor kappaB by the Rho family of GTPases. *J Biol Chem* **273**:12779-12785.
96. **Moorman, J. P., D. A. Bobak, and C. S. Hahn.** 1996. Inactivation of the small GTP binding protein Rho induces multinucleate cell formation and apoptosis in murine T lymphoma EL4. *J Immunol* **156**:4146-4153.
97. **Moraes, T. F., T. Spreter, and N. C. Strynadka.** 2008. Piecing together the type III injectisome of bacterial pathogens. *Curr Opin Struct Biol* **18**:258-266.
98. **Mukhopadhyay, C., A. Bhargava, and A. Ayyagari.** 2003. *Aeromonas hydrophila* and aspiration pneumonia: a diverse presentation. *Yonsei Med J* **44**:1087-1090.
99. **Naumann, M.** 2000. Nuclear factor-kappa B activation and innate immune response in microbial pathogen infection. *Biochem Pharmacol* **60**:1109-1114.
100. **O'Brien, M. C., and W. E. Bolton.** 1995. Comparison of cell viability probes compatible with fixation and permeabilization for combined surface and intracellular staining in flow cytometry. *Cytometry* **19**:243-255.
101. **Osuchowski, M. F., K. Welch, J. Siddiqui, and D. G. Remick.** 2006. Circulating cytokine/inhibitor profiles reshape the understanding of the SIRS/CARS continuum in sepsis and predict mortality. *J Immunol* **177**:1967-1974.
102. **Palu, A. P., L. M. Gomes, M. A. Miguel, I. T. Balassiano, M. L. Queiroz, A. C. Freitas-Almeida, and S. S. de Oliveira.** 2006. Antimicrobial resistance in food and clinical *Aeromonas* isolates. *Food Microbiol* **23**:504-509.
103. **Pazzaglia, G., R. B. Sack, E. Salazar, A. Yi, E. Chea, R. Leon-Barua, C. E. Guerrero, and J. Palomino.** 1991. High frequency of coinfecting enteropathogens in *Aeromonas*-associated diarrhea of hospitalized Peruvian infants. *J Clin Microbiol* **29**:1151-1156.
104. **Pederson, K. J., A. J. Vallis, K. Aktories, D. W. Frank, and J. T. Barbieri.** 1999. The amino-terminal domain of *Pseudomonas aeruginosa* ExoS disrupts actin filaments via small-molecular-weight GTP-binding proteins. *Mol Microbiol* **32**:393-401.

105. **Perona, R., S. Montaner, L. Saniger, I. Sanchez-Perez, R. Bravo, and J. C. Lacal.** 1997. Activation of the nuclear factor-kappaB by Rho, CDC42, and Rac-1 proteins. *Genes Dev* **11**:463-475.
106. **Popoff, M. Y., C. Coynault, K. M., and L. M.** 1981. Polynucleotide sequence relatedness among motile *Aeromonas* species. *Current Microbiology* **5**:109-114.
107. **Portnoy, D. A., S. L. Moseley, and S. Falkow.** 1981. Characterization of plasmids and plasmid-associated determinants of *Yersinia enterocolitica* pathogenesis. *Infect Immun* **31**:775-782.
108. **Presley, S. M., T. R. Rainwater, G. P. Austin, S. G. Platt, J. C. Zak, G. P. Cobb, E. J. Marsland, K. Tian, B. Zhang, T. A. Anderson, S. B. Cox, M. T. Abel, B. D. Leftwich, J. R. Huddleston, R. M. Jeter, and R. J. Kendall.** 2006. Assessment of pathogens and toxicants in New Orleans, LA following Hurricane Katrina. *Environ Sci Technol* **40**:468-474.
109. **Pukatzki, S., S. B. McAuley, and S. T. Miyata.** 2009. The type VI secretion system: translocation of effectors and effector-domains. *Curr Opin Microbiol* **12**:11-17.
110. **Purdue, G. F., and J. L. Hunt.** 1988. *Aeromonas hydrophila* infection in burn patients. *Burns Incl Therm Inj* **14**:220-221.
111. **Radke, J., K. J. Pederson, and J. T. Barbieri.** 1999. *Pseudomonas aeruginosa* exoenzyme S is a biglutamic acid ADP-ribosyltransferase. *Infect Immun* **67**:1508-1510.
112. **Ribardo, D. A., S. E. Crowe, K. R. Kuhl, J. W. Peterson, and A. K. Chopra.** 2001. Prostaglandin levels in stimulated macrophages are controlled by phospholipase A2-activating protein and by activation of phospholipase C and D. *J Biol Chem* **276**:5467-5475.
113. **Robson, W. L., A. K. Leung, and C. L. Trevenen.** 1992. Haemolytic-uraemic syndrome associated with *Aeromonas hydrophila* enterocolitis. *Pediatr Nephrol* **6**:221.
114. **Rose, J. M., C. W. Houston, D. H. Coppenhaver, J. D. Dixon, and A. Kurosky.** 1989. Purification and chemical characterization of a cholera toxin-cross-reactive cytolytic enterotoxin produced by a human isolate of *Aeromonas hydrophila*. *Infect Immun* **57**:1165-1169.
115. **Samie, A., R. L. Guarrant, L. Barrett, P. O. Bessong, E. O. Igumbor, and C. L. Obi.** 2009. Prevalence of intestinal parasitic and bacterial pathogens in diarrhoeal and non-diarrhoeal human stools from Vhembe district, South Africa. *J Health Popul Nutr* **27**:739-745.
116. **Scheffzek, K., M. R. Ahmadian, and A. Wittinghofer.** 1998. GTPase-activating proteins: helping hands to complement an active site. *Trends Biochem Sci* **23**:257-262.
117. **Schmid, I., W. J. Krall, C. H. Uittenbogaart, J. Braun, and J. V. Giorgi.** 1992. Dead cell discrimination with 7-amino-actinomycin D in combination with dual color immunofluorescence in single laser flow cytometry. *Cytometry* **13**:204-208.
118. **Sha, J., T. E. Erova, R. A. Alyea, S. Wang, J. P. Olano, V. Pancholi, and A. K. Chopra.** 2009. Surface-expressed enolase contributes to the pathogenesis of clinical isolate SSU of *Aeromonas hydrophila*. *J Bacteriol* **191**:3095-3107.

119. **Sha, J., E. V. Kozlova, and A. K. Chopra.** 2002. Role of various enterotoxins in *Aeromonas hydrophila*-induced gastroenteritis: generation of enterotoxin gene-deficient mutants and evaluation of their enterotoxic activity. *Infect Immun* **70**:1924-1935.
120. **Sha, J., E. V. Kozlova, A. A. Fadl, J. P. Olano, C. W. Houston, J. W. Peterson, and A. K. Chopra.** 2004. Molecular characterization of a glucose-inhibited division gene, *gidA*, that regulates cytotoxic enterotoxin of *Aeromonas hydrophila*. *Infect Immun* **72**:1084-1095.
121. **Sha, J., M. Lu, and A. K. Chopra.** 2001. Regulation of the cytotoxic enterotoxin gene in *Aeromonas hydrophila*: characterization of an iron uptake regulator. *Infect Immun* **69**:6370-6381.
122. **Sha, J., L. Pillai, A. A. Fadl, C. L. Galindo, T. E. Erova, and A. K. Chopra.** 2005. The type III secretion system and cytotoxic enterotoxin alter the virulence of *Aeromonas hydrophila*. *Infect Immun* **73**:6446-6457.
123. **Sha, J., S. F. Wang, G. Suarez, J. C. Sierra, A. A. Fadl, T. E. Erova, S. M. Foltz, B. K. Khajanchi, A. Silver, J. Graf, C. H. Schein, and A. K. Chopra.** 2007. Further characterization of a type III secretion system (T3SS) and of a new effector protein from a clinical isolate of *Aeromonas hydrophila*--part I. *Microb Pathog* **43**:127-146.
124. **Sha, J., S. F. Wang, G. Suarez, J. C. Sierra, A. A. Fadl, T. E. Erova, S. M. Foltz, B. K. Khajanchi, A. C. Silver, J. Graf, C. H. Schein, and A. K. Chopra.** 2007. Characterization of a new type III secretion system (T3SS)-associated effector protein from a clinical isolate of *Aeromonas hydrophila*. *Infection and Immunity* **Submitted**.
125. **Sierra, J. C., G. Suarez, J. Sha, W. B. Baze, S. M. Foltz, and A. K. Chopra.** 2010. Unraveling the mechanism of action of a new type III secretion system effector AexU from *Aeromonas hydrophila*. *Microb Pathog* doi:10.1016/j.micpath.2010.05.011
126. **Sierra, J. C., G. Suarez, J. Sha, S. M. Foltz, V. L. Popov, C. L. Galindo, H. R. Garner, and A. K. Chopra.** 2007. Biological characterization of a new type III secretion system effector from a clinical isolate of *Aeromonas hydrophila*-part II. *Microb Pathog* **43**:147-160.
127. **Stanley, P., V. Koronakis, and C. Hughes.** 1991. Mutational analysis supports a role for multiple structural features in the C-terminal secretion signal of *Escherichia coli* haemolysin. *Mol Microbiol* **5**:2391-2403.
128. **Stebbins, C. E., and J. E. Galan.** 2001. Maintenance of an unfolded polypeptide by a cognate chaperone in bacterial type III secretion. *Nature* **414**:77-81.
129. **Stebbins, C. E., and J. E. Galan.** 2003. Priming virulence factors for delivery into the host. *Nat Rev Mol Cell Biol* **4**:738-743.
130. **Stiles, B. G., and T. D. Wilkins.** 1986. Purification and characterization of *Clostridium perfringens* iota toxin: dependence on two nonlinked proteins for biological activity. *Infect Immun* **54**:683-688.
131. **Stuber, K., S. E. Burr, M. Braun, T. Wahli, and J. Frey.** 2003. Type III secretion genes in *Aeromonas salmonicida* subsp *salmonicida* are located on a large thermolabile virulence plasmid. *J Clin Microbiol* **41**:3854-3856.

132. **Suarez, G., J. C. Sierra, T. E. Erova, J. Sha, A. J. Horneman, and A. K. Chopra.** 2010. A type VI secretion system effector protein, VgrG1, from *Aeromonas hydrophila* that induces host cell toxicity by ADP ribosylation of actin. *J Bacteriol* **192**:155-168.
133. **Suarez, G., J. C. Sierra, T. E. Erova, J. Sha, A. J. Horneman, and A. K. Chopra.** A type VI secretion system effector protein, VgrG1, from *Aeromonas hydrophila* that induces host cell toxicity by ADP ribosylation of actin. *J Bacteriol* **192**:155-168.
134. **Suarez, G., J. C. Sierra, J. Sha, S. Wang, T. E. Erova, A. A. Fadl, S. M. Foltz, A. J. Horneman, and A. K. Chopra.** 2008. Molecular characterization of a functional type VI secretion system from a clinical isolate of *Aeromonas hydrophila*. *Microb Pathog* **44**:344-361.
135. **Sundin, C., B. Hallberg, and A. Forsberg.** 2004. ADP-ribosylation by exoenzyme T of *Pseudomonas aeruginosa* induces an irreversible effect on the host cell cytoskeleton in vivo. *FEMS Microbiol Lett* **234**:87-91.
136. **Swift, S., M. J. Lynch, L. Fish, D. F. Kirke, J. M. Tomas, G. S. Stewart, and P. Williams.** 1999. Quorum sensing-dependent regulation and blockade of exoprotease production in *Aeromonas hydrophila*. *Infect Immun* **67**:5192-5199.
137. **Tardy, F., F. Homble, C. Neyt, R. Wattiez, G. R. Cornelis, J. M. Ruyschaert, and V. Cabiliaux.** 1999. *Yersinia enterocolitica* type III secretion-translocation system: channel formation by secreted Yops. *Embo J* **18**:6793-6799.
138. **Tato, C. M., and C. A. Hunter.** 2002. Host-pathogen interactions: subversion and utilization of the NF-kappa B pathway during infection. *Infect Immun* **70**:3311-3317.
139. **Tobe, T., S. Nagai, N. Okada, B. Adler, M. Yoshikawa, and C. Sasakawa.** 1991. Temperature-regulated expression of invasion genes in *Shigella flexneri* is controlled through the transcriptional activation of the virB gene on the large plasmid. *Mol Microbiol* **5**:887-893.
140. **Vila, J., J. Ruiz, F. Gallardo, M. Vargas, L. Soler, M. J. Figueras, and J. Gascon.** 2003. *Aeromonas* spp. and traveler's diarrhea: clinical features and antimicrobial resistance. *Emerg Infect Dis* **9**:552-555.
141. **Woestyn, S., M. P. Sory, A. Boland, O. Lequenne, and G. R. Cornelis.** 1996. The cytosolic SycE and SycH chaperones of *Yersinia* protect the region of YopE and YopH involved in translocation across eukaryotic cell membranes. *Mol Microbiol* **20**:1261-1271.
142. **Xu, X. J., M. R. Ferguson, V. L. Popov, C. W. Houston, J. W. Peterson, and A. K. Chopra.** 1998. Role of a cytotoxic enterotoxin in *Aeromonas*-mediated infections: development of transposon and isogenic mutants. *Infect Immun* **66**:3501-3509.
143. **Yu, H. B., P. S. Rao, H. C. Lee, S. Vilches, S. Merino, J. M. Tomas, and K. Y. Leung.** 2004. A type III secretion system is required for *Aeromonas hydrophila* AH-1 pathogenesis. *Infect Immun* **72**:1248-1256.
144. **Zhang, Y., and J. T. Barbieri.** 2005. A leucine-rich motif targets *Pseudomonas aeruginosa* ExoS within mammalian cells. *Infect Immun* **73**:7938-7945.

VITA

Carolina Sierra was born on January 25th, 1978, in Bogota, Colombia. She grew up in Bogota, where she attended the elementary and high school. Then, she attended Javeriana University in Bogota for her Bachelor degree in Bacteriology. She worked in the Samaritana Hospital and the Colombian National Cancer Institute for three years before joining the University of Texas Medical Branch as a visiting scientist in 2003. In 2005, she matriculated at the UTMB Graduate School of Biomedical Sciences. She received the Vale-Asche Scholarship in 2007 and the following year she received the James W. McLaughlin Scholarship. During her graduate student training, she attended two national and four local meetings where she had oral and poster presentations and had own several awards.

Education

B.S., December 1999, Javeriana University, Bogota, Colombia

Publications

1. **Sierra JC**, Suarez G, Sha J, Baze WB, and Chopra AK. Unraveling the mechanism of action of a new type III secretion system effector AexU from *Aeromonas hydrophila*. *In Press*, Microbial Pathogenesis. doi:10.1016/j.micpath.2010.05.011 2010
2. Suarez G, **Sierra JC**, Kirtley M, and Chopra AK. Role of a type VI secretion system effector protein, Hcp, of *Aeromonas hydrophila* in modulating activation of host immune cells. Submitted to Microbiology. 2010 (In revision).
3. Suarez G, **Sierra JC**, Erova TE, Sha J, and. Chopra AK. A type VI secretion system effector protein VgrG1 from *Aeromonas hydrophila* that induces host cell toxicity by ADP-ribosylation of actin. *J. Bacteriol.* 192: 155-168. 2010.
4. Khajanchi BK, Sha J, Kozlova EV, Erova TE, Suarez G, **Sierra JC**, Popov VL, Horneman AJ, Chopra AK. N-Acyl homoserine lactones involved in quorum sensing control type VI secretion system, biofilm formation, protease production, and in vivo virulence from a clinical isolate of *Aeromonas hydrophila*. *Microbiology.* 155: 3518-31. 2009.

5. Zhang F, Suarez G, Sha J, **Sierra JC**, Peterson JW, and Chopra AK. Phospholipase A(2)-activating protein (PLAA) enhances cisplatin-induced apoptosis in HeLa cells. *Cell Signal*. 21:1085-99. 2009.
6. Suarez G, **Sierra JC**, Sha J, Wang S, Erova TE, Fadl AA, Foltz SM, Horneman AJ, and Chopra AK. Molecular characterization of a functional type VI secretion system from a clinical isolate of *Aeromonas hydrophila*. *Microb Pathog*. 44:344-61. 2008.
7. Zhang F, Sha J, Wood TG, Galindo CL, Garner HR, Suarez G, **Sierra JC**, Peterson JW, and Chopra AK. Alteration in the activation state of new inflammation-associated targets by phospholipase A₂-Activating protein (PLAA). *Cell Signal*. 20: 844-61. 2008
8. **Sierra JC**, Suarez G, Sha J, Foltz SM, Popov VL, Galindo CL, Garner HR, Chopra AK. Biological characterization of a new type III secretion system effector from a clinical isolate of *Aeromonas hydrophila*-Part II. *Microb Pathog*. 43:147-60. 2007
9. Sha, J, Wang, S.F, Suarez, G, **Sierra, J.C**, Fadl, A.A, Erova, T.E, Foltz, S.M, Khajanchi, B.K, Silver, A.C, Graf, J, Schein, C.H, Chopra, A.K. Further characterization of a type III secretion system (T3SS) and of a new effector protein from a clinical isolate of *Aeromonas hydrophila*-Part I. *Microb Pathog*. 43:127-46. 2007
10. Bland D, Suarez G, Beswick EJ, **Sierra JC**, and Reyes VE. *H. pylori* receptor MHC class II contributes to the dynamic gastric epithelial apoptotic response. *World J of Gastroenterol*. 12:5306-10. 2006
11. Beswick EJ, Pinchuk IV, Suarez G, **Sierra JC**, and Reyes VE. *Helicobacter pylori*-CagA-dependent macrophage migratory inhibitory factor produced by gastric epithelial cells binds to CD74 and stimulates procarcinogenic events. *J Immunol*. 176:6794-801. 2006
12. Das S, Suarez G, Beswick E, **Sierra JC**, Graham DY, and Reyes VE. Expression of B7-H1 on gastric epithelial cells: its potential role in regulating T cells during *Helicobacter pylori* infection. *J Immunol* Mar 176:3000-9. 2006
13. Beswick EJ, Pinchuk IV, Minch K, Suarez G, **Sierra JC**, Yamaoka Y, and Reyes VE. The *Helicobacter pylori* urease B subunit binds to CD74 on gastric epithelial cells and induces NF-kappaB activation and interleukin-8 production. *Infect Immun* Feb 74:1148-55. 2006
14. Das S, **Sierra JC**, Suarez G, Kizhake S, Luxon B, and Reyes VE. Differential protein expresión profiles of gastric ephithelial cells following *Helicobacter pylori* infection using protein chips. *The Journal of Proteome Research* May-June 4:920-30. 2005
15. Barrera CA, Beswick EJ, **Sierra JC**, Bland D, Espejo R, Mifflin R, Adegboyega P, Crowe SE, Ernst PB, and Reyes VE. Polarized expression of CD74 by gastric epithelial cells. *The Journal of Histochemitry and Cytochemistry* Dec 53:1481-9. 2005

Abstracts and Posters

1. **Sierra JC**, Suarez G, Foltz SM, Wallace B, Baze and Chopra AK. Unraveling the mechanism of action of a new type III secretion system effector AexU from *Aeromonas hydrophila*. McLaughlin Colloquium on Infection and Immunity. Galveston, TX. 2010
2. Suarez G, **Sierra JC**, Kirtley M, and Chopra AK. Role of a type VI secretion system effector protein, Hcp, of *Aeromonas hydrophila* in modulating activation of host immune cells. McLaughlin Colloquium, Galveston, TX. 2010.
3. **Sierra JC**, Suarez G, and Chopra AK. A type 3 secretion system (T3SS) effector AexU from *Aeromonas hydrophila* SSU has ADP-ribosyltransferase and GTPase-activating protein activity. ASM General Meeting. Philadelphia, PA. 2009.
4. Suarez G, **Sierra JC**, Sha J, Erova TE, Horneman A, and Chopra AK. A type VI secretion system effector protein, VgrG1, from *Aeromonas hydrophila* induces host cell toxicity by ADP-ribosylation of actin. ASM General Meeting. Philadelphia, PA. 2009.
5. Suarez G, **Sierra JC**, Sha J, Erova TE, Horneman A, and Chopra AK. A type VI secretion system effector protein, VgrG1, from *Aeromonas hydrophila* induces host cell toxicity by ADP-ribosylation of actin. Graduate Student Festival, NIH, Bethesda, MD. 2009.
6. **Sierra JC**, Suarez G, Foltz SM, Baze WB, and Chopra AK. Unraveling the mechanism of action of a new type III secretion system effector AexU from *Aeromonas hydrophila*. Graduate Student Festival, NIH, Bethesda, MD. 2009.
7. **Sierra JC**, Suarez G, Sha J, Erova TE, Foltz SM and Chopra AK. Identification and biological characterization of new type III secretion system effector proteins from an emerging human pathogen *Aeromonas hydrophila*. McLaughlin Colloquium on Infection and Immunity. Galveston, TX. 2008
8. **Sierra JC**, Suarez G, Sha J, Fadl AA, Wang S, Foltz SM, Erova TE, Schein CH, and Chopra AK. A new type III secretion system effector protein in an emerging human pathogen *Aeromonas hydrophila*. McLaughlin Annual Colloquium. Galveston, TX. 2007
9. Suarez G, **Sierra JC**, Sha J, Erova TE, Foltz SM, and Chopra AK. Initial characterization of a new and novel type six secretion system (T6SS) in an emergent human pathogen *Aeromonas hydrophila*. McLaughlin Annual Colloquium on Infection & Immunity. Galveston, TX. 2007.
10. **Sierra JC**, Suarez G, Sha J, Galindo CL, Chopra AK. Functional and biological characterization of a new type III secretion system effector from an emerging human

pathogen *Aeromonas hydrophila*. Submitted to The Texas Branch American Society of Microbiology, Galveston, 2006.

11. Suarez G, **Sierra JC**, Sha J, Fadl AA, Wang S, Foltz SM, Erova TE, Schein CH, and Chopra AK. A new type III secretion system effector protein in an emerging human pathogen *Aeromonas hydrophila*. Texas Branch 2006 ASM Meeting. Galveston, Texas. 2006